EARTHQUAKE HAZARD EVALUATION FOR SWITZERLAND

Erik RÜTTENER

Adresse de l'auteur:

Schweizerischer Erdbebendienst
Institut für Geophysik
ETH-Hönggerberg
CH-8093 Zürich

Préface de l'éditeur

La présente publication intitulée " Earthquake Hazard Evaluation for Switzerland " est la 29ième de la série des Matériaux pour la Géologie de la Suisse, série Géophysique.

Cette publication présente le travail de thèse de Monsieur Erik Rüttener, effectué à l'Institut de Géophysique de l'Ecole Polytechnique Fédérale de Zürich, sous les directions du Professeur Stephan Mueller et du Dr. Dieter Mayer-Rosa.

Ce travail consiste en une évaluation du risque sismique pour un site donné en tenant compte des incertitudes dont sont entachées les données. Pour ceci, Monsieur Rüttener a utilisé une technique d'estimation Bayesienne dans laquelle les estimations "a priori" des paramètres de risques sont corrigées à l'aide des données observées. Finalement la méthode proposée a été appliquée aux risques sismiques en Suisse

La Commission Suisse de Géophysique remercie très vivement l'auteur pour cette intéressante contribution à la recherche géophysique.

L'Académie Suisse des Sciences Naturelles à supporté entièrement les coûts d'impression de cette publication; qu'elle veuille bien accepter ici l'expression de notre gratitude.

Zurich, Août 1995

Au nom de la Commission Suisse
de Géophysique

Le Président:

Prof. Emile Klingelé

Vorwort

Die Installation und der Betrieb eines modernen seismischen Netzes in der Schweiz hat seit 1975 die Kenntnisse über die Vollständigkeit und Genauigkeit seismischer Daten wesentlich gefördert. Damit war es möglich, die Erdbebengefährdung und im weiteren Sinn das dadurch verursachte Risiko in der Schweiz systematisch zu untersuchen. Die erste landesweite Gefährdungskarte konnte 1977 veröffentlicht werden. Sie hat ihren Niederschlag sowohl in der seismischen Beurteilung von Standorten als auch den "Schweizerischen Baunormen SIA 160" gefunden.

Verschiedene wissenschaftliche Projekte, die in Zusammenarbeit mit anderen Instituten seitdem in der Schweiz durchgeführt wurden, unterstreichen das wachsende Interesse an diesem aktuellen Thema.
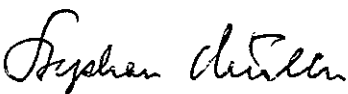
1990 konnte eine Neubearbeitung dieses Themas mit einer Dissertation ins Auge gefasst werden, die von Herrn Erik R ü t t e n e r ausgeführt und im Frühjahr 1995 mit dem Titel: "Earthquake Hazard Evaluation for Switzerland" an der Eidgenössischen Technischen Hochschule (ETHZ Nr.11048) abgeschlossen wurde. Sie wurde von Prof. Dr. Stephan Müller (ETH und Universität Zürich) als Hauptreferent, Dr. Dieter Mayer-Rosa (Schweizerischer Erdbebendienst, ETH Zürich), 1. Korreferent, und Prof. Dr. Juan Jose Egozcue (Technische Universität Barcelona), 2. Korreferent, betreut.

Diese Dissertation ist im Rahmen der Hauptaufgaben des Schweizerischen Erdbebendienstes an der ETH Zürich zu sehen, wozu eine realistische Bestimmung der Erdbebengefährdung in der Schweiz und damit verbunden die Entwicklung von neuen Berechnungsmethoden gehört.

Von 1993 bis 1995 wurde diese Arbeit vollumfänglich durch das Nationale Forschungsprojekt NFP 31 des Schweizerischen Nationalfonds in Bern finanziert. Herr E. Rüttener hat ausserdem in den Jahren 1992 bis 1993 im "Mikrozonierungs- und Gefährdungsprojekt Obwalden" mitgearbeitet, das vom Schweizerischen Nationalkomitee für die "International Decade for Natural Disaster Reduction" unterstützt wurde.

Die vorliegende Veröffentlichung entspricht in ihrem Inhalt der Dissertation von E. Rüttener.

Unser Dank geht an die Schweizerische Geophysikalische Kommission für die Möglichkeit, im Rahmen ihrer Publikationsreihe "Materiaux pour la Géologie de la Suisse, Série Géophysique" diese Untersuchung zu veröffentlichen.

(Stephan Müller)   (Dieter Mayer-Rosa)

CONTENTS

To

STEFANIE

who always encouraged me

"So far as Mathematics do not tend to make men more sober and rational thinkers, wiser and better men, they are only to be considered as an amusement, which ought not to take us off from serious business."

Reverend Thomas Bayes, 1736

ABSTRACT

Earthquake hazard analysis is of considerable importance for Switzerland, a country with moderate seismic activity but high economic values at risk. The evaluation of earthquake hazard, i.e. the determination of return periods versus ground motion parameters, requires a description of earthquake occurrences in space and time. In this study the seismic hazard for major cities in Switzerland is determined.

The seismic hazard analysis is based on historic earthquake records as well as instrumental data. The historic earthquake data show considerable uncertainties concerning epicenter location and epicentral intensity. A specific concept is required, therefore, which permits the description of the uncertainties of each individual earthquake. This is achieved by probability distributions for earthquake size and location.

Historical considerations, which indicate changes in public earthquake awareness at various times (mainly due to large historical earthquakes), as well as statistical tests have been used to identify time periods of complete earthquake reporting as a function of intensity. As a result, the catalog is judged to be complete since 1878 for all earthquakes with epicentral intensities greater than IV, since 1750 for intensities greater than VI, since 1600 for intensities greater than VIII, and since 1300 for intensities greater than IX.

Instrumental data provide accurate information about the depth distribution of earthquakes in Switzerland. In the Alps, focal depths are restricted to the uppermost 15 km of the crust, whereas below the northern Alpine foreland earthquakes are distributed throughout the entire crust (30 km). This depth distribution is considered in the final hazard analysis by probability distributions.

An analysis of intensity attenuation versus distance, based on more than 6,000 macroseismic observations and taking into account the uncertainty of the individual estimates, yields three distinct regions with different attenuation properties. The highest attenuation is observed in the subalpine chains (which comprise Helvetic and Ultrahelvetic nappes), and the lowest in the crystalline basement and Penninic nappes of the Alps. The northern Alpine foreland is characterized by an intermediate attenuation.

Since previous models did not take into account uncertainties of epicenter location, earthquake size and intensity attenuation, a new approach for calculating seismic hazard was adopted. The method is based on Bayesian statistics and incorporates the uncertainties in the input data in order to determine the uncertainties in the final hazard estimates.

Seismic hazard curves have been calculated for twelve major cities in Switzerland.

These curves are compared with results of a study carried out in 1978. The results of the previous study almost always range within the 90% probability interval of the new results, but generally lie at the upper bound of the probability intervals. It is concluded that taking the uncertainties into account results in smaller return periods. Return periods for intensities greater than VIII in regions with low seismic activity cannot be determined with confidence. This is a consequence of the limited time period of observations available, which does not constrain such large return periods (greater than 10'000 years). Additional data, such as paleoseismological data, must be used in order to reduce the large uncertainties in the return periods. However, when such data are available, they can be readily integrated into the method developed.

ZUSAMMENFASSUNG

In Europa gehört die Schweiz zu den Ländern mit einer geringen bis mittleren seismischen Aktivität. Wegen der hohen Konzentration von ökonomischen Sachwerten darf jedoch die Gefährdung durch Erdbeben in der Schweiz nicht vernachlässigt werden. Die Bestimmung der Erdbebengefährdung, d.h. der möglichen Bodenerschütterung in Abhängigkeit der Wiederkehrperiode, erfordert Kenntnisse über das räumliche und zeitliche Auftreten von Erdbeben. Das Ziel dieser Studie ist es, die Erdbebengefährdung für 12 wichtige Städte in der Schweiz zu berechnen.

Dazu werden sowohl historische Erdbebendaten als auch instrumentelle Aufzeichnungen miteinbezogen. Die Bestimmung der Stärke und des Epizentrums von historischen Erdbeben ist mit grossen Unsicherheiten verbunden. Um diese Unsicherheiten zu beschreiben, werden Wahrscheinlichkeitsverteilungen eingeführt. Sie gewährleisten eine realistische Darstellung der Unsicherheiten jedes einzelnen Bebens.

Zeitperioden, in welchen Erdbeben einer gewissen Stärke vollständig erfasst wurden, müssen bestimmt werden. Starke Erdbeben in der Vergangenheit sind dabei von Bedeutung, da sie das Bewusstsein gegenüber Erdbeben verstärkten und somit zu detaillierteren Chroniken führten. Statistische Tests bestätigen diesen Einfluss. Folgende Zeiträume zeigen eine vollständige Erfassung der Erdbeben: ab 1878 für Intensitäten grösser als IV, ab 1755 für Intensitäten grösser als VI, ab 1600 für Intensitäten grösser als VIII und ab 1300 für Intensitäten grösser als IX.

Instrumentelle Aufzeichnungen der letzten 20 Jahre liefern genaue Angaben über die Tiefenverteilung der Erdbeben. Es zeigt sich, dass Erdbeben in den Alpen auf die obersten 15 km der Kruste beschränkt sind, im nördlichen alpinen Vorland hingegen sind sie über die ganze Kruste (30 km) verteilt. Diese Tiefenverteilung wird durch Wahrscheinlichkeitsverteilungen in der Gefährdungsberechnung berücksichtigt.

Über 6'000 makroseismische Beobachtungen beschreiben die Abminderung der Intensität mit der Distanz. Drei geographische Regionen können unterschieden werden, welche verschiedene Abminderungscharakteristiken aufweisen: 1) Die subalpinen Ketten (Helvetikum und Ultrahelvetikum) mit der stärksten Abminderung, 2) das nördliche alpine Vorland und 3) das kristalline Grundgebirge und die Penninischen Decken der Alpen mit der geringsten Abminderung. Die hergeleiteten Abminderungsbeziehungen, welche auch die Unsicherheiten in den makroseismischen Beobachtungen berücksichtigen, erlauben eine Modellierung der Intensitätsabnahme mit der Distanz.

Da gebräuchliche Algorithmen zur seismischen Gefährdungsberechnung es nicht erlauben, die Unsicherheiten in der Lokalisierung, der Stärke und der Intensitätsabnah-

me mit der Herdentfernung von Erdbeben zu berücksichtigen, musste eine spezifische Methode erarbeitet werden. Basierend auf dem Konzept der Bayesian-Statistik wird eine Methode eingeführt, die aus den Unsicherheiten in den Eingangsdaten und in den verwendeten Modellen die Unsicherheiten in den Resultaten bestimmt.

Für zwölf Orte in der Schweiz werden Wiederkehrperioden in Abhängigkeit der Intensität berechnet. Ein Vergleich der Resultate mit denjenigen aus der Studie von 1978 zeigt, dass die früheren Werte nahezu immer im 90% Wahrscheinlichkeitsintervall liegen, jedoch meistens an dessen oberen Begrenzung. Dies deutet darauf hin, dass der Einbezug von Unsicherheiten in die Berechnung tendenziell zu kürzeren Wiederkehrperioden führt. Lange Wiederkehrperioden (grösser als 10'000 Jahre), die in der früheren Studie für hohe Intensitäten berechnet wurden, zeigen sehr grosse Unsicherheiten. Dies ist eine Folge der kurzen Beobachtungszeiten im Verhältnis zu den Wiederkehrperioden. Hier müssen zusätzliche Daten herangezogen werden (z.B. aus der Paläoseismologie), um die Wiederkehrperioden genauer einzugrenzen. Der entwickelte Algorithmus ist beschaffen, dass solche zusätzlichen Informationen miteinbezogen werden können.

Chapter 1

INTRODUCTION

1.1   Goals and Overview

Over the last two decades, earthquake risk mitigation has gained worldwide attention and its need has been repeatedly demonstrated by disastrous earthquakes, which claimed thousands of lives and caused huge economic losses to industry and infrastructure (e.g. Armenia earthquake 1988 (Wyllie and Filson, 1989) or Northridge earthquake in Los Angeles 1994 (Hall, 1994)). It was recognized that reduction of losses caused by earthquakes has to be a primary aim of the international community - a postulate which has lead to the UN proclamation of the International Decade of Natural Disaster Reduction (IDNDR) (UNO, 1989).

Earthquake risk is defined as the product of earthquake hazard and vulnerability, where vulnerability defines the degree of loss to a given element resulting from the occurrence of a natural phenomenon of a given magnitude. Earthquake hazard includes any physical phenomenon, such as ground shaking or ground failure resulting from an earthquake and its probability of occurrence. Therefore, earthquake risk is not only a matter of concern in regions with high seismicity, i.e. with high seismic hazard, but is particularly important in areas with a high population density and/or with an accumulation of significant values in infrastructure and economy, i.e. areas with a high vulnerability.

Switzerland, as part of the Alpine orogenic belt, has undergone a pronounced lithospheric convergence and shearing between the African and Eurasian plates. This lasting crustal deformation produces a slightly higher seismicity compared to low seismic activity in the northern part of Europe. The seismic activity since 1974 in Switzerland and adjacent regions is displayed in figure 1.1. The level of seismic activity and the high population density obviously justifies the assessment of seismic hazard in Switzerland.

To reduce losses caused by earthquakes a clear picture of earthquake hazard and vulnerability in a particular area is necessary. Earthquake hazard analysis is performed to obtain the necessary characterization of possible ground-shaking severity that could be expected at a particular site. However, the data and information, which serve as a primary input for a seismic hazard analysis, are inherently imprecise and inaccurate.

Usually seismic hazard is represented by a point estimate of the probability function, which describes the exceedance of a ground motion level at a site in a certain number of years. A frequently used point estimate, especially for mapping, is the ground motion value that will not be exceeded in a certain number of years with a given prob-

ability. The reduction of the probability function to a point estimate makes it impossible to understand the accuracy of the results.

The main goal of this work is to estimate the seismic hazard for a certain site taking into account the uncertainty of the input data and to quantify the uncertainty of the hazard estimate. This is achieved by using a Bayesian estimation technique, where a prior estimate of the hazard parameter (occurrence probabilities of a ground motion level or return periods) is corrected by observed data. This method takes uncertainties in the input parameters into account and gives probability intervals of the calculated seismic hazard. Before the method can be applied, however, an earthquake database has to be built up, and models have to be defined that describe the uncertainty of different parameters (e.g. epicentral intensity, location).

The text is structured as follows:

Chapter 1 reviews State-of-the-art methods covering the historic and deductive approaches in seismic hazard analysis. The basic assumptions and limitations of the different techniques are discussed. Furthermore, a summary of the situation in Switzerland is given.

Chapter 2 introduces the concept of probability distributions in order to account for the uncertainty of earthquake size and location. Appropriate error models are assessed, with special attention to epicentral intensity estimates. It is shown that with the developed models the uncertainties can appropriately be represented. The compiled earthquake catalog covering Switzerland and adjacent regions is presented. The seismicity in Switzerland regarding spatial and temporal distribution is discussed. Time periods of complete reporting of earthquakes for different intensity levels are defined.

Chapter 3 gives first an introduction in Bayesian estimation techniques. The Bayesian model developed for seismic hazard analysis is presented. The chapter ends with a comparison of the influence of different prior estimates on posterior probability distributions.

Chapter 4 describes macroseismic intensity attenuation models. A new attenuation model is defined, which represents the different characteristics of the northern Alpine foreland, the Helvetic and Ultrahelvetic nappes and the crystalline basement and Penninic nappes of the Alps. The model also takes into account the integer-based definition of intensity values by a discretized normal distribution.

Chapter 5 verifies the applicability of the defined intensity attenuation relation of Chapter 4 in combination with the error models of Chapter 2 by modelling intensity distributions for individual earthquakes. It is shown that intensity distributions can properly be modelled. Next, return periods versus intensity are calculated to characterize seismic hazard for 12 sites in Switzerland. The seismic hazard obtained is compared with results of previous studies. The chapter ends with a discussion of the methods developed along with recommendations for future work.
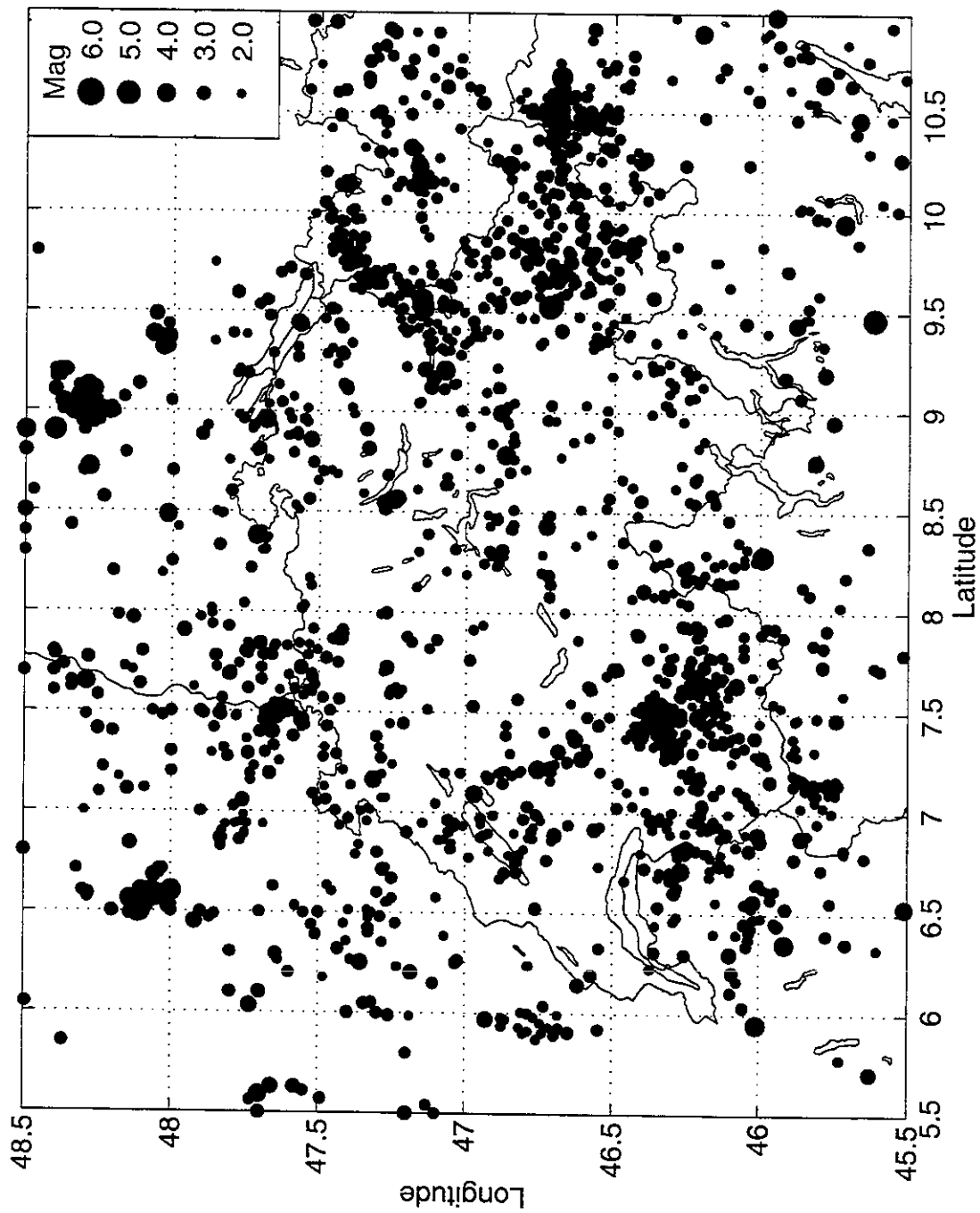
Figure 1.1: Epicenter map of instrumentally determined earthquakes for the time period 1974 to 1994 in Switzerland and adjacent regions. The magnitude range is 2.5 to 5.5.

1.2 Review of Methods in Seismic Hazard Analysis

Seismic hazard is defined as the probability of occurrence of a certain ground motion caused by earthquakes. Parameters of ground motion are usually either macroseismic intensity determinations or parameters derived from instrumental measurements (e.g. peak or spectral peak acceleration, respectively velocity). The selection of a specific parameter depends on the available data for the region under study. In European countries, many macroseismic investigations have been carried out to describe the damages of historic earthquakes. A systematic collection of historic earthquake data of the last centuries has produced a large databases that describe earthquake severity in terms of macroseismic intensity. On the contrary, only few countries in Europe have installed strong motion instruments. Therefore, not enough strong motion records of significant earthquakes were obtained for all regions up to now. Consequently, the "unreliable" macroseismic data with sufficient geographical coverage, or the "reliable" strong motion records with insufficient geographical coverage have to be used.

Methods used to calculate seismic hazard can be grouped into two categories (McGuire, 1993): the "**historic**" methods and the "**deductive**" (or seismic source) methods. The historic method is based on the historic occurrences of earthquakes, from which the ground shaking severity at a site is calculated. The methods are called deductive, if the occurrence of earthquakes is interpreted and characterized by seismic sources. Seismic sources are defined as geographical features with homogeneous distributed seismicity.

The "historic" methods (cf. Veneziano et al., 1984) model, in principle, the occurrence of ground shaking at a particular site in the past, caused from each event of the earthquake catalog. The methods accept that the knowledge about the historic occurrence of ground shaking at a site is sufficient and adequate to describe the earthquake hazard. This assumes that the future pattern of seismic activity will not substantially differ from that observed in the past. As a consequence, areas with high seismic activity in the past will have a higher probability for the occurrence of earthquakes in the future. This hypothesis is only justified if there are no other reliable data at hands either to predetermine future epicenters in areas without observed activity, or to define quiet sources, where a high activity has been observed in the past.

The general steps involved in the historic procedure (Veneziano et al., 1984) are shown in figure 1.2. Starting from an earthquake catalog, which contains date, location and size of historic earthquakes, the seismic ground motion of each earthquake at a specific site is calculated using an appropriate ground motion attenuation function. The summation over all calculated site intensities leads to an estimation of seismic hazard as the mean rate at which different intensity levels have been exceeded.

If enough observations of ground motion intensity for a site are available, they can also be used directly without the employment of an attenuation function. Egozcue et al. (1991) and Grünthal (1991) developed procedures that use either observed site intensities of strong earthquakes or theoretically calculated intensities by using empirical attenuation functions. In the seismic hazard analysis, therefore, observed intensity anomalies, usually neglected when applying attenuation functions, are taken into account.

Historic methods should be adopted in regions, where the identification of earthquake sources with homogenous seismicity is impossible because of lack of data and knowledge. However, the historic method is not adequate and will give rather unrealistic and unstable results if the earthquake record is not long enough to reveal the general characteristics of the seismicity pattern. This is especially evident for long return periods (low probabilities). In these cases a method has to be applied which allows for interpretations and assumptions of the future seismicity pattern.
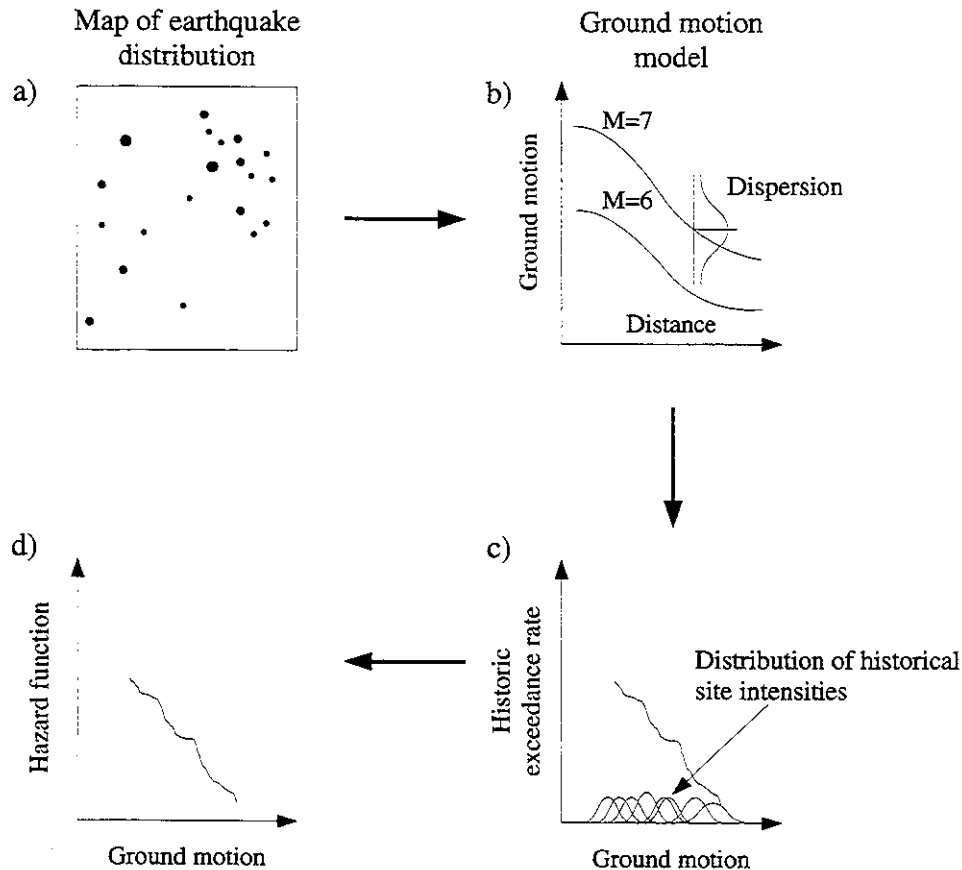

Figure 1.2: The main steps involved in the historic hazard approach (cf. Veneziano et al., 1984): a) earthquake catalog, b) ground motion attenuation functions, c) historical site intensities and d) probability analysis.

In 1968, Cornell published an approach, which is known as the "deductive" or "seismic source" method and which is the standard methodology in seismic hazard assessment. There now exist a number of modifications of Cornell's method. Various easily applicable computer codes have been developed, such as SRAMSC by McGuire (1976) and SEISRISK by Bender and Perkins (1987). The method has been widely applied in the United States (cf. Shah et al. (1975), Algermissen and Perkins (1976) and Algermissen et al. (1982)) and in Europe (Sägesser and Mayer-Rosa, 1978).

The main steps involved in the deductive method are illustrated in figure 1.3. Based on the spatial distribution of earthquakes and on often rather intuitive seismotectonic

criteria, seismic sources are defined. The seismicity of each source is described by a recurrence relationship. This is often done by the simple cumulative magnitude-frequency law known as the Gutenberg-Richter relationship (Gutenberg and Richter, 1944):

$$\log N\,(m) = a - b \cdot m \qquad (1\text{-}1)$$

where

$N\,(m)$ number of earthquakes with magnitude $\geq$ m

10^{a} number of earthquakes above magnitude 0

b slope of the cumulative magnitude distribution

The parameter b characterizes the seismicity of a region. This relationship has been shown to be applicable in various areas throughout the world (e.g. Evernden, 1970). Typically b values around the world range from 0.7 to 1.1. It can be necessary to modify this relation either in areas where seismic data show another behavior or if intensity is used instead of magnitude. Merz and Cornell (1973) modified the linear exponential law to a quadratic exponential law for an application in Boston, and Shah et al. (1975) used a bilinear law for their study of seismic risk in Nicaragua.

Usually the parameters of the magnitude-frequency law are determined by least-square methods. From the magnitude-frequency law a probability density function can be derived, which gives the probability that, if an earthquake occurs, it will be of magnitude m. For the Gutenberg-Richter relationship the probability density is:

$$f_{m} = k\beta \exp\left[-\beta\,(m - m_{0})\right],\,(m_{0} < m < m_{u}) \qquad (1\text{-}2)$$

where

β $= b \ln\,(10)$

k normalizing constant

$m_{0},\,m_{u}$ lower-bound magnitude and upper-bound magnitude

The use of a lower-bound magnitude assumes that smaller events are not relevant for the overall hazard and therefore can be neglected. The upper-bound magnitude, which accounts for the largest possible earthquake, is usually determined by assumptions about the physical characteristics of the source. However, it is also possible to model an unlimited magnitude distribution by Cornell's method (1968).

In seismic hazard calculations it is assumed that the seismic activity of the source is homogeneously distributed over the seismic source, i.e. that it is of equal likelihood that an earthquake happens anywhere in the defined source region or along a defined fault. The evidently abrupt changes in the seismic activity at the border of the seismic sources were addressed in the algorithm SEISRISK III of Bender and Perkins (1987). They introduced an earthquake-location uncertainty, which allows the earthquakes in a seismic source to be normally rather than uniformly distributed. As a consequence the calculated seismicity does not drop abruptly at the seismic source boundaries, but changes rather smoothly across the boundary.
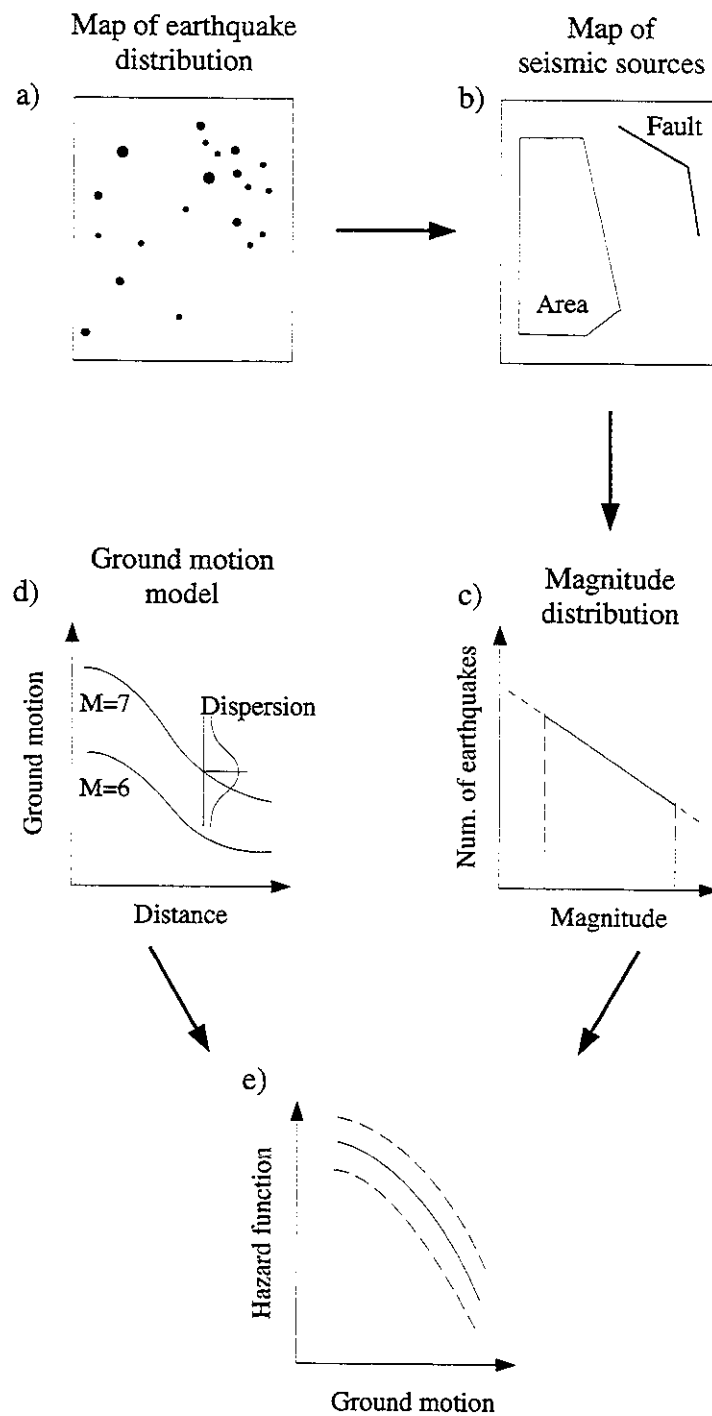
Figure 1.3: The main steps involved in the deductive approach (Cornell, 1968): a) earthquake catalog, b) delineation of seismic sources, c) magnitudes-frequency distribution, d) ground motion attenuation functions and e) probability analysis.

The occurrence of earthquakes in time is commonly modelled by a Poisson process (Cornell (1968), Lomnitz (1973)). The Poisson distribution has been applied many times and it has been shown to be reasonable, when aftershocks are removed, especially for large shocks (see for example Gardner and Knopoff, 1974). The probability distribution of a Poisson process for n events in time t is given by:

$$P\,(N_t = n) \ = \ \frac{(\lambda t)^n \exp\,(-\lambda t)}{n!} \qquad (1\text{-}3)$$

where

λ mean occurrence rate

N_t number of occurrences in time

A Poisson process assumes that the events are random in time and independent of each other. Therefore, it is not possible to model the sudden release of continuously accumulated strain or either fore- or aftershocks patterns. Other models have been developed which can account for the time dependence of earthquake occurrence. The assumptions that stress accumulates at a constant rate and is released once a threshold level is reached leads to the "time-predictable" model (Anagnos and Kiremidjian, 1984). Thereby the time to the next event is governed by the magnitude of the previous earthquake. If it is assumed that each event brings the stress level back to zero, the magnitude of the next event is dependent on the time elapsed since the last event. This assumption is incorporated in the "slip-predictable" model (Kiremidjian and Anagnos, 1984). The two models take into account the time elapsed since the last event (memory models) and estimate a stress accumulation and a release process. The applicability of these models depend on the possibility to define and characterize seismic sources by their mechanisms, which is usually only the case for fault sources. However, the correlation between the inter-arrival times of earthquakes and the preceding magnitude has to be tested for each seismic source.

The next step in the deductive seismic hazard analysis consists of the selection of an appropriate ground motion model. Given the earthquake size and distance, the ground motion at a site is influenced by the source characteristics, the path of the seismic waves and the local soil conditions. Campell (1985) showed that most of the developed attenuation relations have the general form:

$$Y = b_1 \cdot f_1\,(m) \ \cdot f_2\,(r) \ \cdot f_3\,(m, r) \ \cdot f_4\,(p) \ \cdot \varepsilon \qquad (1\text{-}4)$$

where

Y ground motion parameter of interest

m magnitude

r distance between source and site

f_1, f_2, f_3 functions of the magnitude and the distance

$f_4\,(p)$ function of the travel path and site conditions

ε scatter parameter of the uncertainty of the ground motion

The first implemented attenuation models in the programs of Cornell (1968) and McGuire (1976) assumed a radial symmetric behavior of ground motion attenuation. This behavior was not proposed based on physical considerations but lack of data usually did not allow to define a more exact model. However, in order to accommodate the apparent variation of observed ground motion measurements, a standard deviation is assigned to the attenuation function (ε in formula (1-4)). As a first-order approximation to the observed form of isoseismals in Switzerland, an elliptical attenuation model was used by Mayer-Rosa and Merz (1976) in a first seismic hazard analysis for Switzerland.

The last step in seismic hazard analysis is the so-called site severity analysis, i.e. the calculation of the probability per unit time that a certain ground motion level is exceeded at a site. The probability $G_{gm|(m,r)}(a)$, that an earthquake with a given magnitude m at a distance r, exceeds the ground motion level a at the site, can be calculated combining the magnitude-frequency relation (1-2), the Poisson distribution of earthquake occurrence in time (1-3) and the ground motion attenuation function (1-4). If the probability density functions for the magnitude distribution and for the distance between earthquake and site are known, the integration over all magnitudes and distance ranges leads to the desired probability:

$$P\left[gm > a|t\right] = v_i \int_{r_{min}}^{r_{max}} \int_{m_{min}}^{m_{max}} G_{gm|(m,r)}(a) f_M(m) f_R(r|m)\ (dm)\ dr \qquad (1\text{-}5)$$

where

a	ground motion level
m	magnitude
r	distance between source and site
f_M	magnitude probability density function
m_{min}, m_{max}	minimum and maximum magnitude being considered
f_R	distance probability density function
r_{min}, r_{max}	minimum and maximum distance being considered
v_i	mean rate of earthquakes between min. and max. magnitude
P	probability, that the ground motion is larger than a in time t

1.3   Previous Works and Seismic Instrumentation in Switzerland

The method used in the seismic hazard study for Switzerland was first described by Mayer-Rosa and Merz (1976). A procedure was chosen which followed in principle the probabilistic approach proposed by Cornell (1968). This hazard analysis led to comprehensive hazard maps (Sägesser and Mayer-Rosa (1978), Mueller and Mayer-Rosa (1980)) and risk studies for critical industrial facilities, i.e. nuclear power plants. Macroseismic intensity was chosen as the ground motion parameter to be assessed, because of the availability of macroseismic data and isoseismal maps for practically all strong earthquakes in Switzerland in this century (cf. Swiss Seismological Service (1911-1963), Mayer-Rosa and Baer (1993)) and the lack of strong motion records.

Figure 1.4 shows the historical seismicity since 1300 and the 22 seismic sources that have been defined for these hazard studies. The delineation of the sources follows mainly the pattern of the historical seismicity and takes into account the general seismotectonic trends. An intensity-frequency distribution was used to characterize the seismic activity of each seismic source, represented by a quadratic law:

$$\log N\,(I_0) \;=\; \alpha + \beta \cdot I_0 + \gamma \cdot I_0^{\,2} \qquad\qquad (1\text{-}6)$$

where

N cumulative number of earthquakes

I_0 epicentral intensity

α, β, γ parameters to be fitted

The attenuation of intensity with distance was modelled by a formulation proposed by Sponheuer (1960) (see equation (4-3)). For some isoseismal patterns in Switzerland an azimuthal variation of intensity attenuation can be recognized. An elliptic attenuation relation as a first-order approximation was adopted by Sägesser and Mayer-Rosa (1978) in order to better take into account these observations.

After modifications of McGuire's program (1976) with respect to elliptic attenuation and quadratic intensity-frequency relationships, seismic hazard was calculated for a grid of 10 by 10 km. Based on these results contour maps showing intensities for a given probability or showing probabilities for a given intensity were drawn. Figure 1.5 shows one of the calculated hazard maps, which depicts the calculated intensities for a return period of 1000 years. The region of the Canton Valais shows the highest intensities with values greater than 8. Four zones with intensities of about 7.5 can be identified: the region of Basel, central Switzerland, the Engadine and the Rhine Valley in northeastern Switzerland.

The Swiss national seismic network, in operation since the mid-seventies (figure 1.6), permits to accurately locate earthquakes in Switzerland. The accuracy of the locations is usually better than ± 3 km, which leads to an improved understanding of the earthquake distribution in Switzerland. The recent installation of the Swiss national strong motion network (cf. Smit and Mayer-Rosa (1993) and Smit (1994)) will provide

valuable information on the attenuation of ground motion and about the influence of local soil conditions for future applications. With the availability of strong motion records, it will be possible to assess other parameters than intensity, as. e.g. narrow-band peak ground accelerations. Nevertheless, as the seismicity in Switzerland is moderate, it will take some time until a significant number of strong motion records are obtained. Therefore, these data could not yet be used in the present hazard analysis.

The earthquake hazard of a particular site is influenced by the local geologic settings (site effect) which are not yet taken into account. The importance of site effects is widely recognized and must therefore be accounted for in site-specific earthquake hazard studies. The ongoing projects in Switzerland within the framework of the Swiss National Science Foundation Program 31 (Climate Changes and Natural Hazards) and the national projects of the IDNDR will help to improve our knowledge about local geology and site effects.
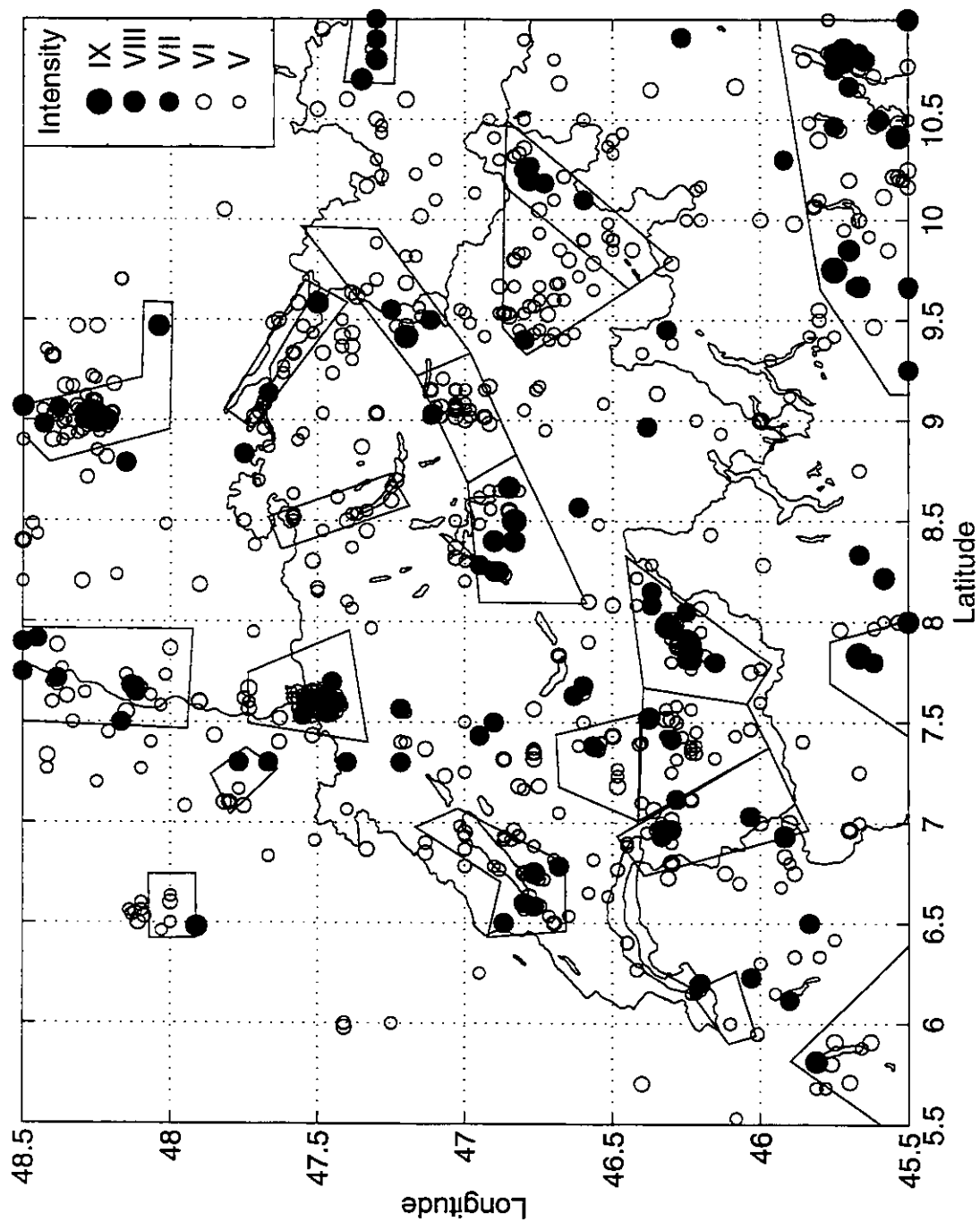
Figure 1.4: Historical seismicity map of Switzerland for the time period of 1300 to 1994. Only earthquakes with an epicentral intensity ≥ V are shown. Superimposed is the geographic distribution of the seismic sources used in the previous seismic hazard study (Sägesser and Mayer-Rosa, 1978).
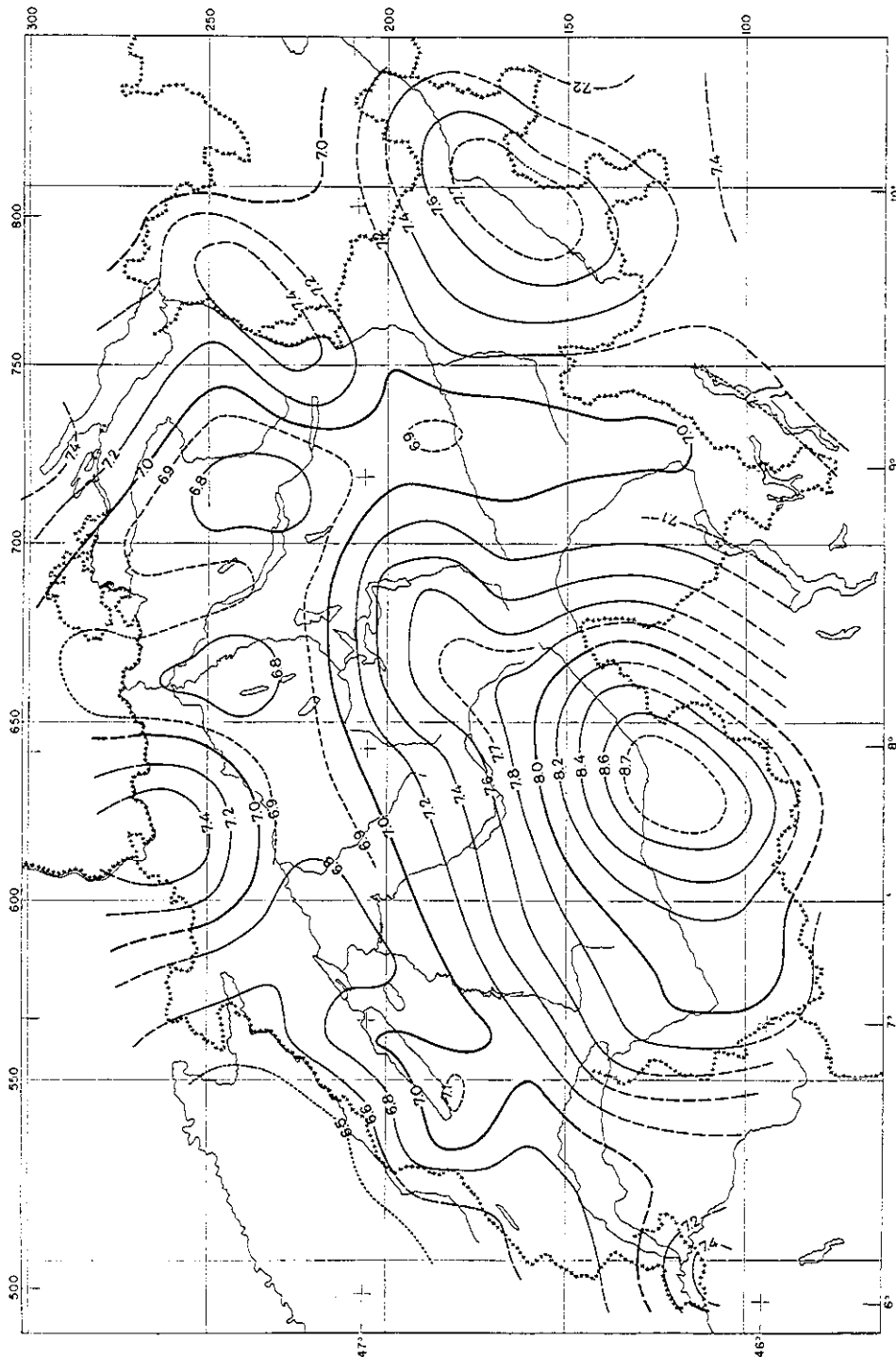
Figure 1.5: Seismic hazard map for Switzerland after Sägesser and Mayer-Rosa (1978). Contour lines of calculated intensities (here to one decimal place that indicates calculated intensity values) are presented for a return period of 1000 years.
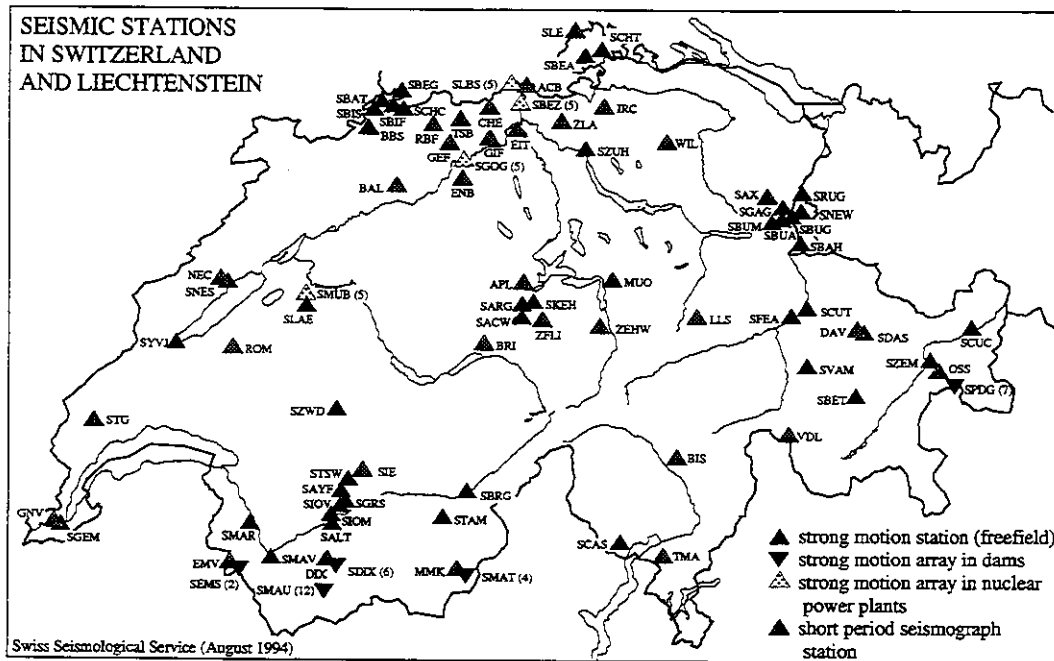
Figure 1.6: Short-period seismograph network and strong motion (accelerograph) stations and arrays in Switzerland (Smit, 1994) (numbers in parentheses give the number of strong motion instruments installed at that site).

Chapter 2

EARTHQUAKE DATABASE FOR SWITZERLAND

Development of an accurate and homogeneous earthquake database is an essential step in earthquake hazard assessment. The earthquake database provides most of the information needed to describe the temporal and spatial seismicity pattern. It is not only location, time and size of historic earthquakes which provide basic information for hazard analysis, but also the uncertainty of the determined parameters must be assessed explicitly and with great care in order to be correctly applied in the hazard calculation. Without an estimate of the accuracy of the assessed parameters, seismic hazard cannot be properly evaluated.

In order to build up an earthquake catalog for this study, macroseismic data as well as instrumental data have been compiled. Based on assessed error estimates of earthquake intensity and location, models had to be defined that represent the distribution of earthquake intensity and location. The compiled database combined with error models provides a description of the seismicity in Switzerland.

2.1 Imprecise Data and Error Models

2.1.1 Macroseismic Intensity Data

Macroseismic intensity is one of the parameters most frequently used to represent ground motion in seismic hazard analysis. It is the only parameter that can be directly assessed for historic earthquakes and therefore contribute valuable data for the seismic hazard analysis (Guidoboni and Stucchi, 1993). An observed damage picture is classified with the application of an intensity scale (in Switzerland at the beginning of this century with the Rossi-Forell scale (Forell, 1880) and more recently with the MSK 64 intensity scale (Medvedev et al., 1965)). The assessed intensity degree is represented by an integer value. Although intensity values are not a priori applicable as numerals, they can be used as such as long as it is assumed that intensity degrees represent equally-spaced ground motion levels.

For most historic earthquakes macroseismic intensity estimates are based on historical documents, which contain descriptions of the observed effects caused by various earthquakes. In some regions in Europe, historic seismological compilations are frequently available, which already contain intensity estimates. The sources of consider-

able disparity in intensity estimates are:

- reports which describe the effects of the earthquake often contain subjective interpretations and they usually neglect to take into account buildings or structures that did not suffer any damage. Therefore, they tend to be "reports of maximum observed effects";

- intensity scales used to classify the observations have been changed over time and vary from country to country. Therefore, intensity estimates cannot be compared with each other before they are converted;

- number and quality of single observations are strongly heterogeneous with respect to time and location of the earthquake.

As a consequence the intensity for historic earthquakes cannot be exactly determined and requires an error estimate. A proper error evaluation of an intensity should indicate an intensity range, e.g. VII to VIII. Sometimes, intensity ranges are represented in half intensity degrees or even smaller units (cf. the Austrian catalog (Lenhardt, 1993), where intensities are given as numerical values to one decimal place), which implies a higher accuracy than actually can be assessed. One aim of the present work is a correct treatment of estimated intensity values and their errors. This is achieved by modelling the uncertainty in intensity estimates by a probability density distribution. The probability distribution has to be assessed from the given intensity values and errors.
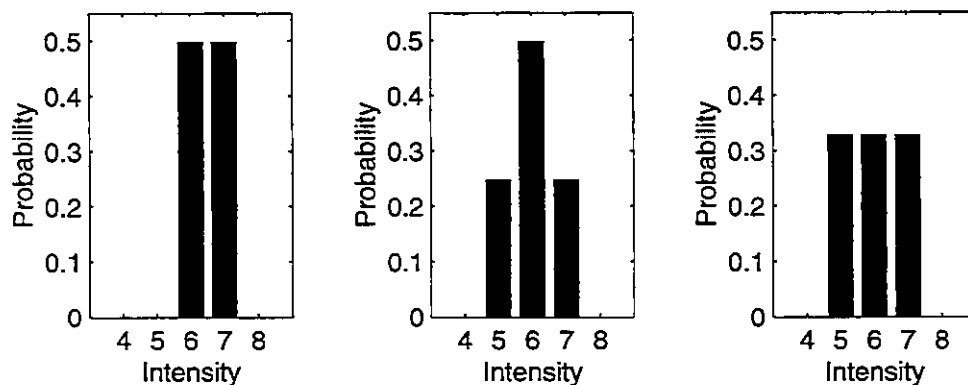

Figure 2.1: Probability distributions for the representation of uncertainties in intensity estimates. For a given intensity of VI to VII, equal probabilities are assumed for intensity VI and VII (left). For a given intensity VI with an error of ± 1 two probability distributions are conceivable (center and right).

Figure 2.1 shows, in order to illustrate the procedure, possible probability distributions for two examples. The first example shows a probability distribution for an intensity ranging from VI to VII (often indicated as 6.5). An equal probability (0.5) is assigned to intensity VI and VII. The second example shows two interpretations of intensity VI with an error estimate of ± 1: in the first interpretation it is assumed that intensity VI is the most likely intensity degree, therefore a higher probability for intensity VI than for intensity V and VII is chosen. In the second interpretation it is assumed that the possible

intensity ranges from V to VII. Therefore, a distribution with equal probability is preferred. These examples illustrate the flexibility of probability distributions to codify uncertainties of intensity estimates. The assessment of appropriate probability distributions is discussed in chapter 2.3.

2.1.2   Earthquake Location

The macroseismic epicenter locations give the most probable location of the highest intensity value of an earthquake. It is obvious that these locations do not have to coincide with the instrumentally determined epicenter, because various factors influence the intensity distribution (e.g. density of the population, surface geology). The macroseismic locations of earthquakes are further affected by the number and accuracy of the reported single observations as well as by the geometric distribution of the observations. In addition, the exact geographic locations of the reported damages of historic earthquakes are often unknown or ambiguous, which yield large errors in the assessment of macroseismic locations.

For recent earthquakes, the errors in the macroseismic epicenter locations are usually only determined by the geometric distribution of single observations. This factor is of little importance for earthquakes located in areas with a high population density, and consequently densely distributed observations.

The accuracy of instrumental locations is determined by:

- epicenter and stations distribution;

- number of phase readings per event;

- accuracy of each phase reading;

- velocity model used for location.

For the best resolved earthquakes the horizontal location error of the present seismic network in Switzerland is on the order of 1-2 km, but it can grow easily to several kilometers, if only few readings are available or if the earthquake occurs outside the recording station network (Kradolfer, 1989).

Instrumental as well as macroseismic locations can be seen as maximum likelihood estimations affected by several parameters as discussed above. In this context a maximum likelihood estimation of the earthquake location can best be modelled by a two-dimensional normal distribution, whose density for circular symmetry with covariance equal 0 is given by (2-1). More explicitly, the probability P that the epicenter lies in an area $(\Delta x \Delta y)$, assuming that the most probable epicenter is at (0,0) and that the standard deviation is σ, is equal to the integral over this area of the probability density function (2-2):

$$f(x_1, y_1) = \left(\frac{1}{2\pi\sigma^2}\right) \exp\left(-\frac{1}{2\sigma^2}\left(x_1^2 + y_1^2\right)\right) \qquad (2\text{-}1)$$

and

$$P\left(\Delta x, \Delta y\right) = \int\limits_{\Delta x \Delta y} f(x, y)\, dx dy \qquad\qquad (2\text{-}2)$$

where

x_1, y_1 point of interest

σ standard deviation (location error)

$\Delta x, \Delta y$ area for which probability is calculated

According to this formulation, there is a probability of 68.3% that the epicenter is within a radius equal to σ around the determined location. Figure 2.2 shows the probability distribution within gridded areas (5 km x 5 km) assuming that the earthquake epicenter is at (x=0,y=0) and the location error is 10 km, respectively 20 km. By this representation, the error in earthquake location can be expressed satisfactorily.
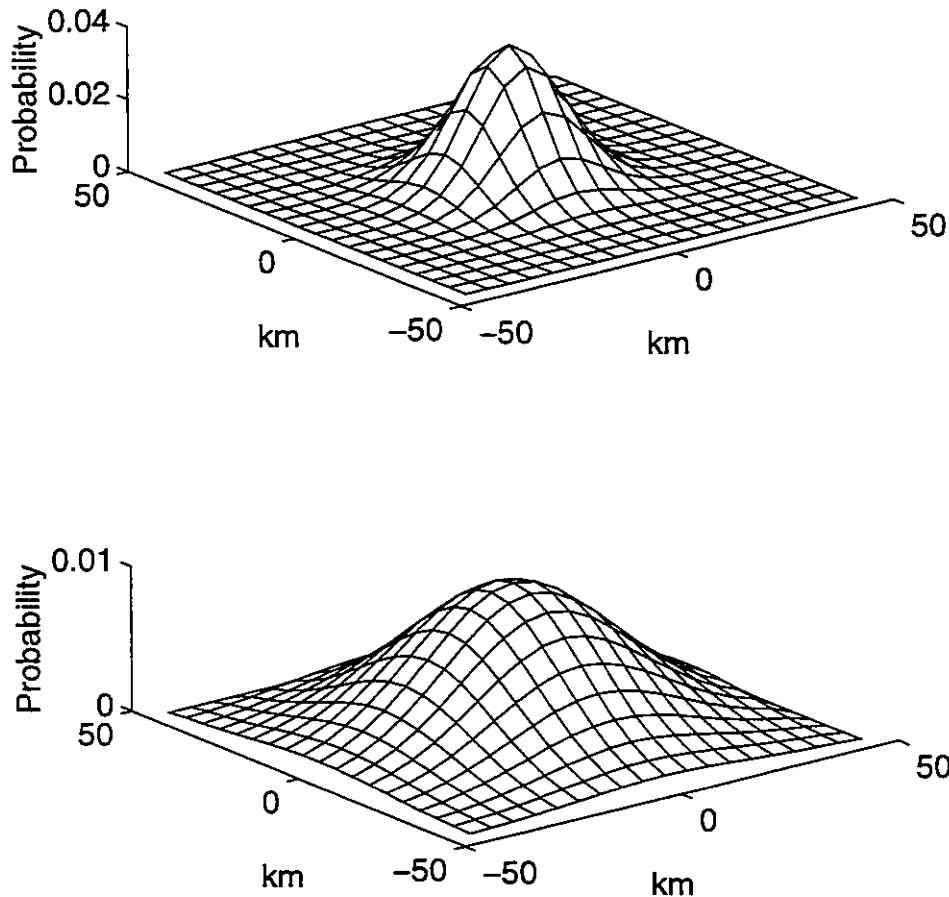

Figure 2.2: Earthquake location probabilities within gridded areas (5 km x 5 km) assuming an epicenter at (x=0,y=0) and a location error of 10 km (top), respectively 20 km (below).

2.2   Earthquake Catalog

The main source of the compilation of the earthquake data catalog is the earthquake database of the Swiss Seismological Service. This database contains not only all instrumentally localized earthquakes since 1974, but also all historic earthquake data which were originally collected for the seismic hazard studies of Switzerland in 1976 (Sägesser and Mayer-Rosa (1978), Mueller and Mayer-Rosa (1980)). This catalog will herein be referred to as the "Swiss Earthquake Catalog" (SEC). The boundaries of the region for the data collection have to extend further than the Swiss territory in order to closely estimate seismic hazard in sites near the Swiss border. The final region encompasses 5.5 to 11.0 longitude East and 45.5 to 48.5 latitude North. A time window from 1300 to 1993 and a magnitude threshold of Ml=2.0 of the instrumentally located earthquakes was applied for the catalog compilation.

The SEC is supplemented, especially in the bordering regions of Switzerland, with entries from the catalog, which was prepared for the joint seismic hazard study for Austria, Germany and Switzerland (Grünthal et al., 1994). This extended catalog will herein be referred as the "Extended Swiss Earthquake Catalog" (ExSEC). For the original sources of the added catalog, which itself is a compilation of various national catalogs, see Grünthal et al. (1994).

Table 2.1: Characteristics of the Extended Swiss Earthquake Catalog (epicenter maps see figures 2.11 and 2.12)

	Before 1990	1900 - 1974	1975 - 1993
Number of Events in total	1708	2125	1921
Number of Events with I≥VI	263	87	7
Number of Events with I≥VII	97	29	1
Maximum Intensity	IX	VIII-IX	VII-VIII

In order to establish the ExSEC, macroseismic and instrumental earthquake data have to be combined into a single earthquake catalog. The identification of duplicate earthquakes reported in the macroseismic data as well as in the instrumental data is an important step when merging two earthquake catalogs. Possible duplicates of the same earthquake were identified by applying a time window filter of 120 minutes. About 300 earthquakes have been marked as possible duplicates. Each of them was checked manually by reviewing the original earthquake catalogs and bulletins. If entries have been identified as belonging to the same earthquake, they were accordingly marked in the

catalog. For some earthquakes, errors could be eliminated that were caused by the transfer of historical seismological compilations and reports into computer files. Table 2.1 shows some characteristics of the ExSEC. Epicenter maps for historic earthquakes are displayed in figure 2.11, for instrumental data in 2.12, respectively.

2.2.1   Macroseismic Intensity Data

The macroseismic intensity data of the Swiss earthquake database are based on historical documents, historical earthquake compilations and on macroseismic surveys of the most recent earthquakes.

Most historic earthquake parameters of the Swiss database stem from the evaluation of existing historical seismological compilations. The most important historical sources are the compilations of Volger (1857), Wanner (1932), Montandon (1942,1953), Sieberg (1940), Sponheuer (1952) and Karnik (1971). Intensity assessment was usually made with the information contained in the historical earthquake compilations. Only for very few earthquakes the original historical documents have been investigated, e.g. for the Basel earthquake in 1356 (Wechsler, 1987). The assessment of earthquake parameters based on reports is a crucial step in the compilation of an earthquake data catalog. It is of great importance not only to assess the earthquake data, e.g. epicentral intensity or location, but also to give an estimate of the accuracy of the assessed parameters. For the determination of macroseismic locations, two basic rules were applied: first, the epicenter was located where the highest damages were reported and second, the mean distance between the highest intensity values is given as a measure of accuracy of the epicenter location. In order to illustrate this strategy, figure 2.3 displays the determined intensities based on the descriptions in Volger (1857) for the event of 7 February 1777. The deduced earthquake epicenter available in the SEC is indicated with a star and the given error of ±2 km is shown by the circle. The SEC gives an epicentral intensity of VII with an error of ±1 degrees for this earthquake. The applicability of probability distributions to model uncertainties of epicentral location and intensity, as proposed in chapter 2.1, is shown in figure 2.4.

In 1878 the Swiss Earthquake Commission was founded. One year later the commission published its first bulletin. The following yearly bulletins contain isoseismal maps for most events that could be felt in Switzerland. The epicenter locations have to be estimated based on the available isoseismal maps. However, if observations for single sites are missing the location error can only roughly be assessed. The macroseismic database gives only for major earthquakes the observed intensity values with their coordinates. For these events the intensity distribution can be redrawn and the epicentral intensity as well as the uncertainty in epicentral location can be reassessed. Since 1960 the estimated site intensities as well as the number of observations are available in the Swiss macroseismic database. This provides the opportunity to redraw each isoseismal map when needed.

For earthquakes since 1989 the complete information for each single observation is compiled in computer files. The intensities are assessed following a standardized procedure. Each report is interactively codified by a computer program. Since the program

allows qualitative informations (e.g. "felt strongly" or the activity of the observer was "walking") the original information can be recorded. The codified observations are supplemented by name and zip code of the town where the observation was made. For adding geographical coordinates to the observations a geographic reference file has been built up. The program ADDCOR performs this step interactively to avoid mistakes caused by typing errors of zip codes. For each earthquake the output of this procedure is a file which contains intensity, coordinates and number of observations on which the intensity is based. Because the primary informations of the reports are also saved in the database a re-evaluation of the intensity assessment can be easily done. Therefore not only isoseismal maps can be reconstructed, but also the assessed intensity values can be re-evaluated.
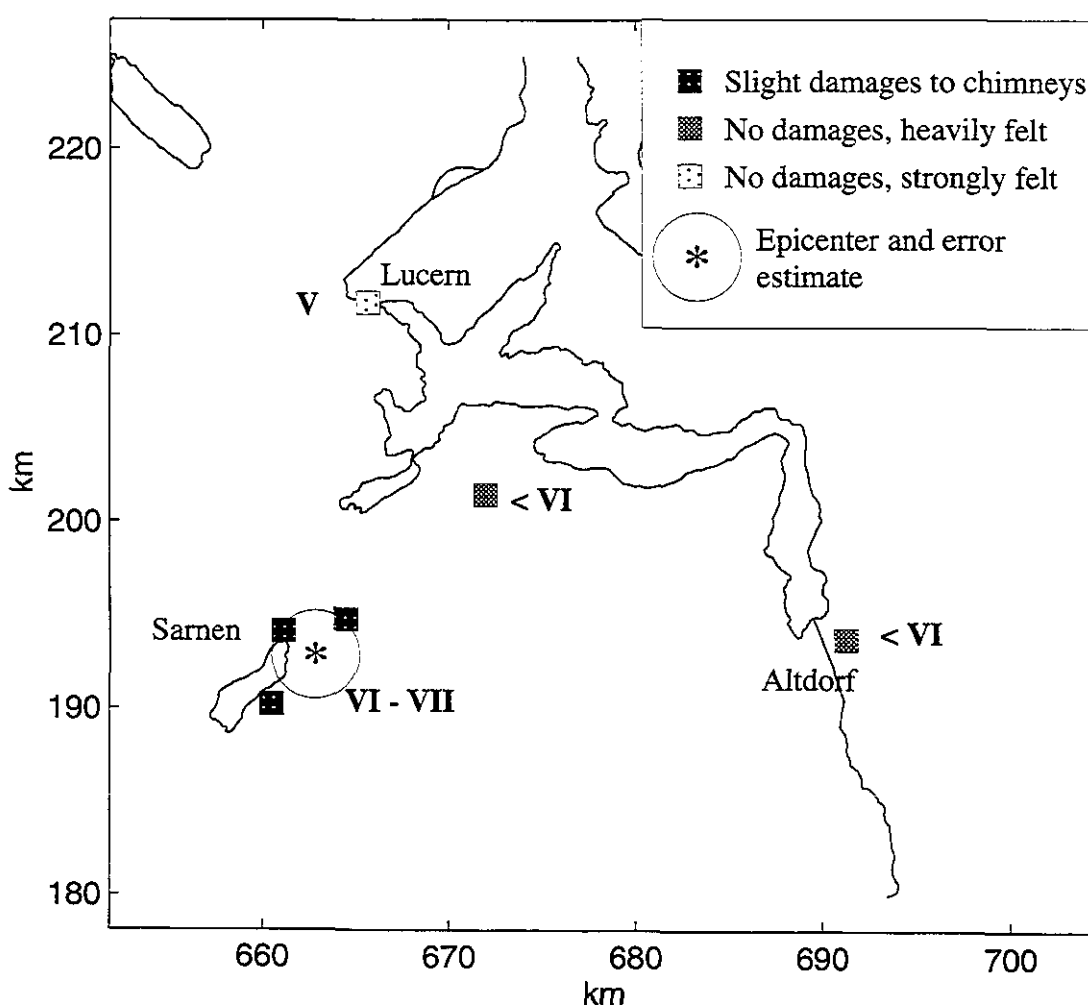

Figure 2.3: Locations described in the seismological compilation by Volger (1857) for the earthquake on 7th February 1777. For these locations intensity values have been assigned.
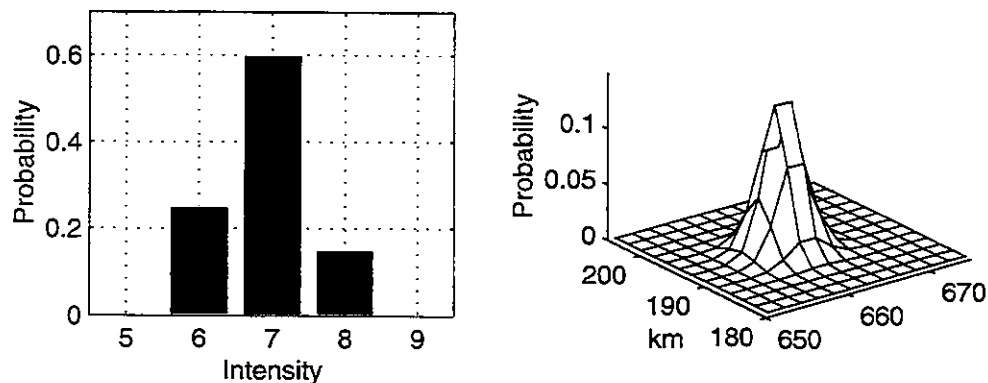
Figure 2.4: Probability distribution for the epicentral intensity and for the earthquake location within a gridded area of 2 km x 2 km for the earthquake of 1777/02/07.

2.2.2   Instrumental Data

In Switzerland instrumental data are available since 1911 when the first seismograph was installed near Zurich. Up to 1975, most of the locations of the Swiss Seismological Service are based only on 4 stations resulting in quite erroneous locations. Since 1964 the earthquake database contains additional locations that were determined by the "Bureau Central International de Séismologie" in Strasbourg (BCIS) and by the International Seismological Centre (ISC) in Edinburgh and later in Newbury (U.K.). The quality of these locations varies strongly in time (see chapter 2.3.2). With the deployment of the new Swiss seismograph network in 1975 reliable locations can be determined for earthquakes occurring within the network.

The location error for instrumental data is usually calculated with the covariance matrix of the calculated and observed arrival times (cf. Lee and Lahr, 1975). These error estimates depend on the number of readings used and on the damping values applied in the inversion. The calculated location errors should only be taken as a rough estimate and have to be compared with the number of readings used for the location, because the location algorithm gives meaningless small errors when only few arrival times are used. A more accurate determination of the error can be achieved by comparing the calculated locations of quarry blasts with their well-known positions. Kradolfer (1989) has relocated 20 quarry blasts and found that the errors in the locations are 2.3 ± 1.2 km in horizontal direction and 5.5 ± 4.4 in vertical direction. These error estimates can be taken as lower limits for instrumentally located earthquakes since 1975.

2.3 Assessment of Error Models

The proposed modelling of uncertainties in earthquake size and location by means of probability distributions (see chapter 2.1) requires the assessment of error estimates. A standard deviation for the earthquake location has to be defined in order to be able to use it in the error model. The uncertainty in the earthquake size can be modelled either with a discrete probability distribution for epicentral intensities or with a standard deviation for magnitudes.

2.3.1 Error Models for Epicentral Intensities

It was not within the scope of this work to reassess all the macroseismic intensities available in the ExSEC, but it is essential to have knowledge about the accuracy of the given intensities. The ExSEC itself gives error estimates for epicentral intensities in the form of error classes. These five classes are:

(1) intensity error of 0 degrees,

(2) intensity error of ±0.5 degrees,

(3) intensity error of ±1.0 degrees,

(4) intensity error of ±2.0 degrees, and

(5) intensity error is unknown.

Figure 2.5 shows for earthquakes with epicentral intensity greater than IV the distribution of error classes in four different time periods. It can be recognized that the most frequent error estimate before the 17th century is ±1.0 intensity degrees (class 3), and after the 17th century ±0.5 intensity degrees (class 2). The number of earthquakes with no intensity error information (class 5), which stems from earthquake catalogs where no error estimates are indicated (e.g. the Austrian catalog (Lenhardt, 1993)) is increasing with time.
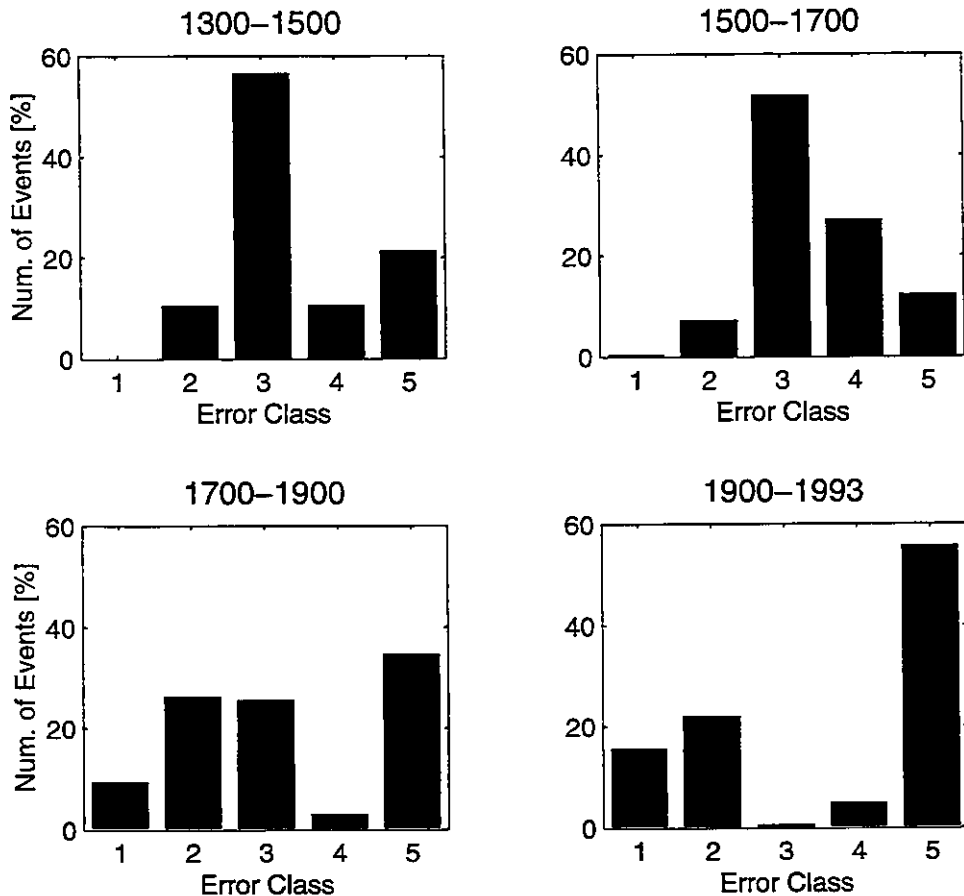
23

Figure 2.5: Distribution of the error classes for epicentral intensities (>IV) for single time periods as indicated in the catalog. The five error classes are: 1=error of 0, 2=error of ±0.5, 3=error of ±1.0, 4=error of ±2.0 and 5=error unknown.

The significance of these error classes can only be understood in combination with the original historical descriptions. Therefore some of the major earthquakes (with epicentral intensity ≥ VIII) have been reviewed for the present study. In order to illustrate the uncertainties involved in the assessed intensities and locations from historic earthquakes, a typical historical description of an event in the eastern part of Switzerland is given:

> "On the 20th of December 1720 at 5.30 p.m., several regions of Switzerland, as e.g. Thurgau, St. Gallen and Lake of Constance were shaken. Some houses collapsed in Appenzell, Reinegg and Lindau. The shaking lasted only for one minute and was accompanied by thunders, a warm wind and a sulfuric scent. The shaking was also felt in Zurich, but only slightly." (translated from Volger, 1857)

The reported damages indicate a maximum intensity of degree VIII. This is the actual intensity given in the SEC. However, an earthquake of intensity VIII would cause damages of degree 2 to 3 (i.e. slight to moderate structural damage (Grünthal, 1993)) to many buildings, which are not described in Volger (1857). Therefore, neither a com-

plete picture of the actual damages is assessable from this historical description nor can the epicentral intensity be accurately estimated. The method of indicating probability distributions provide the possibility to represent this uncertainty of epicentral intensity estimates. An intensity range from VII to VIII with equal probabilities for both intensities is reasonable for this earthquake. In the ExSEC the uncertainty of epicentral intensity is reduced to an error class, in this example to an error of ±1 intensity degrees. With probability distributions for epicentral intensities the complete range of uncertainties can appropriately be represented.

The example above shows a general tendency of epicentral intensities given in the ExSEC. They tend to represent maximum observed damages for historic earthquakes. This implies that intensity estimates for historic earthquakes are usually an upper estimation of epicentral intensity. This conclusion is not valid if the epicenter location is not known accurately, because the epicentral intensity can be underestimated, since there are possibly no observations in the epicentral area. These two controversial aspects influence the uncertainty of epicentral intensity estimates.

A scheme has been developed to convert intensity error classes as given in the ExSEC into probability distributions. It takes the following conditions into account:

- general tendency of reported maximum damages,

- size of epicentral intensity, and

- probable underestimation of epicentral intensities due to location errors.

The applied conversion scheme is displayed in figure 2.6, the exact probability values are summarized in table 2.2. Reasons for the individual probability distributions are:

- Class 1: Intensity error of 0 degrees. The intensity could be assessed without severe doubts. This is valid if a large number of damage descriptions are available in the epicentral area. Consequently, the determination of the earthquake location is also quite accurate. The tendency of reporting maximum damages is accounted for by an asymmetric probability distribution. The determined epicentral intensity is assumed to be almost correct (with a probability of 80%) (figure 2.6a).

- Class 2: Intensity error of ±0.5 degrees. There are some doubts about the size of the assessed intensity, but an error of ±1 is too high. An error of ±0.5 degrees indicates an intermediate accuracy between an error of 0 degrees and an error of ±1 degrees. Consequently, the adopted probability (70%) of the assessed intensity lies also within that range (figure 2.6b). If the intensity in the ExSEC is given in half intensity degrees, the uncertainty is expressed twice. In these cases equal probabilities are assigned to the two corresponding intensity degrees.

- Class 3: Intensity error of ±1 degrees. The assessed intensity is uncertain. Nevertheless, the estimated intensity is assumed to be the most probable intensity degree. Two sources determine the uncertainty of the intensity estimates: 1) the intensity estimate is uncertain due to rare, contradictory or ambiguous historical reports, and 2) widely-distributed intensity observations impede an accurate determination of epicenter location and of epicentral intensity. If the earthquake location is accurate

(location error $\leq$10 km), an asymmetric probability distribution is assumed to take the tendency of reporting maximum effects into account (figure 2.6c). A probability of 60% is then assigned to the indicated intensity. If the location error is >10 km, the tendency of reported maximum damages is probably compensated by underestimating the true epicentral intensity since the intensity decreases by approximately one degree for a distance of 20 km. In these cases, a symmetric probability distribution is chosen (figure 2.6d).

- Class 4: Intensity error of $\pm$2 degrees. The same arguments as for an intensity error of $\pm$1 degrees are valid, but the possible range of intensities is wider. Again, an asymmetric probability distribution is assumed if location errors are small ($\leq$10 km). A probability of 50% is assigned to the indicated intensity (figure 2.6e). A symmetric probability distribution is defined if location errors are >10 km. Then a probability of 50% is assigned to the given intensity. Two intensity degrees higher and lower are also assumed to be possible, but with a very small probability (5%) (figure 2.6f).

- Class 5: The intensity error is unknown. If the intensity error is unknown, the most frequently observed intensity error at that time indicated in the ExSEC (see figure 2.5) is attributed to the earthquake. These "default" errors are $\pm$1 degrees before the 17th century and $\pm$0.5 degrees afterwards. These "default" errors are treated in the way discussed above.

Table 2.2: Probability distributions for the uncertainty in epicentral intensity (loc. er. = epicentral location error)

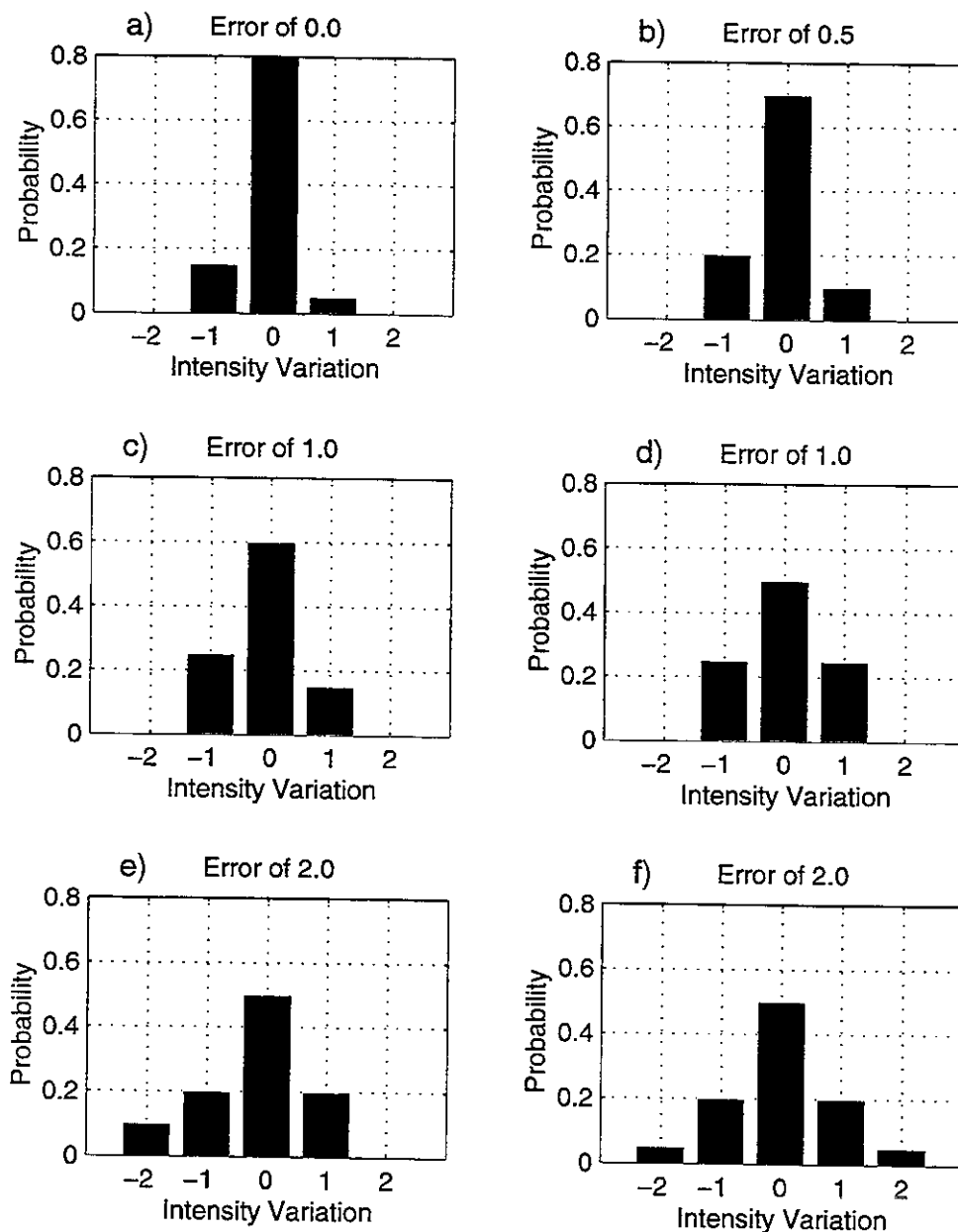| Intensity error	Prob. of I_0	Prob. of I_0+1	Prob. of I_0-1	Prob. of I_0+2	Prob. of I_0-2
0	0.8	0.05	0.15	0	0
$\pm$0.5	0.7	0.1	0.2	0	0
$\pm$1.0	0.6	0.15	0.25	0	0
loc. er. >10 km	0.5	0.25	0.25	0	0
$\pm$2.0	0.5	0.2	0.2	0	0.1
loc. er. >10 km	0.5	0.2	0.2	0.05	0.05

26

Figure 2.6: Conversion scheme for intensity errors into probability distributions. Probability distribution for: a) error of 0, b) error of ±0.5, c) error of ±1 and location error ≤10 km, d) error of ±1 and location error >10 km, e) error of ±2 and location error ≤10 km, and f) error of ±2 degrees and location error >10 km.

Intensities represented in the ExSEC by decimal values are also converted into probability distributions. Decimal intensity values stem from the conversion of magnitudes into intensities and from the Austrian earthquake catalog (Lenhardt, 1993), where the authors calculated epicentral intensities based on the distribution of isoseismals. These intensity estimates are proportionally distributed to the corresponding intensity degrees, e.g. a value of 7.25 yields an intensity VII with a probability of 75% and to an intensity

VIII with a probability of 25%. The intensity error is treated in a similar manner. In order to illustrate this procedure, figure 2.7 shows two examples, whereby the location error is assumed to be less than 10 km. The first example (figure 2.7a) displays the probability distribution of an intensity 7.5 with an error of ±1 degrees. The obtained distribution shows a 80% probability that the intensity was VII or VIII. In the second example (figure 2.7b), the probability distribution of an intensity 7.2 with the same error is displayed. An asymmetric distribution is obtained with the highest probability for intensity VII. Nevertheless, both distributions cover the intensity range from VI to IX which represents the uncertainty of the intensity estimates.
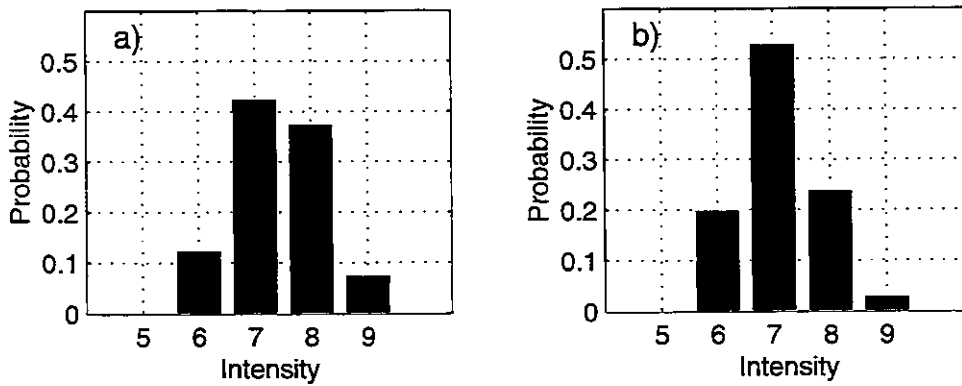
Figure 2.7: Two examples of probability distributions if the intensity values are given by decimal values. a) Probability distribution of an intensity 7.5 with an error of ±1 degrees, and b) probability distribution of an intensity 7.2 with an error of ±1 degrees.

2.3.2   Error Models for Magnitudes

Errors in magnitude estimations are best characterized by standard deviations. In the ExSEC, magnitude estimations are only available for instrumentally-determined earthquakes. Earthquakes with no magnitude estimations (about 3500 earthquakes in the ExSEC) have to be calculated on the basis of epicentral intensity estimates. Formulas to convert intensities into magnitudes have been proposed for Europe (2-3) and for Switzerland (2-4) (Karnik, 1969):

$$M = 0.5I_0 + 1.8 \qquad\qquad (2-3)$$

$$M = 0.67I_0 + 0.3 \qquad\qquad (2-4)$$

where

M magnitude

I_0 epicentral intensity

The formula proposed for Switzerland (2-4) has been defined for epicentral intensities ranging from VI to VII, since no other data were available at that time. This formula

will not be considered here, since it covers only a narrow intensity range. Figure 2.8 displays observed magnitudes versus intensity estimates available in the ExSEC. Superimposed are the relation proposed by Karnik (1969) for Europe (dashed line) (equation 2-3). The relation by Karnik results in higher magnitudes than observed. This is not surprising since a large amount of data used by Karnik stems from deeper earthquakes (assumed to be below 30 km). Earthquakes in Switzerland are above 30 km only in the Alpine foreland and are even shallower in the Alps. The determined relation for Switzerland (equation 2-5 and solid line in figure 2.8) gives, therefore, smaller magnitudes for the same intensity than the relation by Karnik:

$$M = 0.5I_0 + 1.5 \qquad\qquad (2\text{-}5)$$

This simple formula is quite appropriate for taking scatter and accuracy of the data into account. The standard deviation of the calculated magnitudes is 0.4 (and of the calculated intensity 0.8, respectively). A standard deviation of 0.4 will, therefore, be applied in hazard calculations for all converted magnitudes.
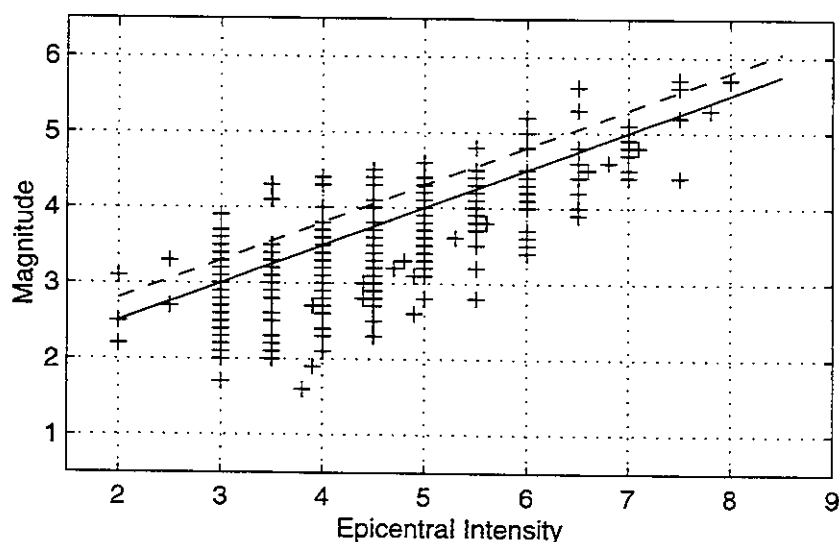

Figure 2.8: Magnitude versus epicentral intensity. Crosses show earthquakes where intensity and magnitude are given. The dashed line represents the formula proposed for Europe (Karnik, 1969), while the solid line represents the formula used in this study.

2.3.3 Error Models for Earthquake Location

Figure 2.9 shows horizontal location errors at different time periods as indicated in the catalog. The number of earthquakes with large errors are decreasing over time as expected. In the time period of 1300 to 1500 more than 50% of the earthquakes have location errors of 50 km and more; for the period of 1700 to 1900 the number decreases to about 10%. Comparison of macroseismic and instrumental determined locations provides a further possibility to check the uncertainties of earthquake locations. For 131

earthquakes since 1900 macroseismic and instrumental locations have been determined. The differences between the two locations are shown in figure 2.10. The mean difference of the locations of the 131 earthquakes is 11.7 km with a standard deviation of the same size. Earthquakes with differences greater than 23.4 km (mean difference plus one standard deviation) have been manually checked. Thereby, location errors were detected. Corrections of these locations (indicated by arrows in figure 2.10) changed the mean difference slightly (to 10.5 km) and reduced the standard deviation significantly (to 7.0 km).

Some earthquakes do not have any error estimates at all. Therefore, a "default" error has to be estimated for these earthquakes. Based on the above discussion a minimum error of 10 km is reasonable for events before 1900. For the time period of 1900 to 1974 a minimum error of 5 km is assigned for macroseismic as well as instrumental data. For the period of 1974 to 1993 the minimum error of instrumental locations is set at 2.5 km.
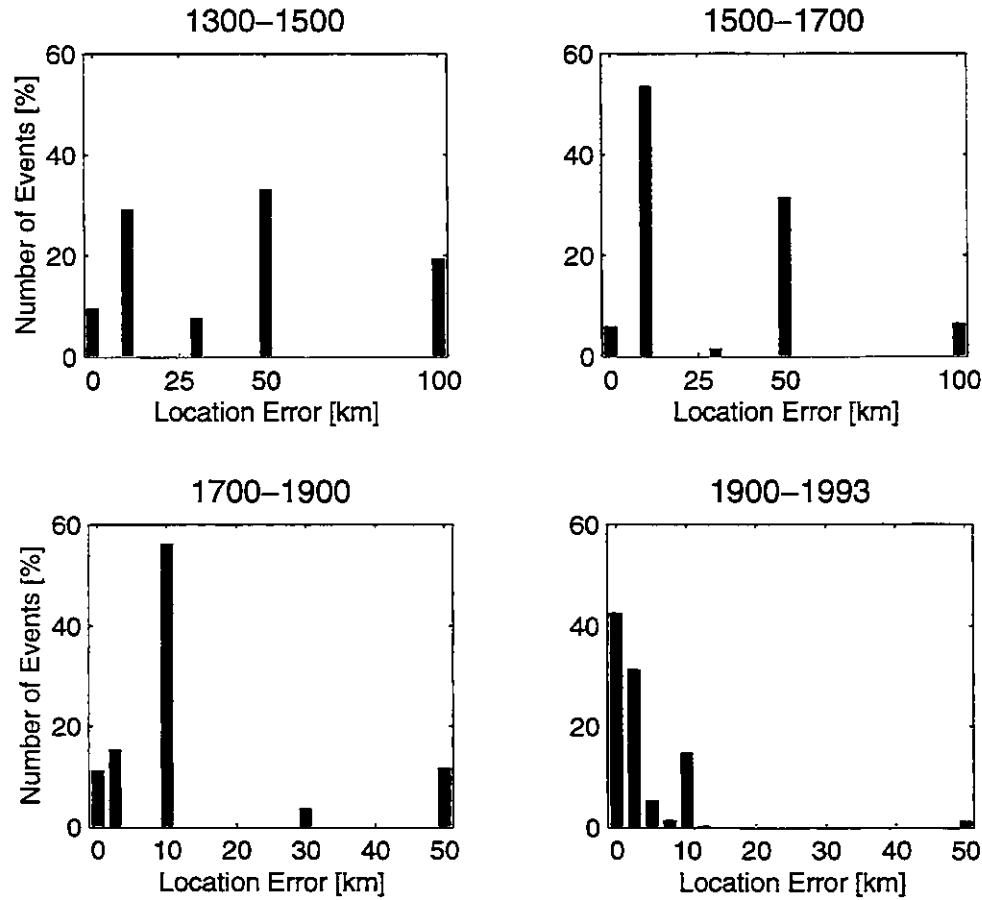

Figure 2.9: Distribution of the horizontal location errors for single time periods as indicated in the earthquake catalog.
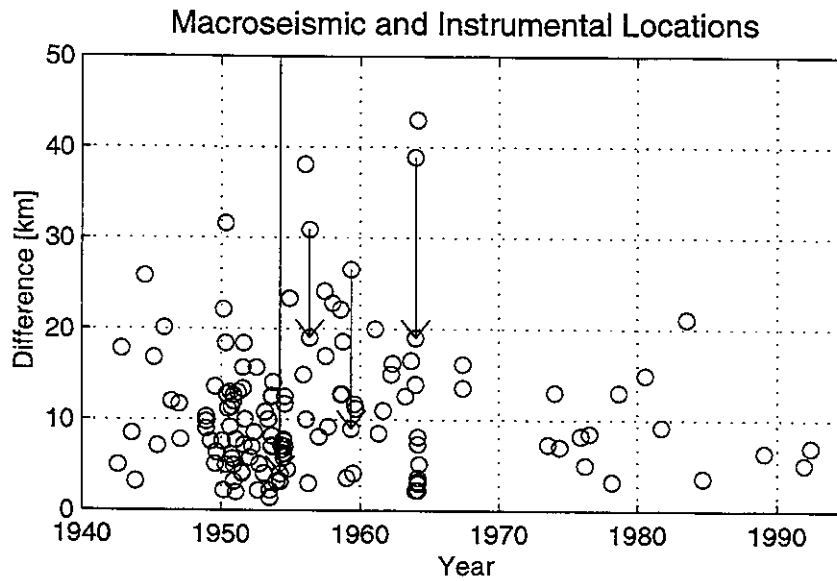
Figure 2.10:Differences between macroseismically and instrumentally determined locations. Errors which have been detected and corrected are indicated by arrows.

2.4   Seismicity

The error models introduced for earthquake locations permit to display historic epicenter maps which take the location uncertainty into account. In order to calculate such epicenter maps, which in this study are called "diffused epicenter maps", the probabilities of all events in a given area are summarized. The probability that the location of a single event is within a given area is calculated by assuming a two-dimensional normal distribution (see chapter 2.1.2). Figure 2.11a shows the "diffused epicenter map" for earthquakes (between 1300 and 1993) with epicentral intensity $\geq$V using gridded areas of 5 km x 5 km. The mean number of earthquakes localized in each area element of the grid is calculated. For comparison, an epicenter map of the same events, but without accounting for the uncertainty is also shown (figure 2.11b).

The "diffused epicenter map" reveals a more correct picture of historical seismicity. Regions with a high seismic activity in the past, i.e. with a high probability that events have occurred, can clearly be distinguished from regions with low seismic activity. Three regions with an increased historical seismicity (more than 1 event per 5 km x 5 km) can be recognized:

- the region of Basel (which is the southward continuation of the Rhinegraben into the Jura) and the Dinkelberg, with a southwest strand to Solothurn;

- the central and the adjoining western Valais and

- the region which extends from central Switzerland to Glarus and Grisons.

Regions with moderate seismic activity are found:

- in the region following the Rhine from Chur to Schaffhausen and then turning south towards Zurich;

- in the Engadine, and

- in the region around the lake of Neuchâtel, which extends to the southeast and joins the active region of the Valais.

This pattern of historical seismicity is confirmed by the instrumental recorded seismicity (figure 2.12). Again, regions with higher seismic activity, i.e. the Valais, the eastern part of Switzerland with Grisons and the Rhine Valley from Chur to the Lake of Constance are visible. The regions of Basel and central Switzerland do not show such a pronounced activity as in the historical seismicity. However, regions with high seismic activity coincide well with the observed historical seismicity.

The same method of diffused epicenters is applied to map the released seismic energy. Therefore, if no magnitude is available, epicentral intensities are converted into magnitudes with the formula (2-5). The corresponding energy is calculated using a log-linear formula (2-6) (Gutenberg and Richter, 1956).

$$\log E = 4.8 + 1.5 M_S \qquad (2-6)$$

where

E Seismic energy in Joules

M_S Surface magnitude

The seismic energy is calculated for gridded areas of 5 km x 5 km and displayed as yearly energy rates per square kilometer. For the time period of 1975-1993 (figure 2.13a), the energy release is distributed over Switzerland, but the major events (with magnitudes $\geq$4.0) can clearly be seen. The energy map for the time period of 1850-1974 (figure 2.13b) shows the pronounced energy release of the Valais, which has been the most active region over the last 125 years. The energy map for the time period 1300-1850 (figure 2.13c) is governed by the biggest historic earthquakes, e.g. the event of Basel in 1356 and the events in central Switzerland of 1601 and 1755. The map of the differences in the yearly energy rates between 1975-1993 and 1300-1974 (figure 2.13d) reveals a large area where energy rates are almost equal, i.e. that the seismic energy release is constant in time. Red and yellow zones show regions, where in the last 19 years the energy rate was higher than in earlier times; blue zones indicate regions, where in the last 19 years the energy rate was lower.

The focal depth distribution along two profiles for well-constrained earthquakes (localized with at least 8 stations and with observations covering an azimuth of more than 180 degrees) is displayed in figure 2.14. In the Alpine foreland the earthquakes are distributed over the entire crust. In the Alps the focal depths are restricted to the upper 10-15 km of the crust (Deichmann and Rybach (1989), Deichmann and Baer (1990), Roth et al. (1992) and Maurer (1993)). Deichmann (1992) explained the deeper earthquakes in

the Alpine foreland with an increased pore pressure in the lower crust that, due to a decrease in the limiting strength, allows for brittle faulting instead of ductile deformation. Figure 2.15 gives the depth distribution in percentage of the number of events. This information will be used in the seismic hazard analysis (see chapter 5).
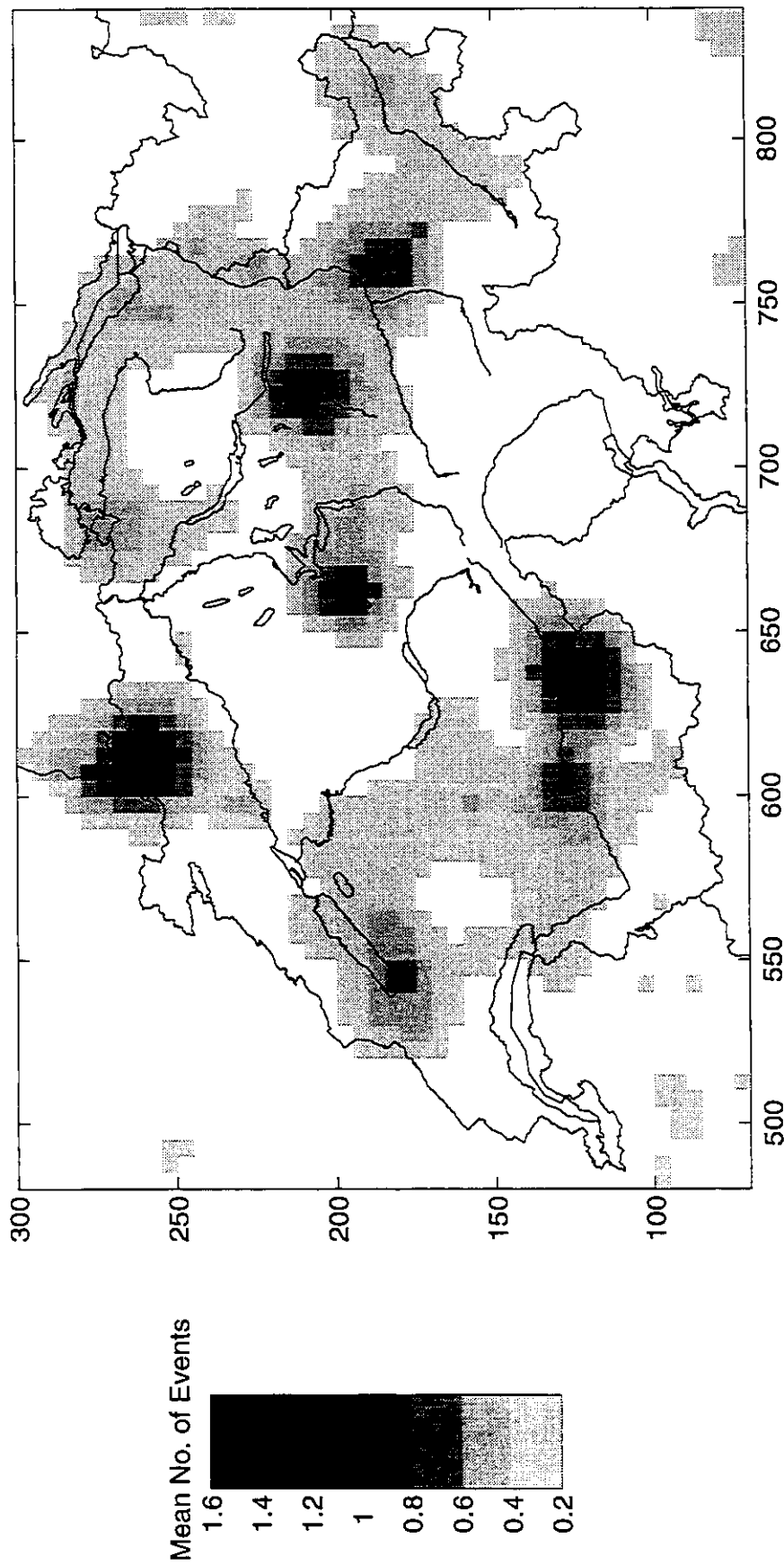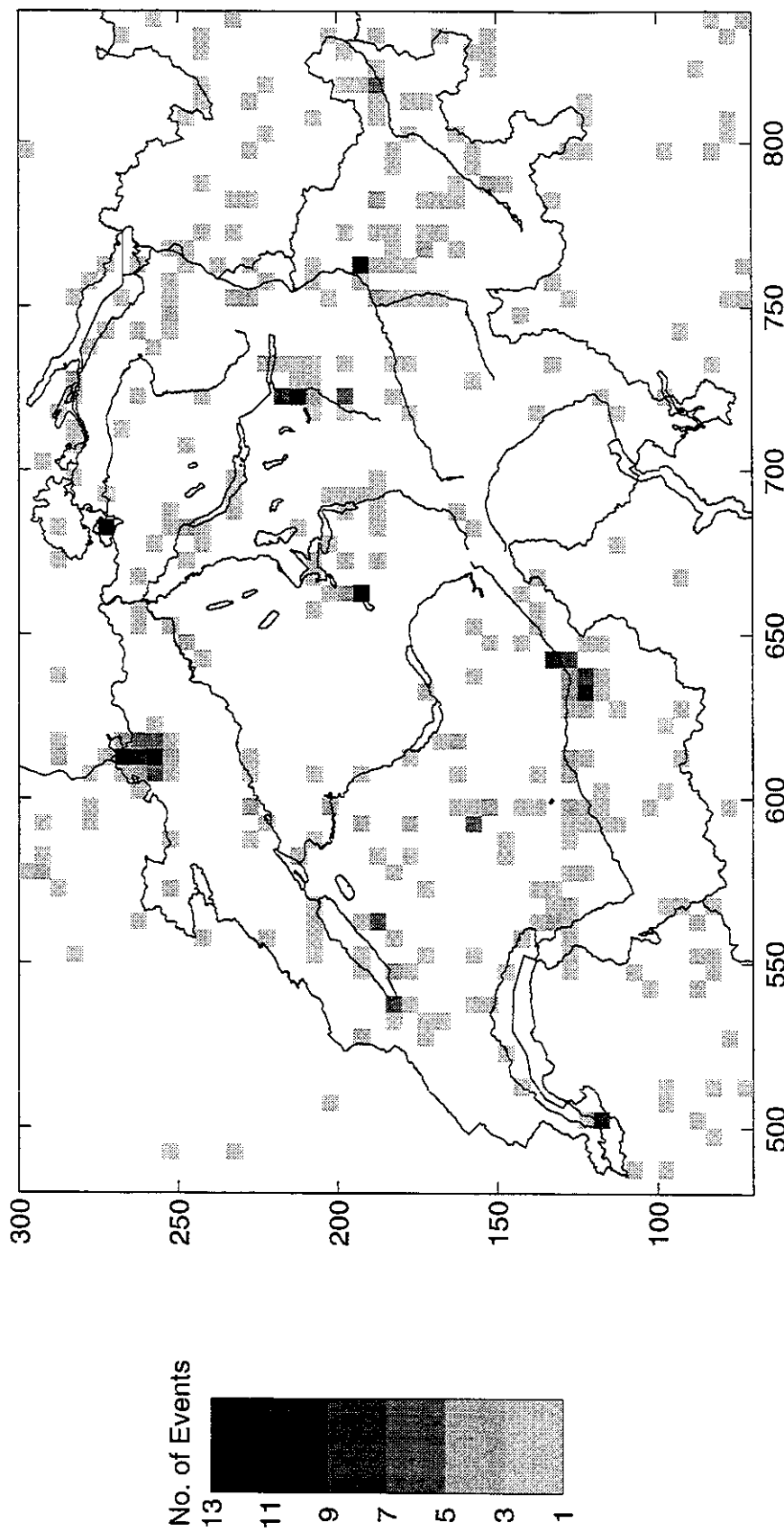
Figure 2.11:a) "Diffused epicenter map" of earthquakes with intensities ≥V from 1300 to 1993. The mean number of earthquakes localized within gridded areas of 5 km x 5 km is given. The location error indicated in the catalog is considered.
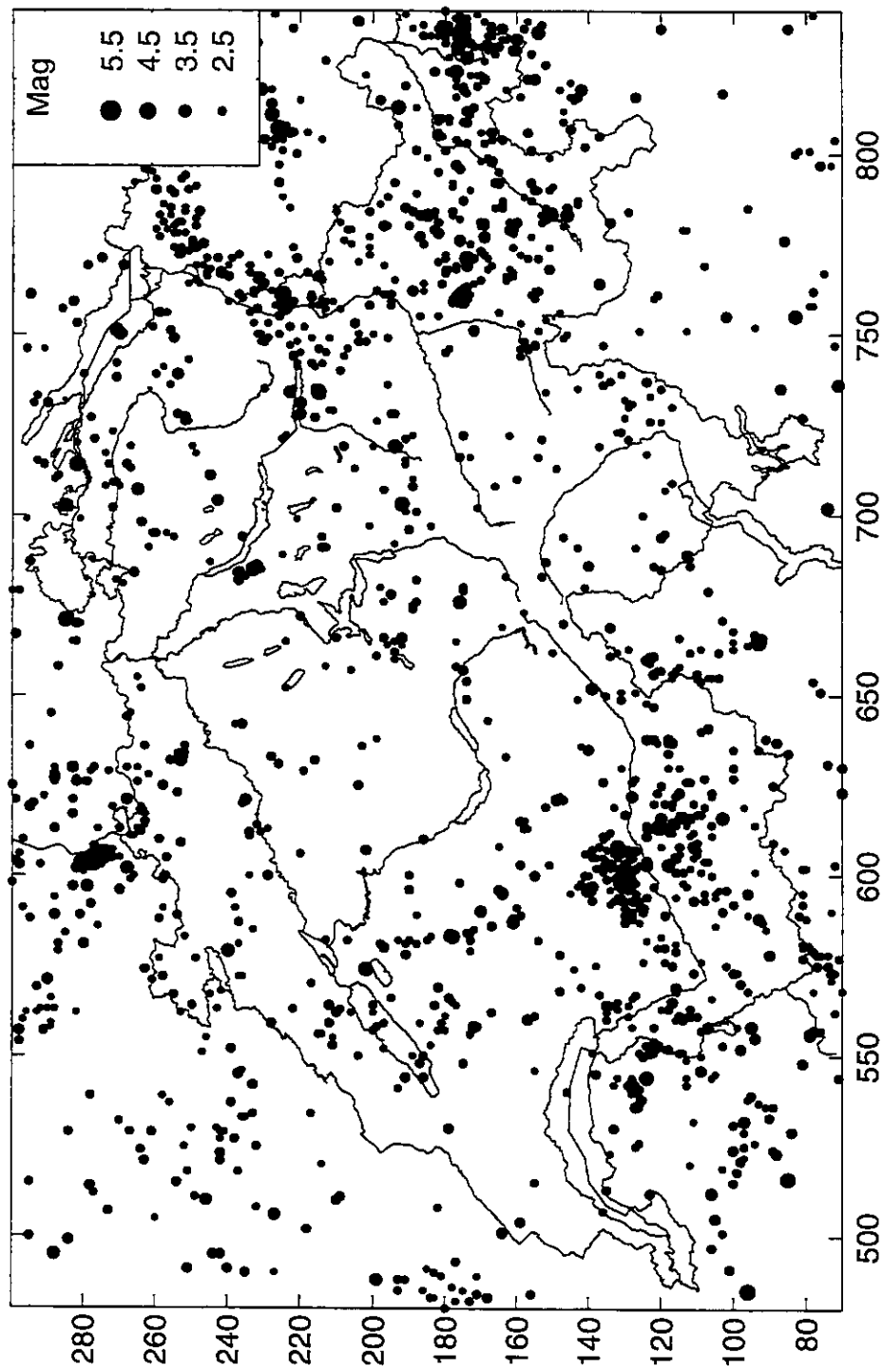
Figure 2.11:b) "Diffused epicenter map" of earthquakes with intensities ≥V from 1300 to 1993. The mean number of earthquakes localized within gridded areas of 5 km x 5 km is given. The location error indicated in the catalog is not considered.

Figure 2.12:Epicenter map of the instrumental data of 1975-1993 in Switzerland.
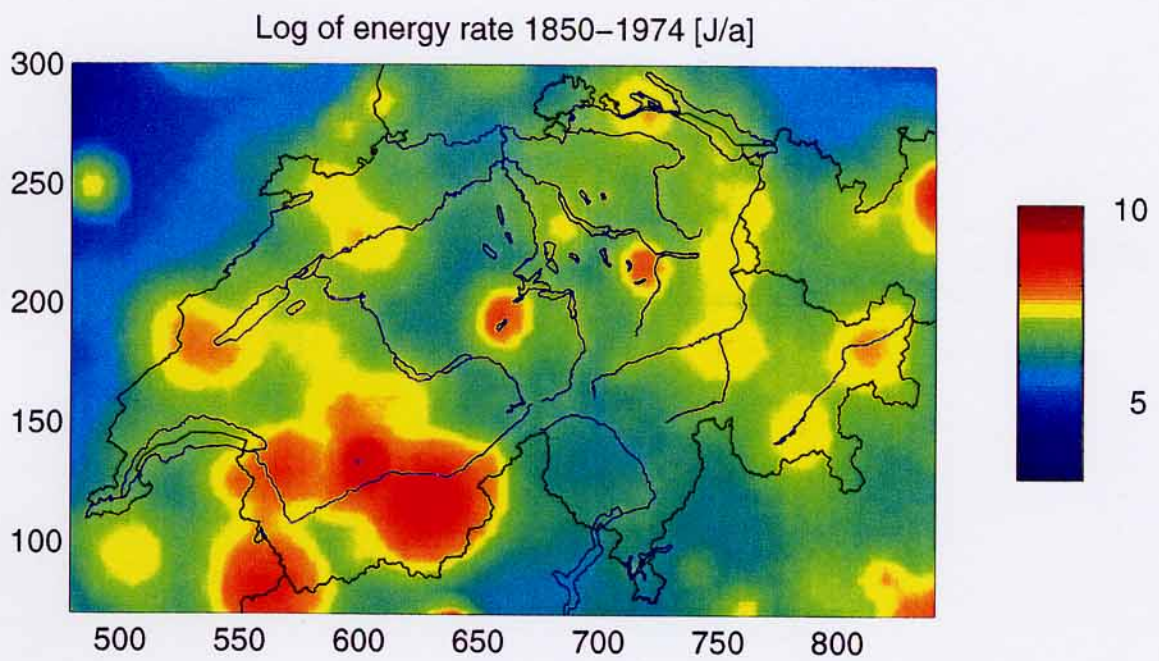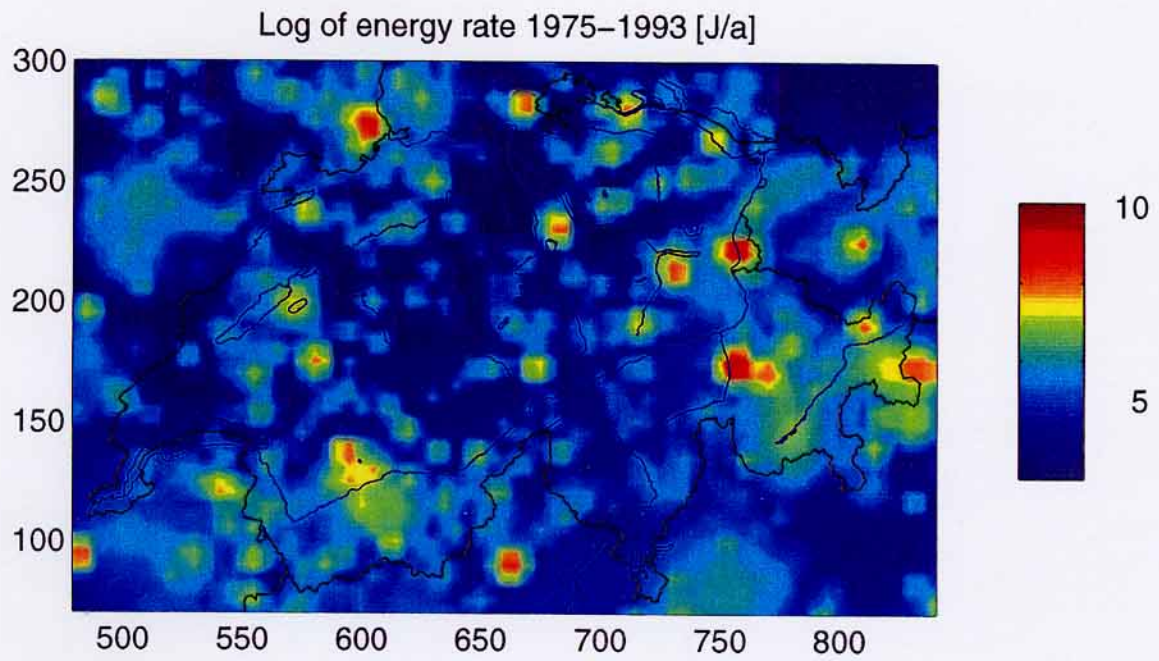The magnitude range is 2.5 to 5.5

36

Figure 2.13: Yearly energy release per square kilometer: a) for the instrumental time period (1975 - 1993), and b) for the historical time period 1850 - 1974.
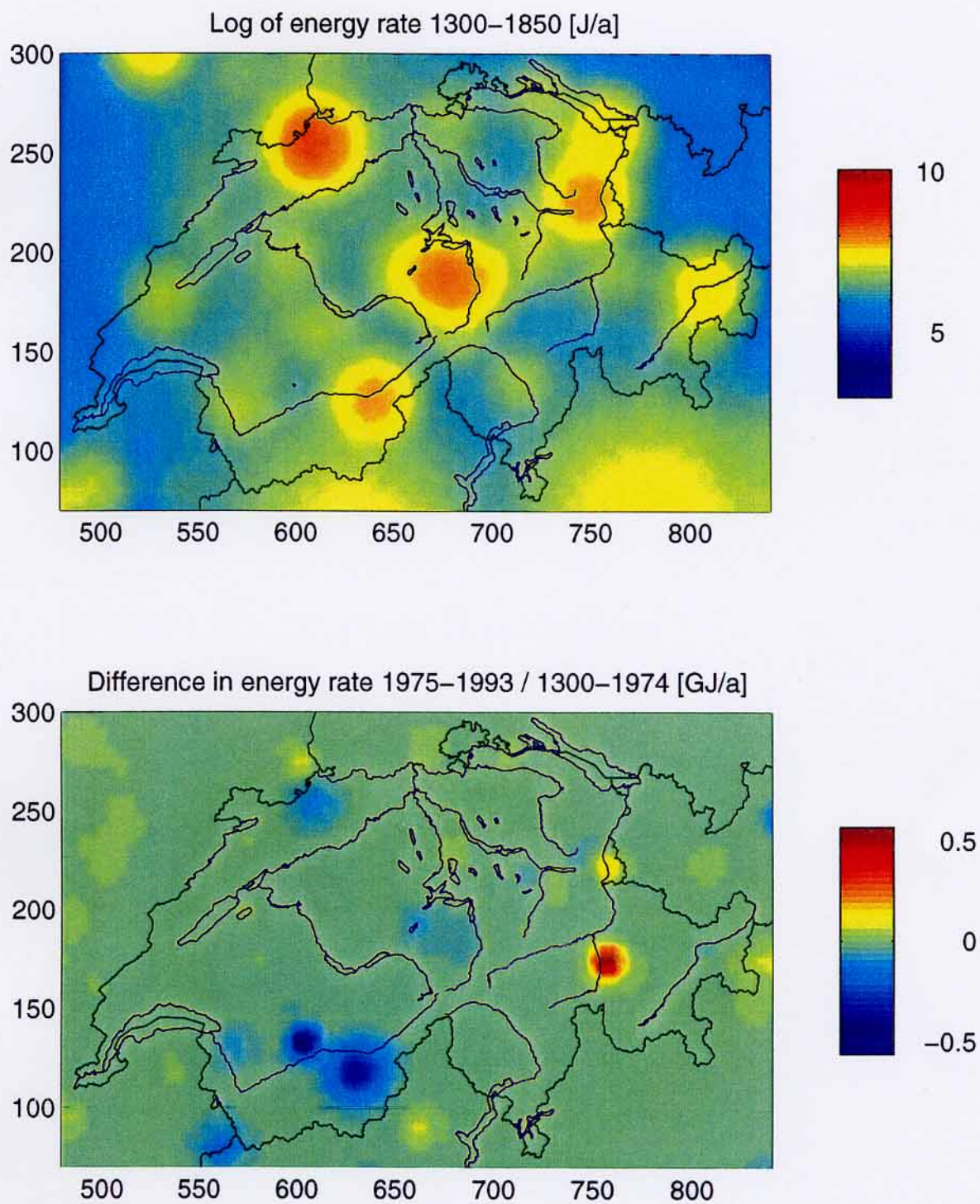
Figure 2.13: Yearly energy release per square kilometer: c) for the historical time period 1300 - 1850, and d) differences in the yearly energy release rates for the instrumental time period compared to the historical time period.
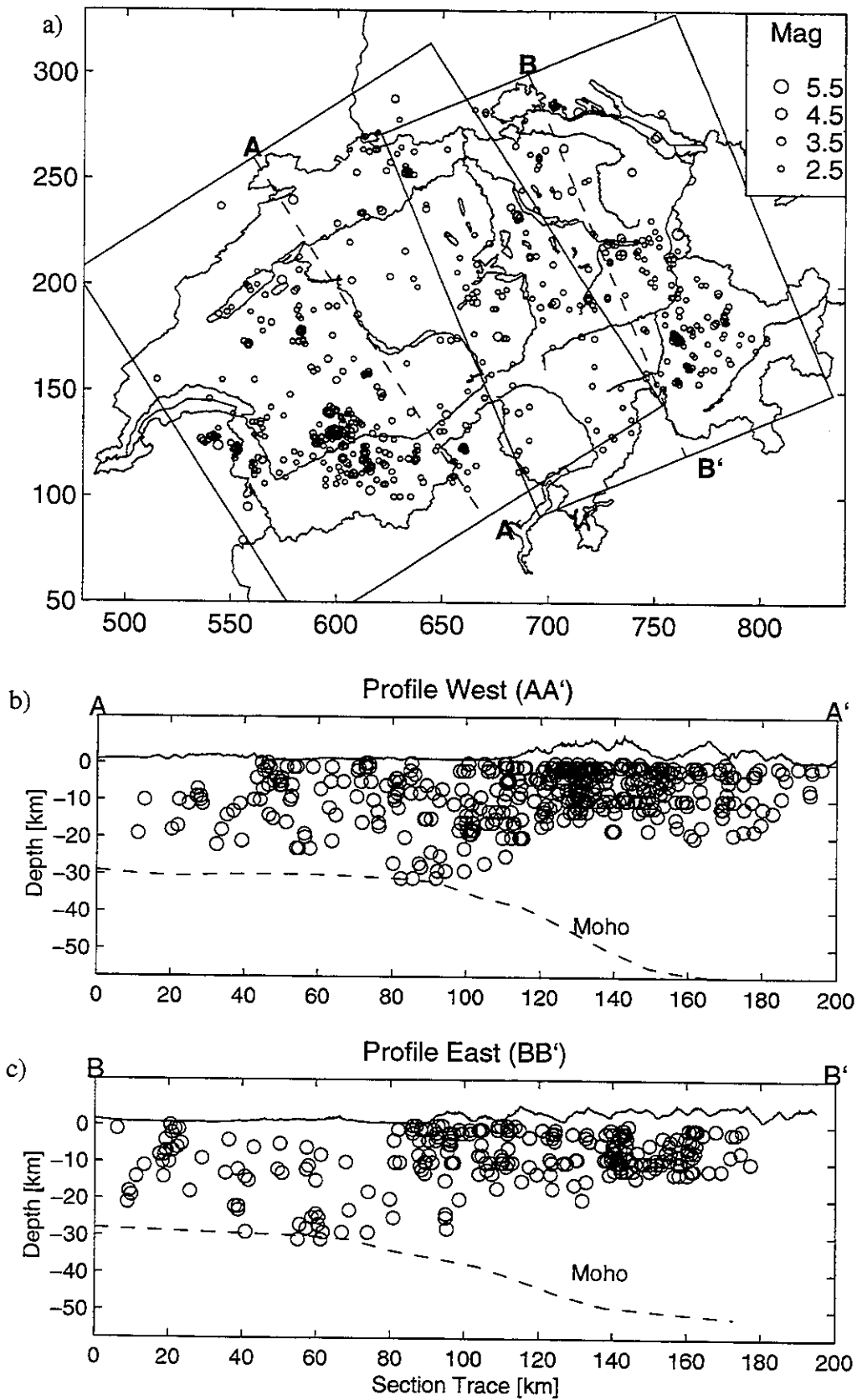
Figure 2.14:Two cross-sections perpendicular to the Alpine belt. The hypocenters are

projected onto vertical planes (AA' and BB') indicated by dashed lines. a) Only the epicenters in the rectangles drawn are used, b) cross-section in western Switzerland and c) cross-section in eastern Switzerland.
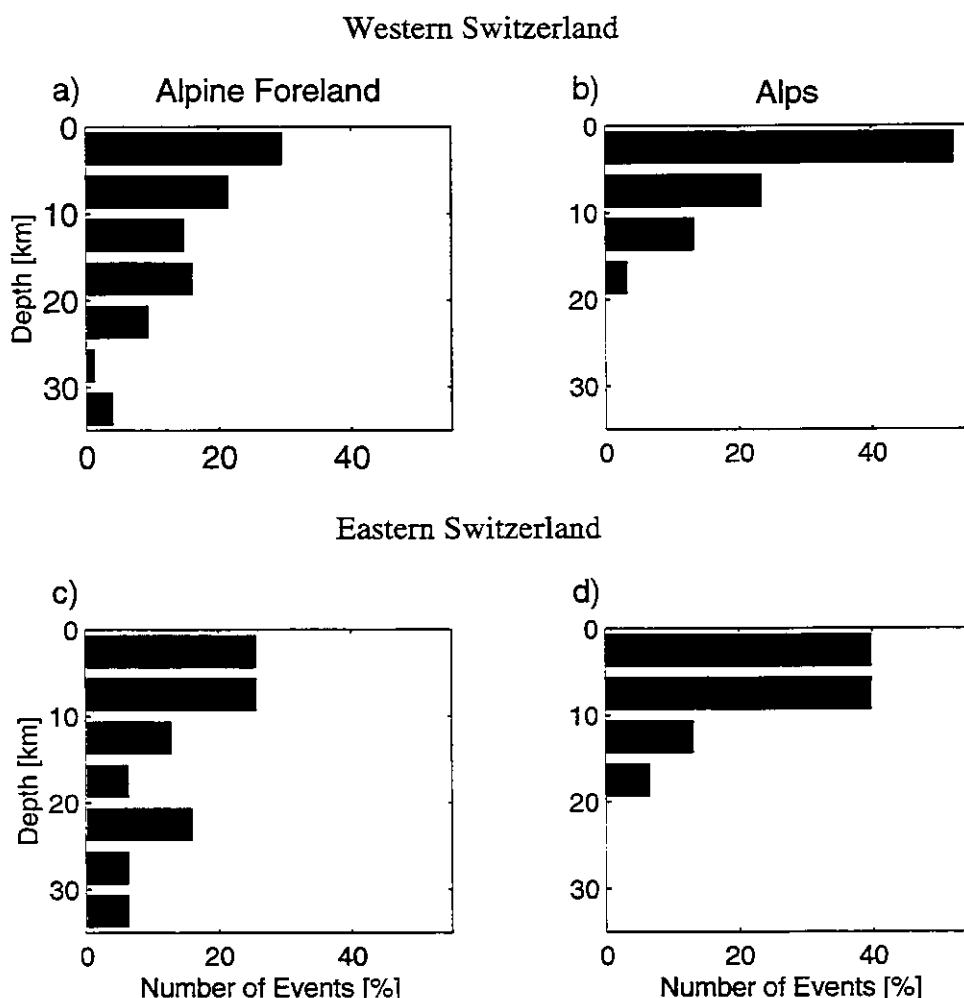
Western Switzerland

Eastern Switzerland

Figure 2.15:Depth distributions of hypocenters along the two profiles in figure 2.14. a,b) Profile AA' in western Switzerland c,d) Profile BB' in eastern Switzerland.

Up to this point the spatial seismicity pattern has been discussed. The distribution of earthquakes in time is of similar importance in earthquake hazard analysis. Figure 2.16 shows the number of all earthquakes exceeding a given intensity threshold in a 5 year time interval. It demonstrates that for smaller intensity values the number of observed events per time interval increases with time. At two points in time the number of observed events changes significantly (indicated by number 1 and 2). A first significant change is found in the second half of the 18th century, where an increased number of events with intensities ≥VI had been reported. This point coincides with the great earthquake in Lissabon (1755), which awakened interest in the earthquake phenomenon at that time. The second sudden change is found at the end of the 19th century, where the number of observed events with intensity ≥V increases. Once again the point coincides with the occurrence of a strong earthquake, this time with an earthquake of intensity VIII to IX in Visp (Volger, 1858). This event triggered the earthquake awareness in

Switzerland and motivated Volger (1858) and others to compile their comprehensive earthquake catalogs for Switzerland. Twenty years later, the Swiss Earthquake Commission was founded who immediately began to publish yearly bulletins.

The cumulative number of earthquakes for different intensity levels (figure 2.17) shows quite a similar picture. By assuming a constant seismicity rate, time periods for completely reported events can be estimated. Table 2.3 summarizes the assumed time periods of complete reporting for different intensity levels, which stem from historic facts and from the analysis of the earthquake catalog. Intensities IV and V are assumed to be completely reported since yearly bulletins appeared, i.e. since 1878. The time period of completeness for intensities VI and VII is accepted since the Lissabon earthquake of 1755. Intensity VIII is assumed to be complete since 1600. Finally, intensities higher than VIII are assumed to be complete for the whole period covered by the Ex-SEC, i.e. since 1300.

For verification of the completeness ranges, a statistical method is applied (Stepp, 1971). The method assumes that earthquake occurrence can be described by a Poisson process with constant recurrence rate. It is then possible to estimate mean recurrence rates and their variance for different time periods, starting at present and going back in time. If the assumption of a stationary recurrence rate is valid, its standard deviation should follow a linear behavior, depending on the time interval chosen. A deviation from the linear behavior implies either that the recurrence rate is not stationary or that the events are not completely reported in the catalog. Figure 2.18 shows the standard deviations for epicentral intensity IV, V, VI and VII versus time intervals and the curves with a linear behavior. If there is a change in the seismicity rate, the deviation of a linear behavior would occur at the same time for all intensities. Since this cannot be observed, it is confirmed that the deviations are due to incomplete reporting of earthquakes (or otherwise the assumption of a Poisson process is wrong). The completeness ranges which would be determined following Stepp's analysis coincide with the historic events mentioned above.

Table 2.3: Results of completeness analysis of the Swiss earthquake catalog (1300-1993)

Intensity	Year since events are completely reported
IV	1878
V	1878
VI	1750
VII	1750
VIII	1600
IX	1300

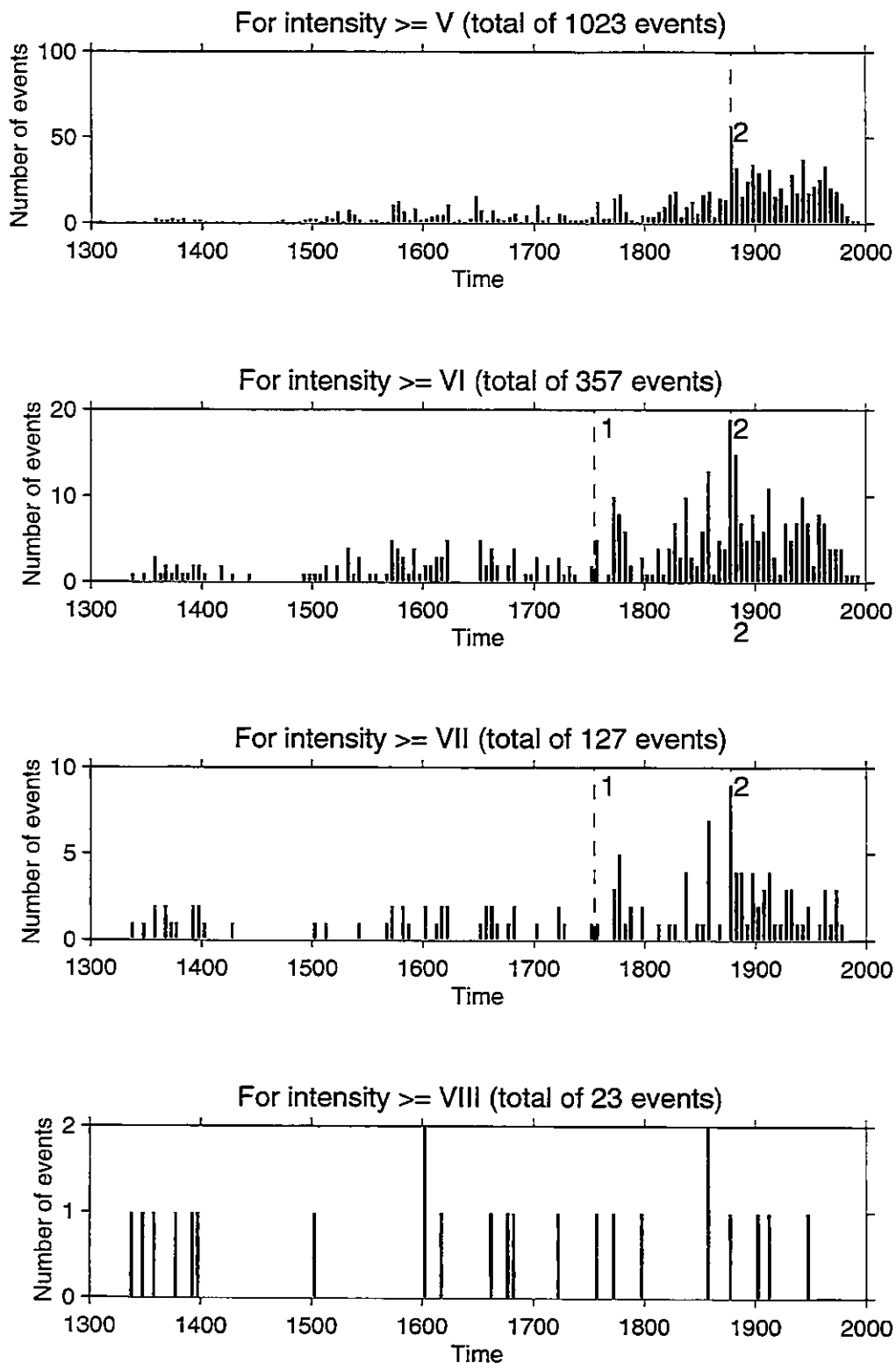Figure 2.16:Temporal distribution of earthquakes since 1300. The number of earthquakes in a 5 year time interval for different intensity thresholds is displayed. Number 1 indicates the date of the Lissabon earthquake in 1755, and number 2 indicates the date of the founding of the Swiss Earthquake Commission (1878).
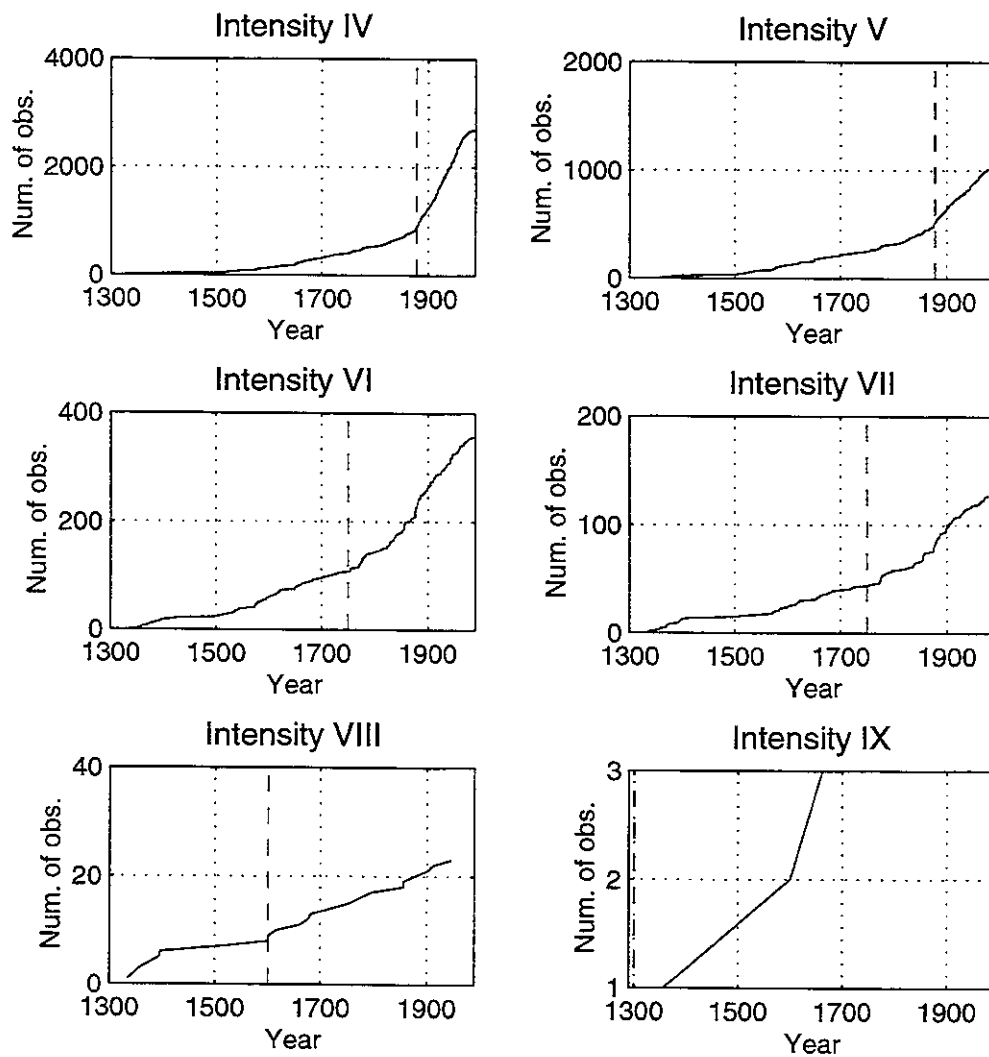
Figure 2.17:Cumulative number of earthquakes since 1300 for different intensity levels. Dashed lines indicate the date, after that the catalog can be assumed to be complete.
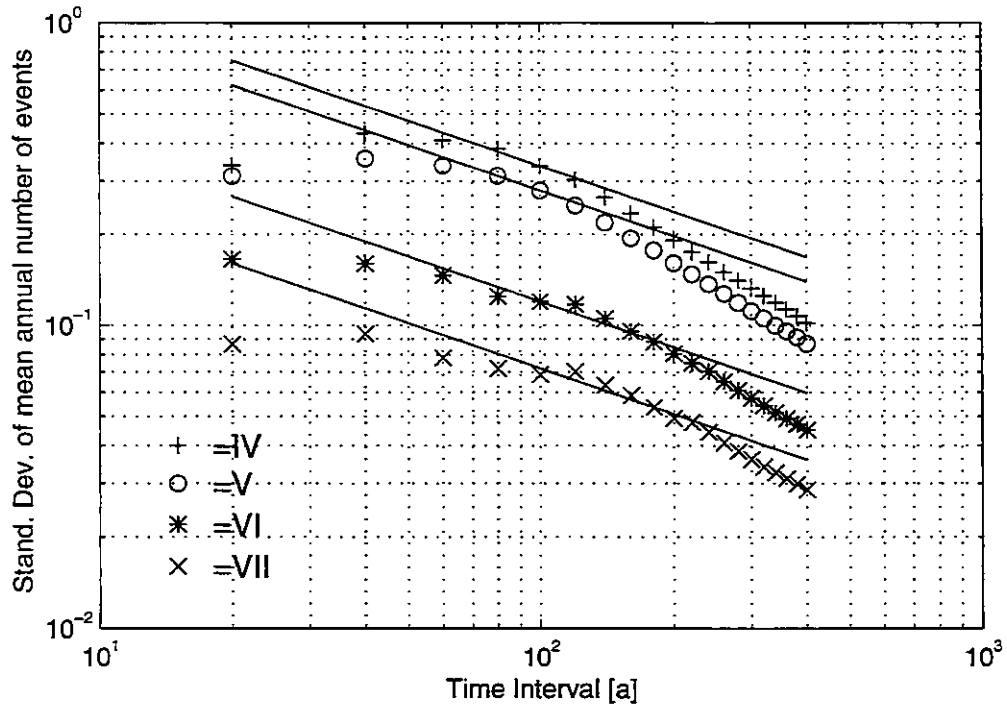
Figure 2.18:Earthquake catalog completeness for different intensity levels. The standard deviation of the estimated mean of the annual number of events as a function of the sample length is displayed. The solid lines give the *linear* trend, which is valid for a complete data catalog and stationary recurrence rate.

Chapter 3

SEISMIC HAZARD ANALYSIS

3.1   Introduction

Estimation of seismic hazard relies on data and models which are both sources of uncertainties in the resulting seismic hazard. In an appropriate decision making process direct knowledge about the uncertainty of the result is required. It is necessary, therefore, to account for the variabilities involved in the hazard assessment and to calculate its influence on the results. The variabilities in seismic hazard consist of two types, statistical and model variability (or uncertainty) and randomness.

- Statistical variability (or uncertainty) stems from a limited sample size and inaccurate samples, which precludes the exact determination of model parameters. With the collection of additional data, the model parameters can be estimated with increased accuracy and the statistical variability will be reduced.

- Model variability (or uncertainty) is attributed to the ability of the models to represent the physical process. With the improvement of our understanding of the physical phenomena the model uncertainty can be reduced.

- Randomness is the probabilistic variability resulting from the nature of physical processes. It cannot be reduced by the collection of additional data, but it can be accounted for by the use of stochastic models.

In seismic hazard analysis, the time of occurrence of a single earthquake is the only source of true randomness. With a satisfactory approximation (if the events are truly independent of each other), the earthquake occurrence can be described by a Poisson process. All other variabilities in seismic hazard have the character of either statistical or modelling uncertainties. These uncertainties lead to multiple combinations of possible models and input parameters to describe seismic hazard. The most common method for combining various models and input parameters is called the logic tree method (Benjamin and Cornell (1970), Coppersmith and Youngs (1986), Araya and Der Kiureghian (1988)). A logic tree is a decision flow path consisting of nodes and branches. Each branch is a possible combination of different models and input parameters. At each node, the different branches reflect possible alternatives. Assigning probabilities to the different alternatives yields a likelihood for each combination. The seismic hazard is first calculated for each branch individually. The final hazard is obtained combining the results for each branch taking into account its likelihood. The enormous amount of com-

puter time needed to calculate an individual combination restricts the number of combinations which can be carried out.

Bayesian statistical decision theory provides a mathematical model for incorporating statistical and model uncertainties as well as individual and more subjective elements (Benjamin and Cornell, 1970). The method is appropriate where information is based on past observations of a random process, which is clearly the case in seismic hazard analysis. Bayesian estimation techniques have been applied in seismic hazard analysis either in order to estimate single input parameters for standard seismic hazard approaches (Mortgat and Shah, 1979) or to update the results of the seismic hazard result by the observed data (Egozcue et al., 1991). In this study a Bayesian method is presented that estimates the probability distribution of the mean number of occurrences in a Poisson process described by the parameter λ, taking into account the uncertainties of the input parameters.

3.2   Method Developed

The method developed consists of two main steps: firstly to calculate "Earthquake Site Catalogs", which describes the history of (probably) ground motions which occurred at a specific site (figure 3.1), and secondly to estimate the Poisson parameter λ by using Bayesian inference (figure 3.2).

An "Earthquake Site Catalog (ESC)" contains the historic occurrences of ground motions for a particular site. This requires to model ground motions for each event of the earthquake catalog for particular sites. Figure 3.1 displays the steps involved in the calculation of the ESC. For each earthquake, a size, location, attenuation and local geology model has to be defined. The uncertainties in earthquake size and location are accounted for by probability distributions as discussed in chapter 2. Also the influence of local geologic settings on the ground motion can be considered. An attenuation model has to be defined that describes ground motion attenuation versus distance (see chapter 4). If input models are defined by probability distributions, the calculated ground motions at a site are also obtained as probability distributions. An ESC contains, therefore, for a specific site for each earthquake a ground motion probability distribution. The probability distribution is formulated as a discrete distribution, where p_i is the probability, that ground motion I at a given site is within ground motion class C, i.e. $p_i = P[I_i \varepsilon C]$. Index i indicates earthquake number i. The probabilities p_i for all earthquakes define the ESC.

Before the Poisson parameter λ can be calculated with Bayesian estimation, the probability of the number of occurrences for each discrete ground motion class has to be calculated from the ESC (figure 3.2). This is achieved by a mixed Bernoulli approach, which is a standard Bernoulli trial with varying probabilities (equation 3-17). Bayesian estimation techniques require a prior estimate of the examined parameter, in this case of the Poisson parameter λ. This prior estimate of λ, i.e. the mean recurrence rate of a ground motion, provides the possibility to integrate any geophysical information which lead to an estimation of λ. However, if no such prior information is available,

48

the method is still applicable because it allows for non-informative priors as well.

If a prior distribution of λ is assessed, then the distribution is updated with the probabilities of the number of occurrences obtained from the ESC. In other words, Bayesian estimation combines the prior distribution of λ with the sample likelihood calculated from the ESC (see chapter 3.3).

The method developed has some clear advantages compared to standard hazard analysis methods (Cornell (1968), McGuire (1976)) combined with logic tree methods (Coppersmith and Youngs, 1986). The main characteristics of the new method are:

- it integrates all uncertainties in the data and the applied models by probability distributions, i.e. in earthquake size and location as well as in ground motion attenuation models;

- it accounts for an "a priori" knowledge of the mean number of occurrences of a ground motion (e.g. derived from seismotectonic studies or geodetic surveys);

- it gives confidence intervals of the obtained seismic hazard;

- it avoids the difficult (and often unmotivated) delineation of seismic sources (which is quite an important problem in regions with low seismic activity);

- there is no need to use explicitly earthquake size distributions (for example by a Gutenberg-Richter relation (Gutenberg and Richter, 1944)).

Nevertheless, the flexibility of the method developed allows also to account for well-determined epicenters and to model seismic sources. However, the assessment of "a priori" knowledge of the mean number of occurrences of a ground motion from geophysical studies is a very complex and ambitious task, which cannot be treated in this study.
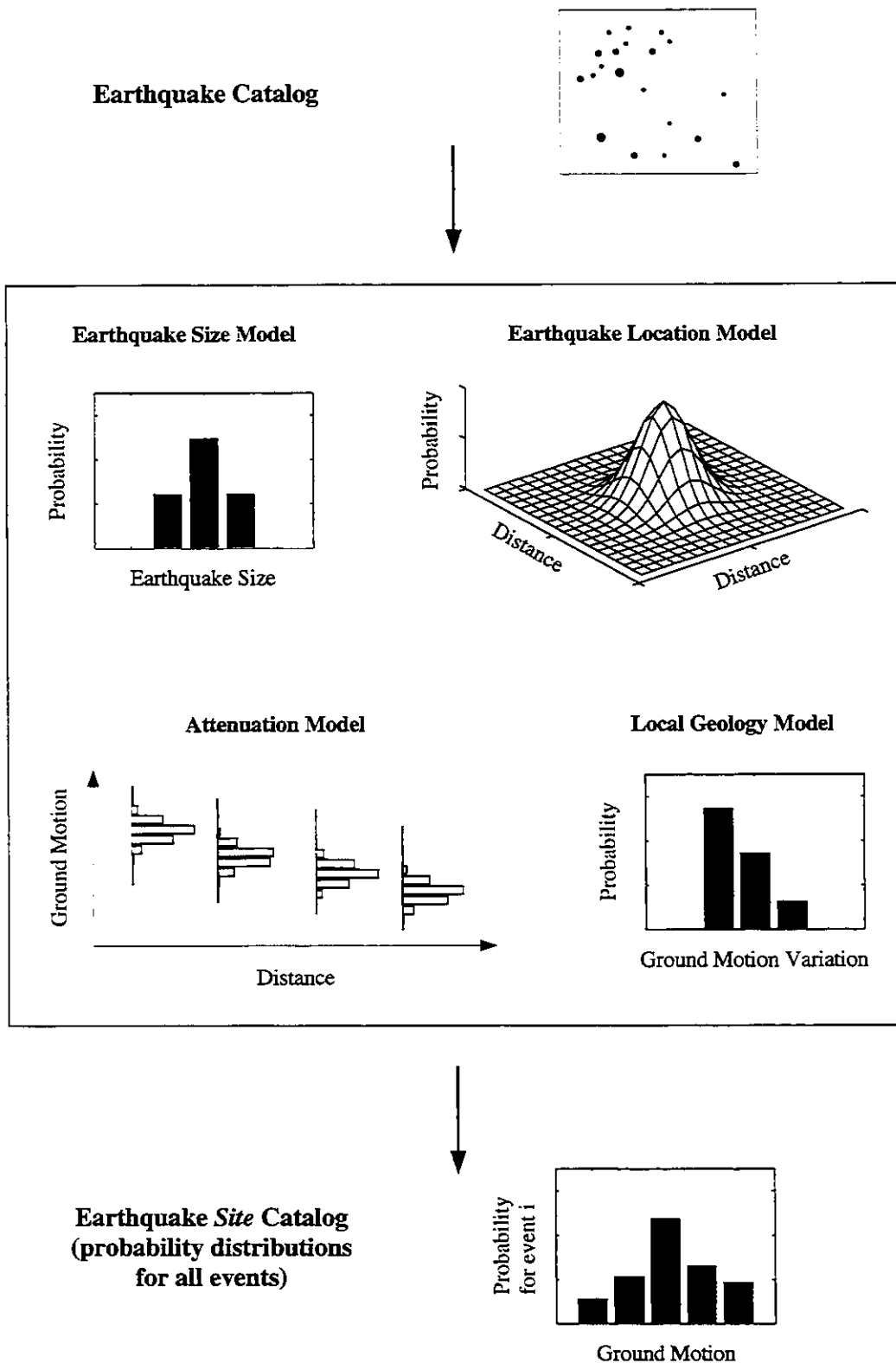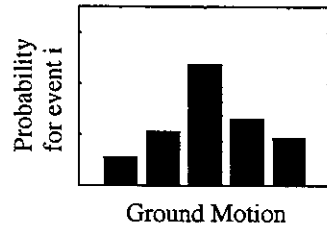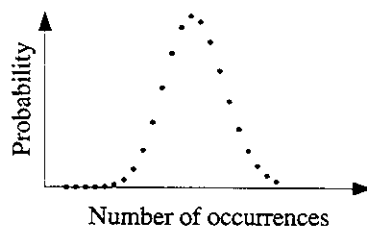
Figure 3.1: Steps involved in the calculation of "Earthquake Site Catalogs". The ground motion probability distribution is calculated for each earthquake taking into account uncertainties in size, location, ground motion attenuation and local geologic settings.
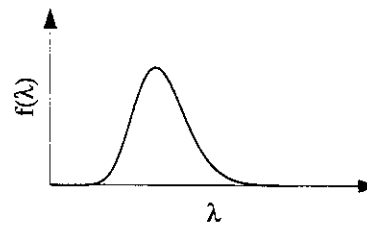
Earthquake Site Catalog

Mixed Bernoulli Trial

**Prior Distribution of
Poisson parameter λ**

Bayesian Estimation
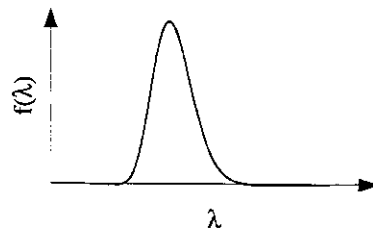
**Posterior Distribution
of parameter λ**

Figure 3.2: Steps involved in the calculation of the Poisson parameter λ. From the "Earthquake Site Catalog" the probability distribution for the number of occurrences of a specific ground motion level is calculated. The posterior distribution of λ is obtained by Bayesian estimation.

51

3.3   Bayesian Estimation

The realistic description of an unpredictable, natural phenomenon led to the concept of probability models, which cover a wide range of applications. In this framework, Bayesian estimation provides a mathematical model for the estimation of the distribution of random variables in the presence of uncertainties. It provides a mathematical procedure, for updating a prior assumption about the distribution of the value of a parameter by additional information, which yields a posterior distribution of the parameter. This chapter introduces the theory of Bayesian estimation. For a more detailed discussion see, for example, Benjamin and Cornell (1970) or Press (1989). In the following paragraphs capital letters denote observable variables and small letters denote an experimental outcome (realization) of the variables.

Bayesian estimation is based on the Bayes' rule (3-3), which is a formal expansion of the total probability theorem (3-1) (Benjamin and Cornell, 1970) and the rule, that the conditional probability for event z, if event x_i has occurred, is equal to the conditional probability for event x_i, if z has occurred:

$$P[z] = \sum_{i=1}^{n} P[z|x_i] P[x_i] \qquad (3\text{-}1)$$

$$P[x_i|z] P[z] = P[z|x_i] P'[x_i] \qquad (3\text{-}2)$$

where

z   event

x_i mutually exclusive, collectively exhaustive events, i=1 to n

Combining (3-1) and (3-2) yields:

$$P''[x_i] = P[x_i|z] = \frac{P[z|x_i] P'[x_i]}{P[z]} \qquad (3\text{-}3)$$

Formula (3-3) is known as Bayes' theorem or Bayes' rule. The probability $P''[x_i]$ is called posterior probability. It is obtained by the multiplication of the former (prior) probability $P'[x_i]$ with the sample likelihood $P[z|x_i]$ and a normalizing constant:

$$\begin{pmatrix} posterior \\ prob \end{pmatrix} = \begin{pmatrix} normalizing \\ factor \end{pmatrix} \begin{pmatrix} sample \\ likelihood \end{pmatrix} \begin{pmatrix} prior \\ prob \end{pmatrix}$$

The sample likelihood describes the relative probability of the various possible outcomes x_i as a function of the observation z. With this model, it is possible to update a prior distribution, if new data are available. Then, the posterior distribution takes into account the observed data.

If observed data are observations of a random process of independent events, they

can be usually described by a probability model (e.g. Poisson model) with unknown parameters. The estimation of these parameters, which describe the random process, can also be estimated following Bayesian inference. Thereby, the parameters of the model are treated as random variables. If $f'_X(X)$ describes a prior probability density of the unknown parameters, (3-3) becomes:

$$f''_X(x) = N \cdot L[X|x_1, x_2...x_n] \cdot f'_X(X) \qquad (3\text{-}4)$$

In (3-4) the prior probability distribution of the unknown parameters is updated by the sample likelihood $L[X|x_1, x_2...x_n]$, which yields a new posterior distribution. N is again a normalizing constant. The influence of the prior distribution on the posterior distribution, which is the product of the prior distribution with the sample likelihood, is shown in figure 3.3. The form of the posterior distributions varies when different forms of the prior distribution or the sample likelihood are assumed. If it is not possible to define an appropriate prior distribution of the unknown parameters, a very flat (or diffuse) prior distribution with almost no information in it can be chosen (figure 3.3). In these cases, the result will almost completely be determined by the data sample. A detailed discussion about the influence of prior distributions on posterior distributions can be found in chapter 3.5.
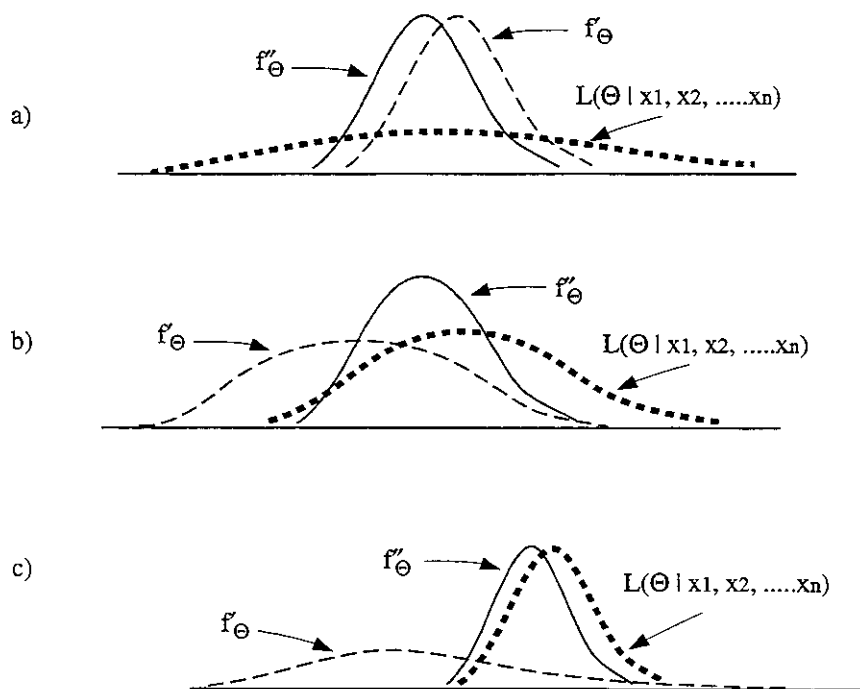

Figure 3.3: Posterior distributions versus prior distribution and sample likelihood (after Benjamin and Cornell (1970)): (a) Well-defined prior distribution and relatively small sample. (b) Prior distribution and sample information of comparable weight. (c) Vague or diffuse prior distribution and relatively large sample.

53

3.4   Bayesian Estimate in Seismic Hazard Assessment

3.4.1   Standard Bayesian Estimate

The parameter that is estimated in seismic hazard analysis, is the Poisson parameter λ, i.e. the mean occurrence rate of a ground motion at a site. This presumes, that the occurrences of a ground motion level can be modelled as a stationary Poisson process. The probability distribution of a Poisson process is given by:

$$P\,(N_t = n)\ =\ \frac{(\lambda t)^{\,n}\exp\,(-\lambda t)}{n!} \qquad\qquad (3\text{-}5)$$

where

n   number of events

N_t number of observations in time interval t

λ mean occurrence rate

The inherent uncertainty of the parameter λ requires a treatment of λ as a random variable. We further assume that the probability distribution of λ is proportional to a Gamma distribution with parameters ν and κ. This somehow arbitrary choice is justified, because the Gamma function is able to fit a large variety of shapes and, therefore, does not introduce substantial limitations in the model. The function covers the range of the positive numbers to infinity, which coincides with the range of the Poisson parameter. It is furthermore an appropriate choice, because the Gamma function is the conjugate prior distribution for the parameter λ of a Poisson distributed random variable, which yields simple relations for the posterior distributions. The prior estimate can thus be written as (Benjamin and Cornell, 1970):

$$f'_\lambda\,(\lambda)\ =\ \frac{\nu^{\kappa}}{\Gamma\,(\kappa)}\lambda^{\kappa-1}\exp\,(-\nu\lambda) \qquad\qquad (3\text{-}6)$$

where

Γ Euler's Gamma function

ν, κ parameters of the Gamma distribution

The parameters ν and κ are directly related to the expectation and variance of λ:

$$E\,[\lambda] = \frac{\kappa}{\nu} \text{ and } Var\,[\lambda] = \frac{\kappa}{\nu^2} \qquad\qquad (3\text{-}7)$$

We have assumed that the number of occurrences of a ground motion level follows a Poisson process with parameter λ. The sample likelihood function on λ, when n occurrences have been observed in the time period T, is:

$$L(\lambda | T, N = n) = \frac{(\lambda T)^n}{n!} \exp(-\lambda T) \qquad (3\text{-}8)$$

where

T time period of observation

n number of occurrences

By applying Bayes' rule (3-3), the posterior distribution f''_λ of λ is:

$$f''_\lambda(\lambda) = f''_{\lambda | N = n}(\lambda) = NL(\lambda | T, N = n) f'_\lambda(\lambda) \qquad (3\text{-}9)$$

$$= \frac{(\lambda T)^n}{n!} \exp(-\lambda T) \frac{v^\kappa}{\Gamma(\kappa)} \lambda^{\kappa - 1} \exp(-v\lambda)$$

or

$$f''_\lambda(\lambda) = \frac{(v + T)^{\kappa + n}}{\Gamma(\kappa + n)} \lambda^{\kappa + n - 1} \exp(-(v + T)\lambda) \qquad (3\text{-}10)$$

From formulas (3-6) and (3-10) follows, that:

$$v'' = v + T \quad \text{and} \quad \kappa'' = \kappa + n \qquad (3\text{-}11)$$

and thus:

$$E''[\lambda | (v, \kappa)] = \frac{\kappa + n}{v + T} \quad \text{and} \quad Var''[\lambda | (v, \kappa)] = \frac{\kappa + n}{(v + T)^2} \qquad (3\text{-}12)$$

From formula (3-12) it can easily be seen that the larger T is, the smaller will be the variance in λ, i.e. that the longer the time period of observation is, the smaller will be the uncertainty in λ. With reference to the Poisson process (3-5) the number of occurrences m in time η can now be calculated allowing for the uncertainty of the parameter λ. This means that the distribution of λ (3-10) has to be combined with the Poisson distribution (3-5). This yields the predictive distribution of the number of occurrences, which represents the probability that m events occur in a time interval of η years (Egozcue, 1994):

$$P_\eta\,[N=m] \;=\; \int_0^\infty \frac{(\lambda\eta)^m}{m!} \exp(\lambda\eta)\cdot f_{\lambda|N=n}\,d\lambda \qquad\qquad (3\text{-}13)$$

$$=\; \frac{\eta^m\,(v+T)^{\kappa+n}\,\Gamma(\kappa+n+m)}{m!\,(v+T+\eta)^{\kappa+n+m}\,\Gamma(\kappa+n)}$$

where

η time interval for prediction

m number of occurrences in time interval η

Formula (3-10) is valid only if the number of occurrences n in time T is known precisely. If the sample is imprecise itself, i.e. if the number n of occurrences can only be estimated with uncertainty, the number n has also to be treated as a random variable. This is the case for the calculated "Earthquake Site Catalog" (see chapter 3.2), which contains probabilities for different ground motion levels. Taking these quantities into account yields the weighted Bayesian estimate.

3.4.2   Weighted Bayesian Estimate

Because of the uncertainty of the data in the earthquake catalog (see chapter 2.3), the number of occurrences of a ground motion level cannot be calculated precisely. This means that the number of occurrences n also follows a probability distribution P[N=n] with n=0,1,,,. The Bayesian estimate (3-10) has now to be rewritten for the value of N=n:

$$\tilde f_\lambda(\lambda) \;=\; \sum_{n=0}^\infty f''_{\lambda|N=n}\cdot P\,[N=n] \qquad\qquad (3\text{-}14)$$

Formula (3-10) can now be expressed as:

$$\tilde f_\lambda(\lambda) \;=\; \sum_{n=0}^\infty \frac{(v+T)^{\kappa+n}}{\Gamma(\kappa+n)}\,\lambda^{\kappa+n-1}\exp\left(-(v+T)\lambda\right)P\,[N=n] \qquad\qquad (3\text{-}15)$$

Combining (3-15) with (3-11) yields:

$$\tilde f_\lambda(\lambda) \;=\; \sum_{n=0}^\infty \frac{v''^{\kappa''}}{\Gamma(\kappa'')}\,\lambda^{\kappa''-1}\exp\left(-v''\lambda\right)P\,[N=n] \qquad\qquad (3\text{-}16)$$

Formula (3-16) will be used for the calculation of posterior distributions of the parameter λ, if the sample data are imprecise.

The probabilities P[N=n] are calculated from the "Earthquake Site Catalog" (ESC). The given probabilities p_i in the ESC can be interpreted as probabilities of a Bernoulli

trial. Then P[N=n] is obtained by a standard Bernoulli trial with varying probabilities p_i for each earthquake:

$$P[N = n] = \sum_{j_1 = 1}^{(x-n+1)} \sum_{j_2 = 1}^{(x-n+2)} \cdots \sum_{j_y = 1}^{x} \prod_{k = 1}^{n} \frac{p(j_k)}{1 - p(j_k)}, \quad n = 1, \ldots, x-1 \quad (3\text{-}17)$$

where

$p(j)$ probability, that event j produces a specific ground motion level at a site

x number of events in "Earthquake Site Catalog"

The expectation and variance of λ is now:

$$\tilde{E}[\lambda| (v, \kappa)] = \frac{\kappa + E(N)}{v + T} \quad \text{and} \quad \tilde{Var}[\lambda| (v, \kappa)] = \frac{\kappa + E(N) + Var(N)}{(v + T)^2} \quad (3\text{-}18)$$

This result shows that the mean of the weighted posterior distribution is that of the standard posterior distribution (3-12), if the number of observations were E(N). But the uncertainty of n influences the variance of the posterior distributions, i.e. the larger the variance in the number of observations is, the larger the variance of λ will be. Figure 3.4 shows two posterior distributions of λ. The dashed line represents the standard posterior, the solid line the weighted posterior, respectively. It is quite obvious, how imprecise data increase the variance of the distribution, whereof the mean of both distributions is equal.

The posterior distribution of the Poisson parameter λ allows to calculate both, point estimates of λ (e.g. mean values, modes, median) and interval estimates of λ. Point estimates from probability densities, e.g. the mean of the posterior density of λ, give a representative point of the value of λ, but do not show the variance of the obtained results. Therefore, whenever possible, probability intervals should be given to indicate the accuracy of the recurrence rate λ. This is valid for the standard Bayesian estimation (with exact data) as well as for the weighted Bayesian estimation (with imprecise data).
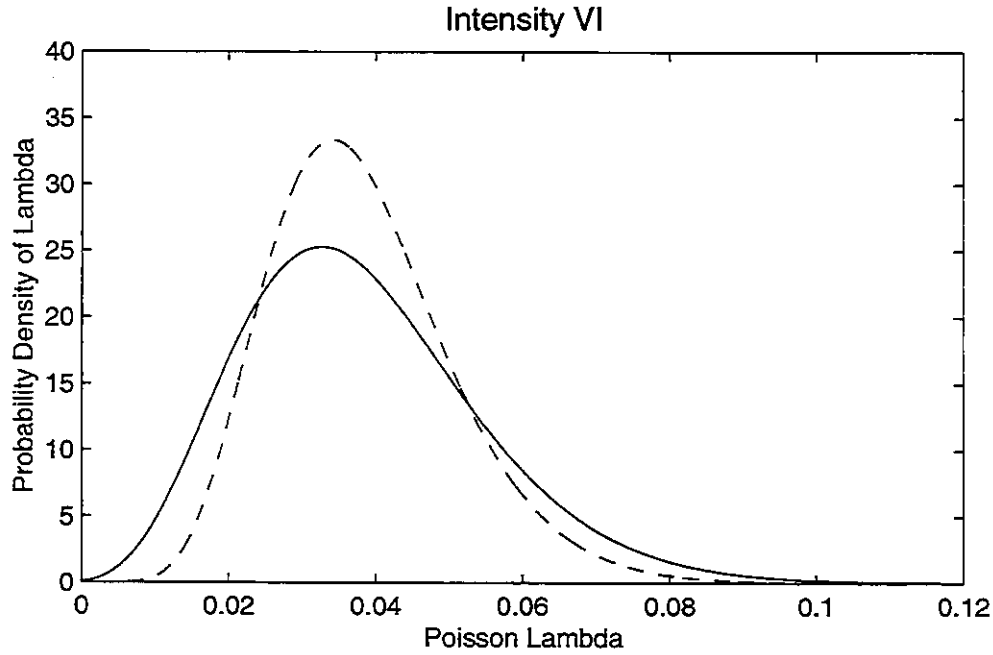
Figure 3.4: Standard posterior distribution of the Poisson parameter λ for exact data (dashed line) and weighted posterior distribution for imprecise data (solid line). The mean value of λ is equal for both distribution, but the variance is increased by imprecise data.

3.5 Prior and Posterior Estimates

As already mentioned, prior distributions can have a significant influence on posterior distributions of λ (cf. figure 3.3). Very flat (or diffuse) prior distributions, which can be called "non-informative priors", will result in posterior distributions almost completely determined by the likelihood of the data sample. Such "non-informative priors" are valuable if no information about the distribution of λ is available. On the other hand, "exact" prior distributions, i.e. with small variance, can hardly be changed by the data sample. However, "non-informative priors" cannot always be mathematically expressed in a proper way, i.e. as a probability density. In combination with the Gamma distribution a "non-informative prior" can be formulated by setting the parameter κ equal to 1 and the parameter ν equal to 1 (cf. equation (3-15)). Then, the prior distribution is an improper distribution, since it cannot be expressed as a density anymore. In the following, examples are given in order to illustrate the method developed of estimating parameter λ by Bayesian inference.

Based on an "Earthquake Site Catalog", probabilities of number of occurrences for a specific ground motion are calculated by applying equation (3-18). A typical result of such a Bernoulli trial with varying probabilities is shown in figure 3.5. For a specific site, the probabilities versus number of occurrences of intensity VI is displayed. The peak in the number of occurrences is recognized to be 9. Assuming a completeness in-

terval of 243 years for intensity VI (chapter 2.4) yields a mean occurrence rate of 0.038. Weighted posterior distributions of λ are calculated for three different prior distributions: 1) a well-defined prior with a relative small variance, which does not correspond to the observed data, 2) a well-defined prior which is confirmed by the data, and 3) a diffuse prior distribution. In order to clarify the influence of prior estimates, posterior distributions based on "non-informative priors" are also calculated. The "non-informative priors" are represented by $\kappa = 1, v = 0$ as parameters of the Gamma distribution.

A prior distribution with an expectation and variance for λ of 0.1 and 0.0005, respectively, is chosen as a well-defined prior, i.e. with a relatively small variance. Figure 3.6 shows that the assumed prior (dotted line) lies almost completely outside the sample likelihood, which is approximately represented by a posterior distribution (dashed line) with a non-informative prior. However, the sample likelihood still shifts the prior distribution towards the observed λ.

In the case of a well-defined prior distribution (with an expectation for λ of 0.05) which is confirmed by the data sample, the posterior distribution (solid line) becomes smaller, i.e. a smaller variance is obtained (figure 3.7). On the other hand, a prior distribution with a wide variance yields almost the same distribution as with a non-informative prior (figure 3.8).

Table 3.1 summarizes the obtained results in terms of return periods. 50% and 90% probability intervals are given. Vaguely defined priors and non-informative priors give similar results, since the posterior distribution is strongly determined by the data sample. A well-defined prior within the data sample reduces the variance of the return periods, while a well-defined prior out of the data sample changes the interval estimates drastically.
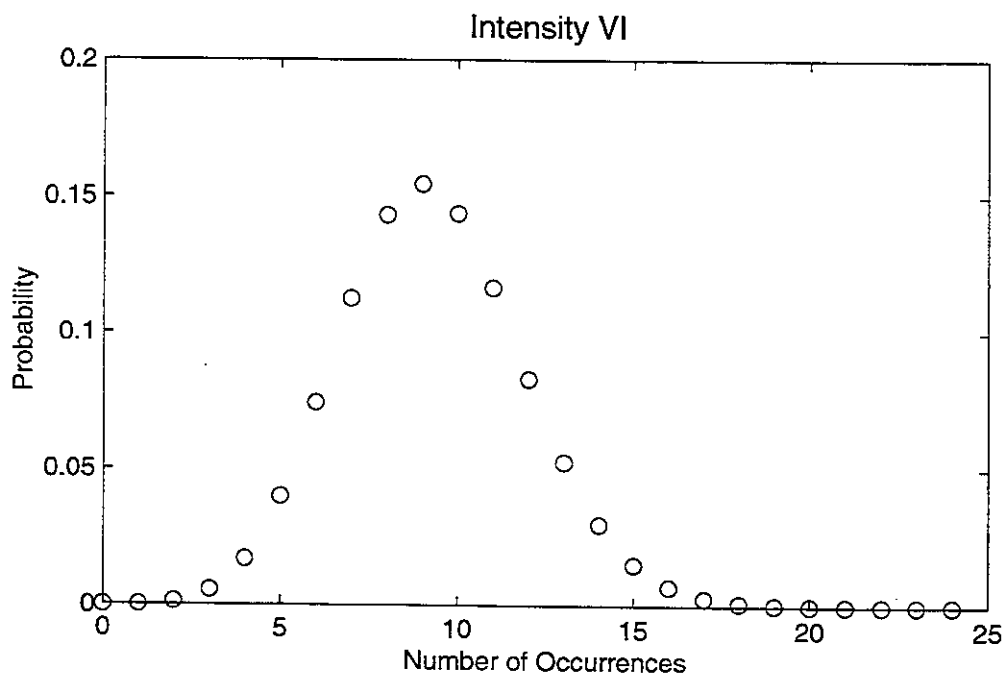

Figure 3.5: Probability versus number of occurrences of intensity VI for a specific site.

Table 3.1: Return periods (in years) in 50% and 90% probability intervals for various types of prior distributions of λ

Type of prior	Expectation and variance of λ	Return period 50% interval	Return period 90% interval
non-informative	k=1 v=0	[21;38]	[15;67]
well-defined	E(λ)=0.1 Var(λ)=0.0005	[13,18]	[11,22]
well-defined	E(λ)=0.05 Var(λ)=0.0004	[20;30]	[15;43]
vaguely defined	E(λ)=0.1 Var(λ)=0.005	[19;32]	[14;53]

The above examples show how the data sample influences the posterior distribution. If probabilities of number of occurrences for a specific ground motion are one for zero observations and consequently zero for n>0, posterior distributions based on non-informative priors can be calculated based on formula (3-15). The posterior distribution of λ reduces to:

$$\bar{f}_\lambda(\lambda) = T\exp(-T\lambda) \qquad (3\text{-}19)$$

Consequently, posterior distributions depend only on the time T of the period of complete observations. Cumulative distributions of (3-19) and probability intervals can explicitly be formulated. Probability intervals are given by:

$$\lambda = -\frac{1}{T}\ln(1-p) \qquad (3\text{-}20)$$

where

T   time period of observation

p   percentile of probability interval

For an observation time of, for example, 700 years, the symmetric 90% probability interval is between 233 years and 13650 years. In fact, if there is only a short time period of observation and no earthquakes are observed, there will be a large uncertainty with regard to the estimated λ values. This is a direct consequence of using a Poisson process of independent events.
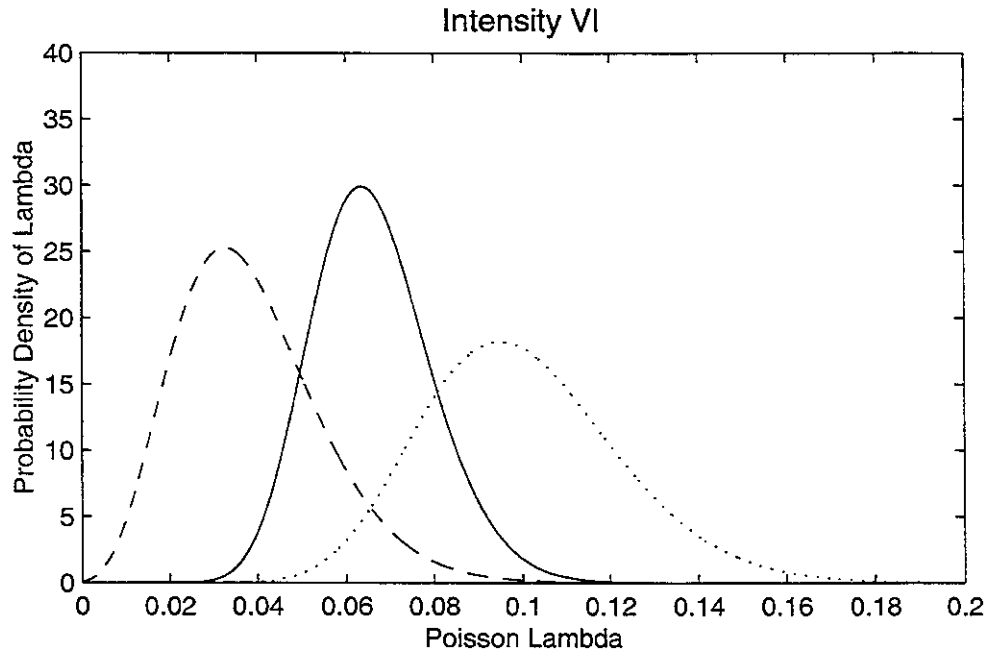
Figure 3.6: Prior and posterior distributions of the Poisson parameter λ. The well-defined prior distribution (dotted line) is shifted by the sample likelihood. The resulting posterior distribution (solid line) lies between prior and non-informative posterior distribution (dashed line).
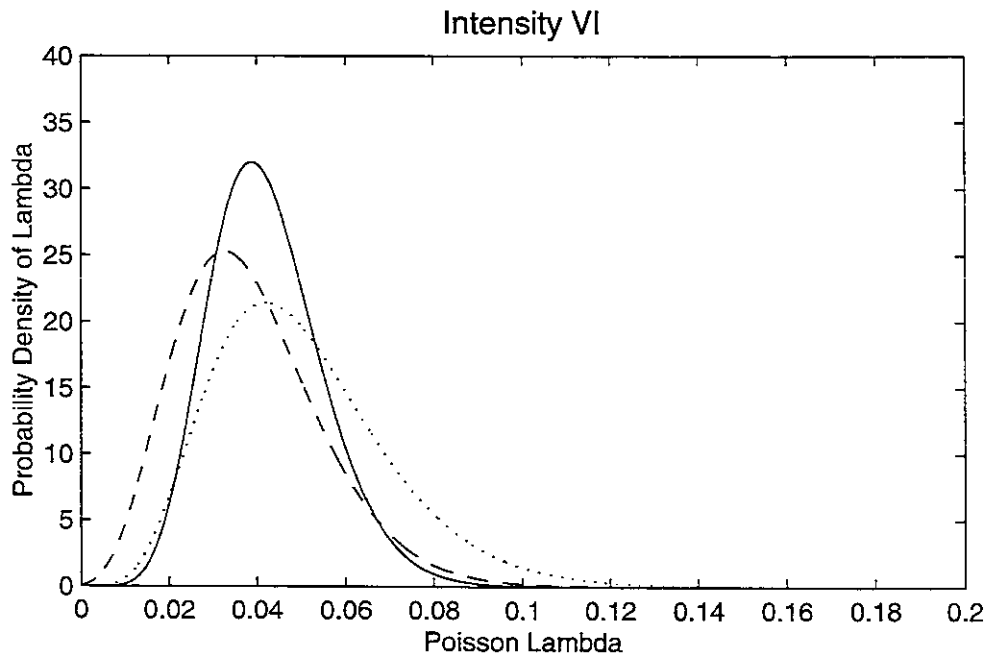

Figure 3.7: Prior and posterior distributions of the Poisson parameter λ. The well-defined prior distribution (dotted line) is confirmed by the sample likelihood. The resulting posterior distribution (solid line) has a smaller variance than the prior and is close
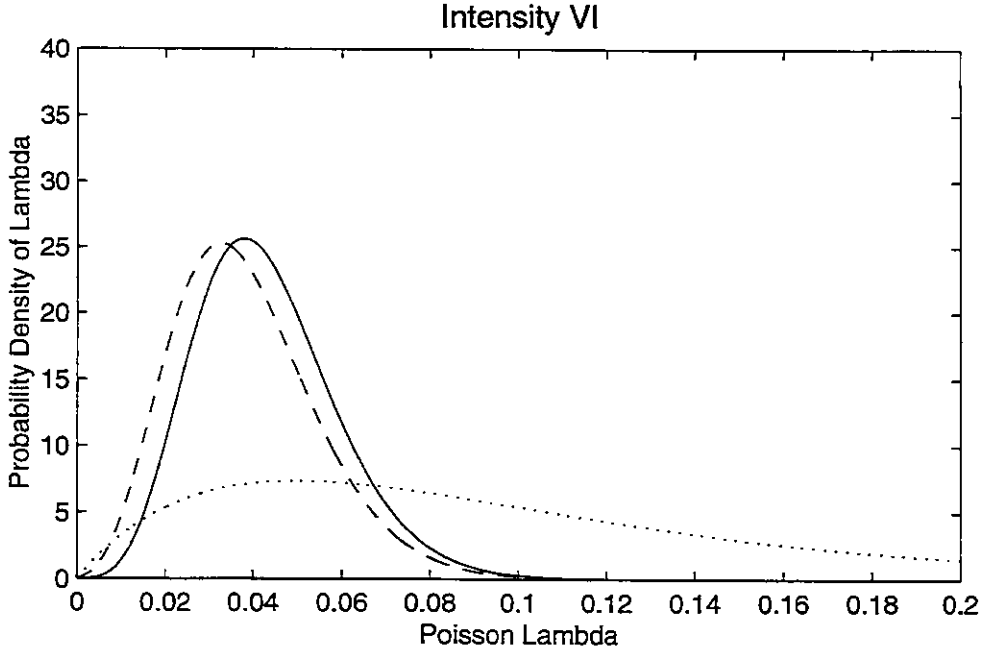
Figure 3.8: Prior and posterior distributions of the Poisson parameter λ. The vaguely defined prior distribution (dotted line) does almost not influence the sample likelihood. The resulting posterior distribution (solid line) has a similar variance as the non-informative posterior distribution (dashed line).

When the parameters λ are estimated for several intensity degrees, a "minimal prior information" that links the different intensity degrees to each other can be accepted. It is called "minimal prior information" since it gives not such a strong relation between different intensity degrees as the widely used frequency-intensity laws (cf. equation (1-1)). The "minimal prior information" states that for two intensity degrees I_1 and I_2, where $I_1 < I_2$, the corresponding Poisson parameters have to follow the relation $\lambda_1 > \lambda_2$. In other words, the return period for intensity I_1 has to be smaller than for I_2. This condition can be formulated by:

$$f_{\lambda_2|\lambda_1}(\lambda_2|\Theta) = \frac{1}{\Theta} I\{0 \leq \lambda_2 \leq \Theta\} \qquad (3\text{-}21)$$

where $I\{\ \}$ stands for the characteristic set function. The prior distribution for λ_2 is obtained by applying the total probability theorem:

$$f_{\lambda_2}(\lambda_2) = \int_0^\infty f_{\lambda_2|\lambda_1}(\lambda_2|\Theta)\tilde{f}_{\lambda_1}(\Theta)\,d\Theta \qquad (3\text{-}22)$$

Figure 3.8 shows an assumed probability density for λ_1 (dashed line) and the derived "minimal prior information" (solid line) for λ_2 following equation (3-22). It can be seen

that values for λ_2 larger than values for λ_1 are not allowed, whereof values of λ_2 smaller than λ_1 have an equal probability of being true values. This "minimal prior information" ensures that values of λ_2 greater than values of λ_1 are not possible. This condition has only an significant influence of posterior distributions if no observations of the corresponding intensity degree are available.
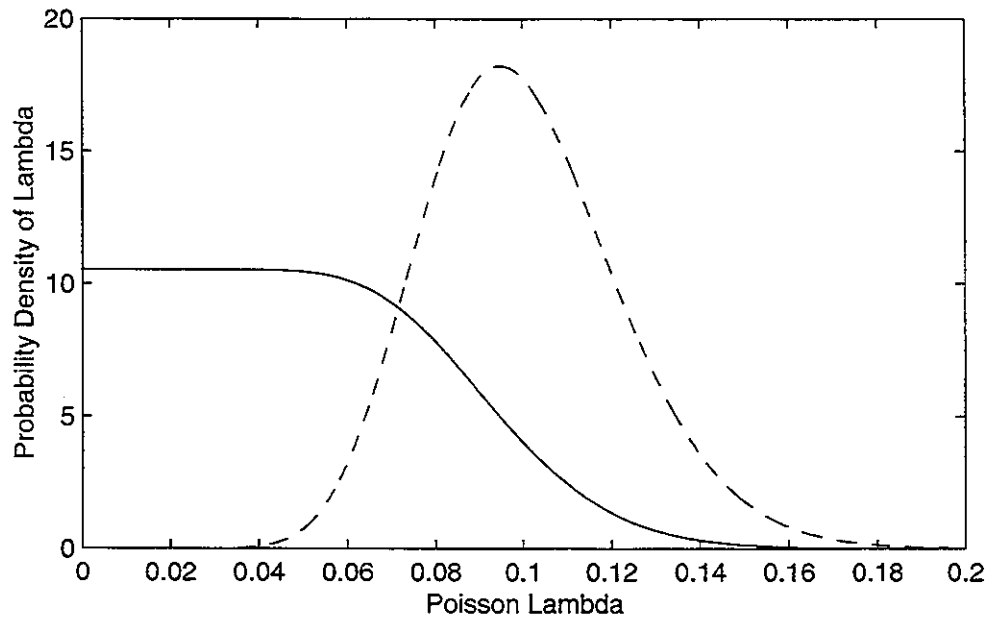

Figure 3.8: Posterior distributions of the Poisson parameter λ_1 (dashed line). From this posterior distribution a "minium prior" distribution for λ_2 (solid line) is calculated. The "minium prior" distribution for λ_2 ensures that values of λ_2 greater than values of λ_1 are not possible.

Chapter 4

GROUND MOTION ATTENUATION

4.1 Macroseismic Intensity Attenuation

Many relationships have been proposed in the past to describe the attenuation of seismic intensity (cf. Kövesligethy (1906), Blake (1941), Sponheuer (1960), Evernden et al. (1981)). Most of them assume that the local intensity I_S is related to the seismic energy E. The assumption, that I_S is proportional to the logarithm of E, yields an attenuation law of the form of equation (4-1). Equation (4-2) is based on the assumption that I_S is proportional to the power of E (cf. Howell and Schultz, 1975).

$$I_s = I_0 - f_1 - g_1 \ln(R) + h_1 R \qquad (4\text{-}1)$$

$$\ln(I_s) = \ln(I_0) - f_2 - g_2 \ln(R) + h_2 R \qquad (4\text{-}2)$$

where

I_0	epicentral intensity
I_S	intensity at a particular site
R	distance between epicenter and site
f, g, h	characteristic parameters

The parameter g describes the geometric attenuation and the parameter h the energy absorption, respectively. The most frequently used relationship in Europe to describe intensity attenuation is the formula proposed by Kövesligethy (1906). It has been empirically verified by Sponheuer (1960) and follows the form of equation (4-1). It may be written as:

$$dI = I_0 - I_s = k \cdot \log\left(\frac{\sqrt{R^2 + H^2}}{H}\right)^b + k \cdot \log(e) \cdot \alpha\left(\sqrt{R^2 + H^2} - H\right) \qquad (4\text{-}3)$$

where

I_0	epicentral intensity
I_S	intensity at a particular site

k	correspondence between intensity and ground motion amplitude (Sponheuer proposed a value of 3)
R	distance between epicenter and site
H	hypocentral depth
b	geometrical spreading coefficient (1 for body waves and 0.5 for surface waves)
α	absorption coefficient

The parameter α is proportional to the energy absorption. In the context of intensity attenuation, however, α does not only describe energy absorption, but also includes radiation effects and objective and subjective judgments involved when an intensity scale is applied.

Sägesser and Mayer-Rosa (1978) and Mayer-Rosa (1986) showed that the attenuation model by Sponheuer (1960) (equation 4-3) appropriately describes intensity attenuation in Switzerland. They introduced the azimuthal dependence of parameter α to achieve a better correlation for some of the observed isoseismal maps.

In this work, the Sponheuer attenuation parameters derived for Switzerland are first reviewed and tested with intensity data gathered over the last 20 years (see table 4.1). Secondly, a probabilistic attenuation law, which accounts for the scatter of the observed intensity data is proposed.

Table 4.1: Earthquakes since May 1976 with epicentral intensity greater than V, used for the assessment of attenuation parameters in Switzerland (I_0 denotes epicentral intensity and N_{obs} number of observations)

Epicentral Area	Date	Lat. / Long.	I_0	N_{obs}
Friuli	1976 05 06	46.353/13.266	VIII	230
Filisur	1976 07 17	46.693 / 9.679	V	45
Friuli	1976 09 15	46.342/13.121	VIII	74
Sils Maria	1978 02 23	46.438/9.815	V	24
Swabian Jura	1978 09 03	48.283 / 9.033	VII	319
Sierentz	1980 07 15	47.628 / 7.518	VI	186
Albis	1984 09 05	47.247 / 8.562	V	486
Vaz	1991 11 20	46.721 / 9.528	VI	352
Buchs	1992 05 08	47.156 / 9.562	V	39

4.1.1 Sponheuer Attenuation Model

For the seismic hazard study in Switzerland, Sägesser and Mayer-Rosa (1978) studied 39 earthquakes with macroseismic observations. In their study, the mean epicentral distances for each observed intensity degree was used to derive parameters of the Sponheuer attenuation law (equation 4-3) for individual earthquakes. Individual α values were then summarized to typical α values for particular seismic sources (see table 4.2) (Sägesser and Mayer-Rosa, 1978).

The attenuation parameter α was determined for different azimuths for intensity IV. If α showed an azimuthal dependence, an ellipse was fitted to the distribution of α as a first-order approximation. An azimuthal dependence could be recognized for 7 out of 39 events. Figure 4.1 shows the intensity decay modelled for an epicentral intensity VIII of the two seismic sources characterized by the strongest azimuthal dependence of α, i.e. the Valais and the Engadine.
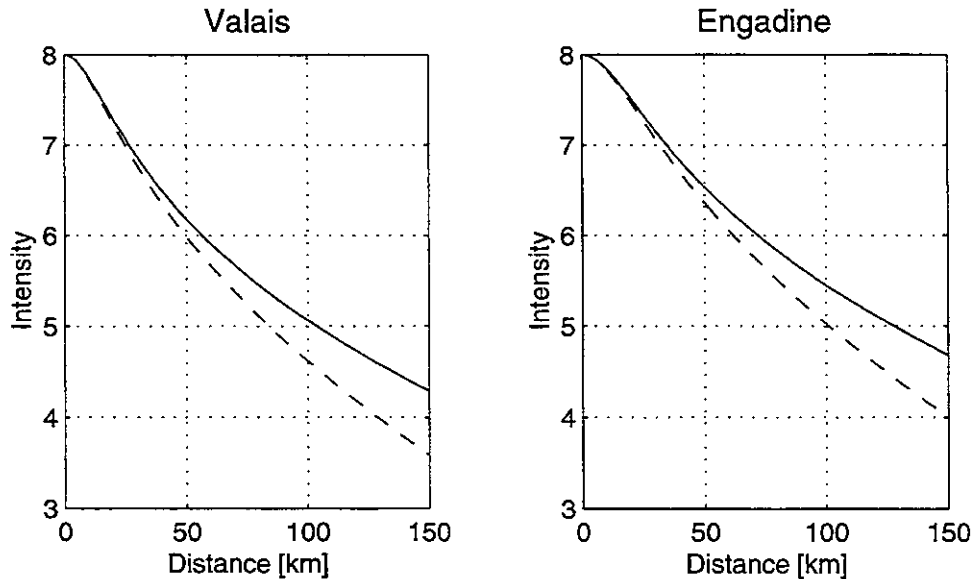

Figure 4.1: Intensity attenuation versus distance for earthquakes of epicentral intensity VIII in the Valais and the Engadine. The dashed curves are for the direction with the highest attenuation, the solid curves for the direction with the lowest attenuation.

The figure shows, that azimuthal dependence of the parameter α has a significant influence on the calculated intensity only for distances greater than 100 km. The azimuthal dependence has, therefore, to be studied with the distribution of the lower intensity degrees. These lower intensities usually have, however, a low resolution and their isoseismal radii are usually badly determined caused by the necessary involvement of neighbouring countries. Higher intensity degrees for the same events do not show such a pronounced directional effect. In addition, other earthquakes of the same seismic sources show a more or less azimuthal symmetry. The azimuthal dependence will, therefore, not be considered in this study. This conclusion is further more supported by recent studies based on instrumental data which stress, that scattering and site effects

are more important than azimuthal dependence (Joyner and Boore, 1988). The azimuthal dependence of α has, however, only a minor relevance for the calculated seismic hazard, since its influence is restricted to the far field.

In this study, a different approach is chosen to estimate the parameters of the Sponheuer attenuation law. For single earthquakes, isoseismal areas are determined for different intensity degrees. Assuming radially symmetric attenuation, radii can be calculated from the corresponding isoseismal areas. Reliable macroseismic data are available for 9 earthquakes since 1976 (see table 4.1). For these events and 25 earthquakes prior to 1976, isoseismal areas have been determined. With the corresponding radii, attenuation parameters were estimated. This was only possible for those seismic sources, where macroseismic data are sufficient. The results are summarized in table 4.2. Differences relative to earlier studies (Sägesser and Mayer-Rosa, 1978) are:

- For the Swabian Jura region the determined radii, including the event of 1978/09/13, match the previous attenuation curve. The original α value of 0.001 is therefore acceptable.

- In the region of Basel, the event of Sierentz on 1980/07/15 provided macroseismic data, which allowed to determine new relations with a lower α value of 0.001.

- In the region of Zurich only very few data were available prior to the event of 1984/05/09. This event provided sufficient data to draw the isoseismal of intensity degree IV. The derived attenuation law shows the best fit for an α value of 0.003 and a hypocentral depth of 20 km. Although only few data are available, the obtained value is reasonable. A focal depth of 15 km for this event was instrumentally determined (Deichmann and Rybach, 1989), which is reasonable close to the macroseismic depth.

- No new data are available for the region of the Lake of Constance. The determined isoseismal radii of the strongest event show an α value of 0.003, which is lower than the value of the 1976 study.

- The very strong attenuation with an α value of 0.056 for the area of Yverdon is confirmed by the determined new isoseismal radii.

- In the region of the Berner Oberland there is only one event with sufficient data to estimate isoseismal areas. This event shows a higher α value of 0.008 and a greater macroseismic depth of 25 km than the value of the previous study (10 km).

- For central Switzerland, four well-documented earthquakes are available before 1976. They show an attenuation α of 0.008, which is slightly higher than the previous value.

- The attenuation law derived for the region of Glarus is mainly determined by the 1971/09/29 event, which shows a clear azimuthal dependence, with stronger attenuation in east-west direction than in north-south direction. If radially symmetric attenuation is assumed, the estimated α value (0.008) lies between the values for the two previously determined attenuation directions.

- The 1992/05/08 event in Buchs is presently the macroseismically best investigated

earthquake for this region. The estimated α value (0.006) is higher than the previous value. This can be accepted, since the determined macroseismic depth is very close to the instrumentally determined hypocentral depth.

- Azimuthal dependence was previously defined for the central and eastern Valais. Estimated α values for these two regions are 0.003 and 0.01 assuming radially symmetry. These values lie within the range of the values of the previous study, with a smaller attenuation for the central Valais and a higher attenuation for the eastern Valais.

- The strongest earthquake in Switzerland since 25 years occurred on 1991/11/20 in Grisons. This event provided a good macroseismic data set with 352 observations. The α value obtained is 0.003.

- No new data are available for the Engadine. The determined α value of 0.006 is slightly higher than the value of the previous study.

The attenuation parameters determined in this study are distributed more consistently over Switzerland than the values of the previous study. In the northern Alpine foreland the new values are generally low (between 0.001 and 0.003). The attenuation increases towards central and eastern Switzerland, with values between 0.006 and 0.008. Earthquakes in the Valais and in Grisons show again lower attenuation values. However, the available macroseismic data are quite poor for some of the seismic sources and, therefore, produce unstable and questionable estimates of the attenuation parameter. These findings emphasize how important the determination of attenuation parameters is for the various regions in Switzerland.

Figure 4.2 displays a simplified tectonic map of Switzerland. Superimposed are the locations of the earthquakes which were used for estimating intensity attenuation parameters. The characteristics in the attenuation behavior suggests a delineation of three regions: 1) the Alpine foreland which covers the area north of the Helvetic and Ultrahelvetic nappes, 2) the Helvetic and Ultrahelvetic nappes and Penninic sediments in detachment nappes, and 3) the crystalline basement and Penninic nappes of the Alps, and the crystalline basement and nappes of the Austroalpine realm. For simplicity, region I will be referred to as the Alpine foreland, region II as the Subalpine chains, and region III as the Alpine chain. In these three regions all macroseismic data have been simultaneously evaluated to determine the attenuation parameter α. In this procedure the macroseismic depth has been kept at the previous determined values in order to account for different depth distributions in different seismic sources. The data and the estimated attenuation laws are shown in figure 4.3. The evaluation of all data within one region results in more stable attenuation parameters. Table 4.3 lists the results for the three regions mentioned.
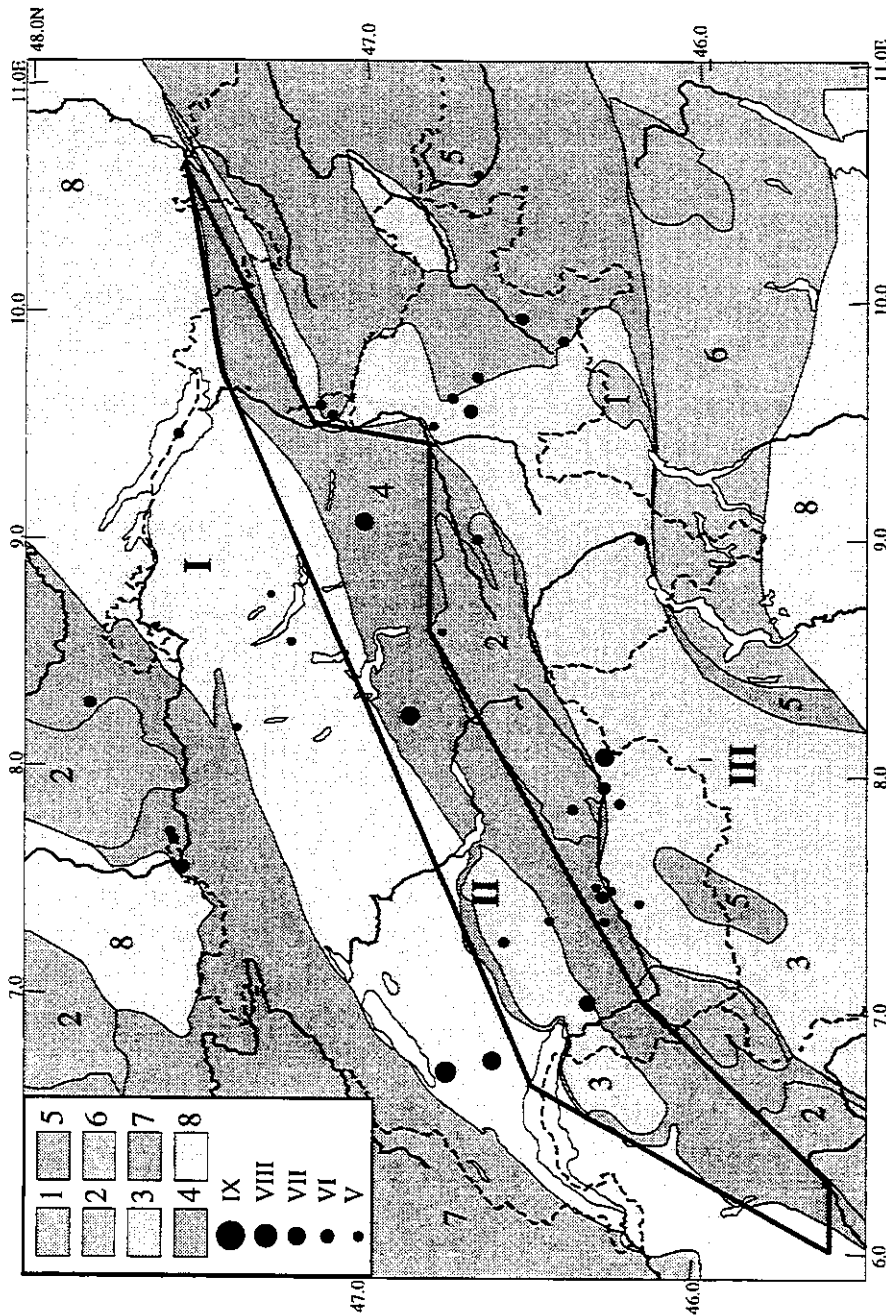
Figure 4.2: Simplified tectonic map of Switzerland with the main tectonic units. Indicated are the three regions, which show different intensity attenuation characteristic, i.e. the Alpine foreland (I), the Subalpine chains (II) and the Alpine chain (III). Superimposed are the locations of earthquakes which were used to estimate the attenuation parameters. The size of the symbol corresponds to the epicentral intensity.

Tectonic units:

1 Tertiary intrusive and volcanic units

2 Crystalline massifs and basement

3 Penninic nappes

4 Helvetic autochthonous sediments, Helvetic and Ultrahelvetic nappes

5 Austroalpine nappes

6 Southern Alps

7 Folded and tabular Jura

8 Tertiary sediments, Molasse

Table 4.2: Determined attenuation parameters α and corresponding macroseismic depths for the 1976 study (Sägesser & Mayer-Rosa, 1978) and for this study

Seismic source	α (1976)	depth (1976)	α (this study)	depth (this study)
Swabian Jura	0.001	10.0	0.001	10.0
Basel	0.025	16.0	0.001	10.0
Zurich	0.005	10.0	0.003	20.0
Lake of Constance	0.01-0.008	10.0	0.003	10.0
Yverdon	0.075	5.0	0.056	5.0
Berner Oberland	0.005	10.0	0.008	25.0
Central Switzerland	0.003-0.005	6.0	0.008	7.5
Glarus	0.017-0.026	6.0	0.007	5.0
Rhine Valley	0.001	5.0	0.006	7.5
Central Valais	0.004-0.008	15.0	0.003	15.0
Eastern Valais	0.004-0.008	15.0	0.011	20.0
Central Grisons	0.001	10.0	0.003	10.0
Engadine	0.0025-0.005	20.0	0.006	15.0
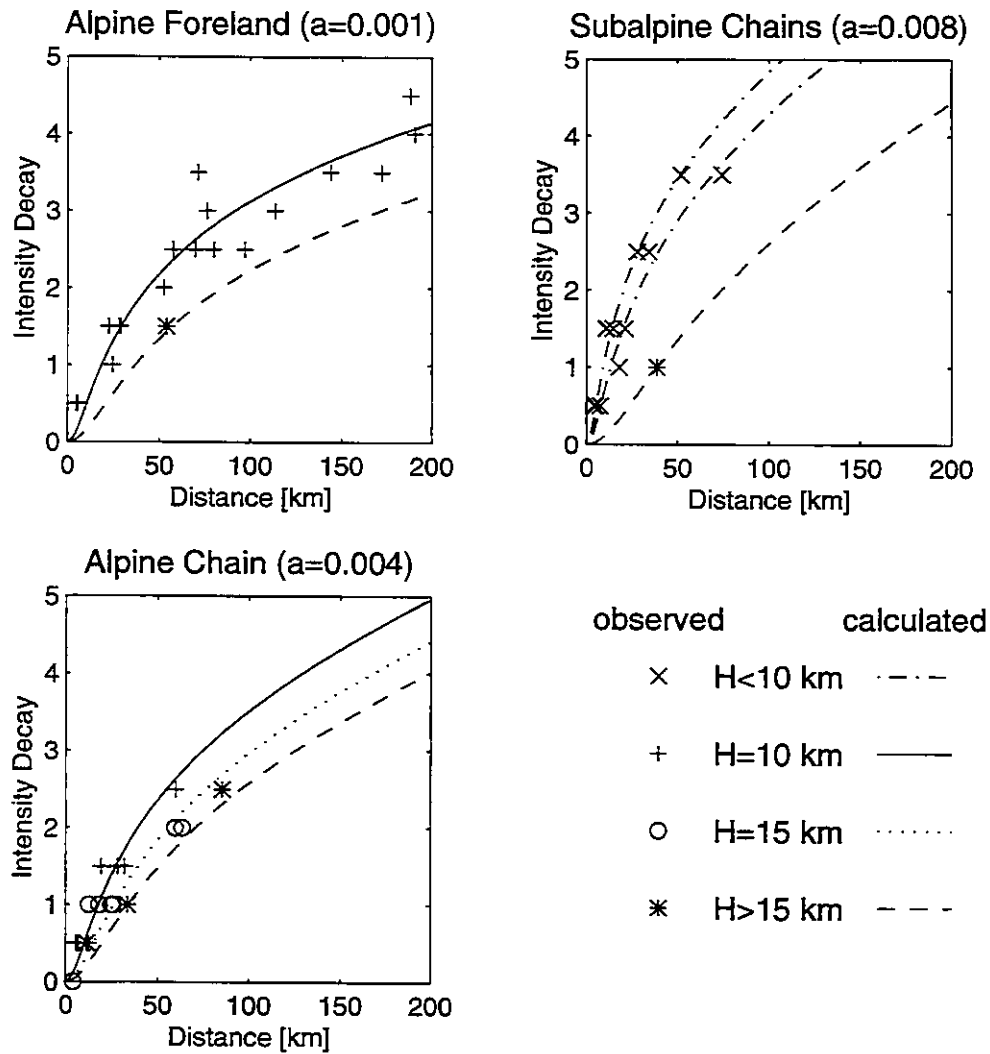
Figure 4.3:Intensity attenuation versus distance for the three defined regions in Switzerland (cf. figure 4.2): The α values determined by the Sponheuer attenuation law are presented. The indicated parameter H corresponds to the focal depth of the seismic events used.

Table 4.3: Attenuation parameter α and its standard deviation σ for the three regions defined in Switzerland

Region	α	σ_α
Alpine Foreland	0.001	0.0006
Subalpine Chains	0.008	0.0027
Alpine Chain	0.004	0.0017

4.1.2 Scattered Attenuation Model

The deterministic attenuation models following the Sponheuer law (Sponheuer, 1960) do not account for the non-negligible scatter of observed intensity data versus distance. Hazard calculations, however, can take scattering into account by assuming a standard deviation in the attenuation law. The observed intensities for the 1964/3/14 earthquake in central Switzerland (figure 4.4) and the Sponheuer attenuation relation determined for this area demonstrate the significant scatter of data. Scattering of intensity values versus distance is firstly caused by physical effects, such as directivity of the radiated energy or influence of local geology settings, and secondly due to the intensity data themselves, which cannot always be exactly determined. The significant scattering observed must be represented by an appropriate attenuation model. A statistical attenuation model is, therefore, introduced in this work to describe attenuation of intensity data.
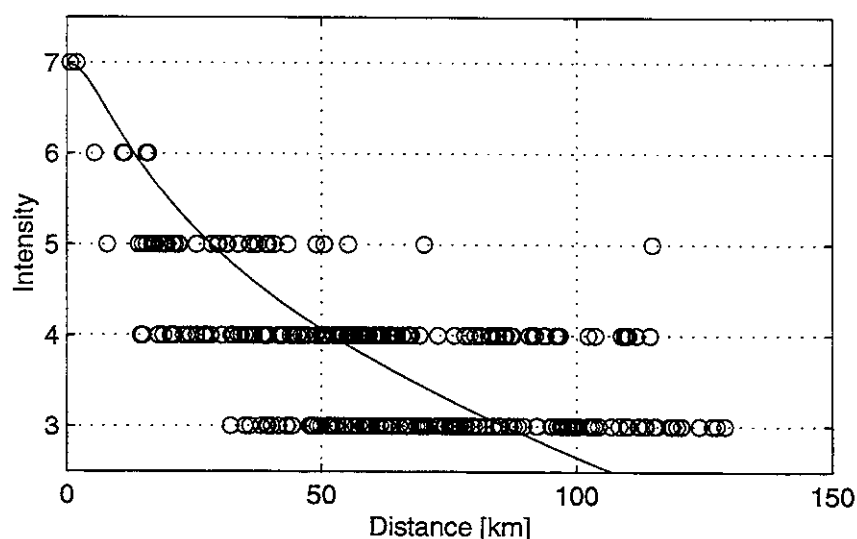

Figure 4.4: Observed intensity distribution (open circles) versus distance for the 1964/ 03/14 event. The solid line represents the determined Sponheuer attenuation law for Subalpine chains.

The fundamental idea is to model the mean intensity attenuation similar to the Sponheuer law, but to allow for the scatter by a standard deviation, which is used in a discretized normal distribution. The discretized normal distribution accounts for the integer-based definition of the intensity scale. In a first step, mean intensity values for discrete distance ranges are calculated and fitted with an isotropic model. The model is chosen on the basis of physical and statistical considerations, with a stronger motivation to fit the observed data rather than base them on a well-founded physical background. The distance ranges used for the calculation of mean intensities are:

- in the near field: 0-2.5, 2.5-7.5 and 7.5-15 km,

- from 15 km to 90 km the distance intervals are 7.5 km wide,

- larger distances: 90-100,100-125,125-150,150-200 km.

Data situated at epicentral distances greater than 200 km from the epicenter are not considered. Other distance ranges have been tested, but no dependence of the chosen ranges on the results could be observed, unless the ranges were so small that they did not provide significant data to estimate mean intensities. Figure 4.5 shows the attenuation of the mean intensity of all earthquakes with an epicentral intensity VII in the Subalpine chains. From this attenuation behavior, which is characteristic for the data in Switzerland, it can be concluded that:

- The mean intensity I_m follows a law, where intensity is proportional to the logarithm of energy (cf. equation 4-1). The applied formula (4-4), which is related to the formula proposed by Blake (1941) is:

$$I_m = I_0 - f - g \ln \left(\frac{\sqrt{R^2 + (H/2)^2}}{(H/2)} \right) \qquad (4\text{-}4)$$

where

I_0 epicentral intensity

I_m mean intensity

R distance between epicenter and site

H hypocentral depth

f, g characteristic parameters

- The standard deviation is constant with distance and has a value of 0.8.

- The mean intensity values are biased for greater distances, because intensity values of degree II and I are missing in the data set.

Further analysis of the behavior of the mean intensity versus distance for single events showed, that the parameter g, which describes the geometric attenuation, depends on the region where the event occurred. On the other hand, the parameter f depends on the epicentral intensity and not on the region considered. In a first step the parameter f has, therefore, been estimated based on all events with equal epicentral intensity. Only observations in the near field, i.e. with epicentral distance R ≤ 30 km, were used, since attenuation in the far field is strongly influenced by the parameter g. A least-square estimation scheme was applied, because the standard deviation is constant with distance. For epicentral intensity V, VI, and VII curves were fitted (figure 4.6) and the parameter f was estimated (table 4.4).

Table 4.4: Attenuation parameter f for different epicentral intensities

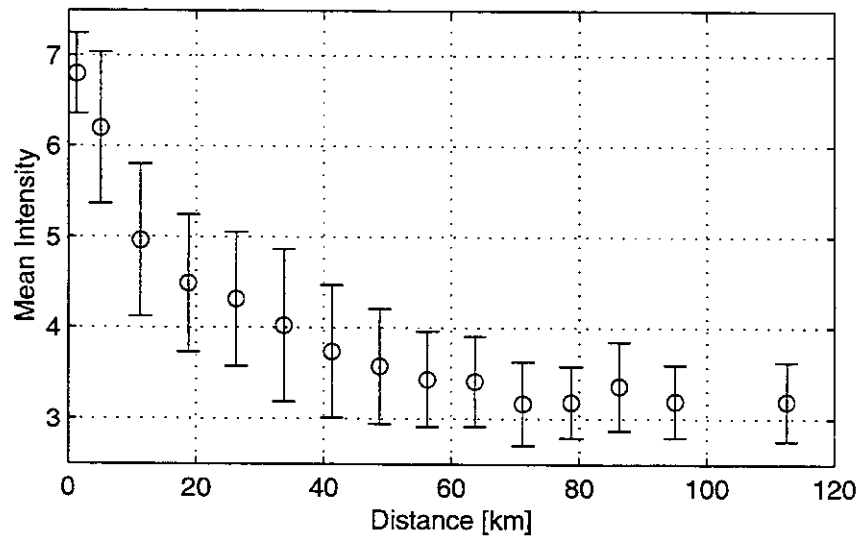| Epicentral Intensity	f	σ_f
V	0.5	0.08
VI	0.5	0.11
VII	0.15	0.10

Figure 4.5: Observed mean intensities and standard deviation in discrete distance ranges for all earthquakes with an epicentral intensity VII in the Subalpine chains.
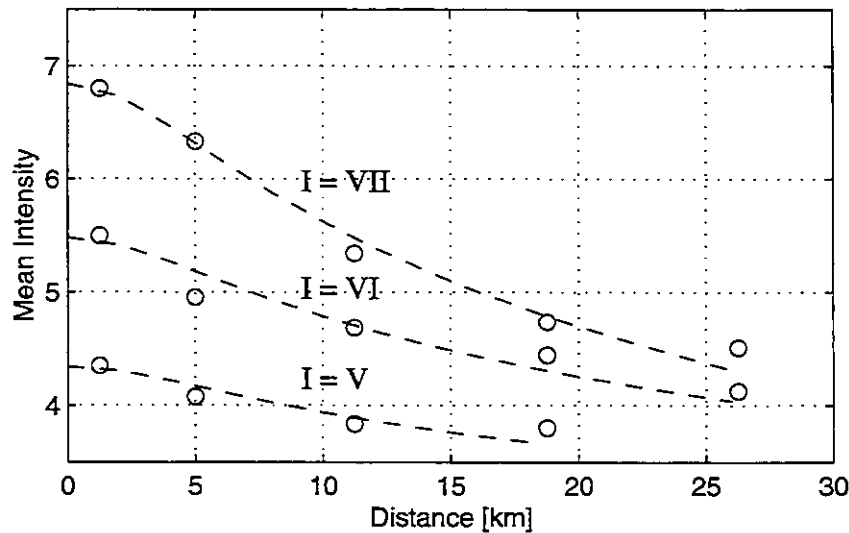
Figure 4.6: Observed mean intensities in the near field in discrete distance ranges (circles) for intensities V, VI and VII. The dashed lines correspond to the logarithmic attenuation model fitted by a least-square algorithm for each individual intensity.

In a second step, the parameter g was estimated for the three characteristic regions, i.e. the Alpine foreland, the Subalpine chains and the Alpine chain (figures 4.7 to 4.9).

In the Alpine foreland, a large number of observations belongs to an epicentral intensity VII (figure 4.7a). The shortcoming of these observations is, that they are only available for distances greater than 60 km, because these events occurred in the Swabian Jura and German macroseismic data are missing. This fact implies a rather unstable least-square estimation. The events with epicentral intensity V and VI yield an estimate of g between 0.81 ± 0.06 and 0.84 ± 0.04 (figures 4.7b and 4.7c). Nevertheless, also the observations from the Swabian Jura fit a model with a g value of 0.84 (figure 4.7d). Hence, a value of g equal 0.84 is adopted for the Alpine foreland.

In the Subalpine chains, about 90% of the observations come from events of intensity VII (figure 4.8a). The mean intensities in this regions show a stronger attenuation than in the Alpine foreland (g = 1.18 ± 0.02).

In the Alpine chain, the parameter g could be estimated for epicentral intensities VI and VII, and varies between 0.68 ± 0.01 (figure 4.9a) and 0.78 ± 0.04 (figure 4.9b). For this region, the mean of the two values is adopted (0.73 ± 0.04).

The attenuation parameters g for the mean intensities show the same variation as the parameters α in the Sponheuer attenuation law (see table 4.5). The Subalpine chains show again the highest value, i.e. the highest attenuation of intensity with distance. The northern Alpine foreland and the Alpine chain show significantly lower attenuation parameters.

Table 4.5: Attenuation parameters g for Switzerland

Regions	g	σ_g
Alpine foreland	0.84	0.04
Subalpine chains	1.18	0.02
Alpine chain	0.73	0.04

Up to now, attenuation laws have been defined for the observed mean intensities. In order to avoid calculated intensity values with decimal places, which are obtained when mean intensities are calculated for a given distance, a truncated normal distribution is applied to reconstruct the original scatter of the data. The probability P for an intensity I with parameters I_m and σ is given by:

$$P = \frac{1}{\sqrt{2\pi}\sigma} \int_{(I-0.5)}^{(I+0.5)} \exp\left(\frac{-(x-I_m)^2}{2\sigma^2}\right) dx \qquad (4\text{-}5)$$

where

I_m mean intensity, i.e. mean of a normal distribution

σ standard deviation of a normal distribution

The mean intensity I_m is determined by the attenuation law (4-4); σ is the standard deviation of the mean intensity. The probability distribution is truncated for values higher than the epicentral intensity. The scaling of the truncated probability distribution to 1 yields a distribution with a smaller variance. Within this definition, it is possible to model the scatter of the intensity data and to take the integer-based character of the intensity values into account.

The defined standard deviation of 0.8 of the observed intensities versus distance is determined by uncertainties in intensity determinations as well as for "real" scattering of attenuation. Also uncertainties in epicentral intensity estimates are affecting the standard deviation of the attenuation model. It is necessary, therefore, to correct the standard deviation in the attenuation model for the uncertainty in epicentral intensities, since this uncertainty is treated separately (cf. Chapter 2.4.3). The uncertainty in the epicentral intensities, which has been used to develop the scattered attenuation model, is half an intensity degree. This uncertainty is accounted for by a distribution which assigns a probability of 0.6 to the determined epicentral intensity, 0.15 to one degree higher and 0.25 to one degree lower, respectively (see table 2.2). Taking this epicentral uncertainty into account, best results are obtained with a standard deviation of 0.4. The chi2-maximum-likelihood ratio test (Meyer, 1975) was used to test different standard deviations. With a standard deviation of 0.4 significance levels between 0.8 and 0.95

for distances less than 40 km are obtained. For greater distances the significance levels lie between 0.05 and 0.25. Significance levels for accepting a model are usually as low as 0.05 or 0.1. A model is rejected if the significance is less than the selected level. The significance levels obtained are much higher and the attenuation model with a standard deviation of 0.4 can be accepted.
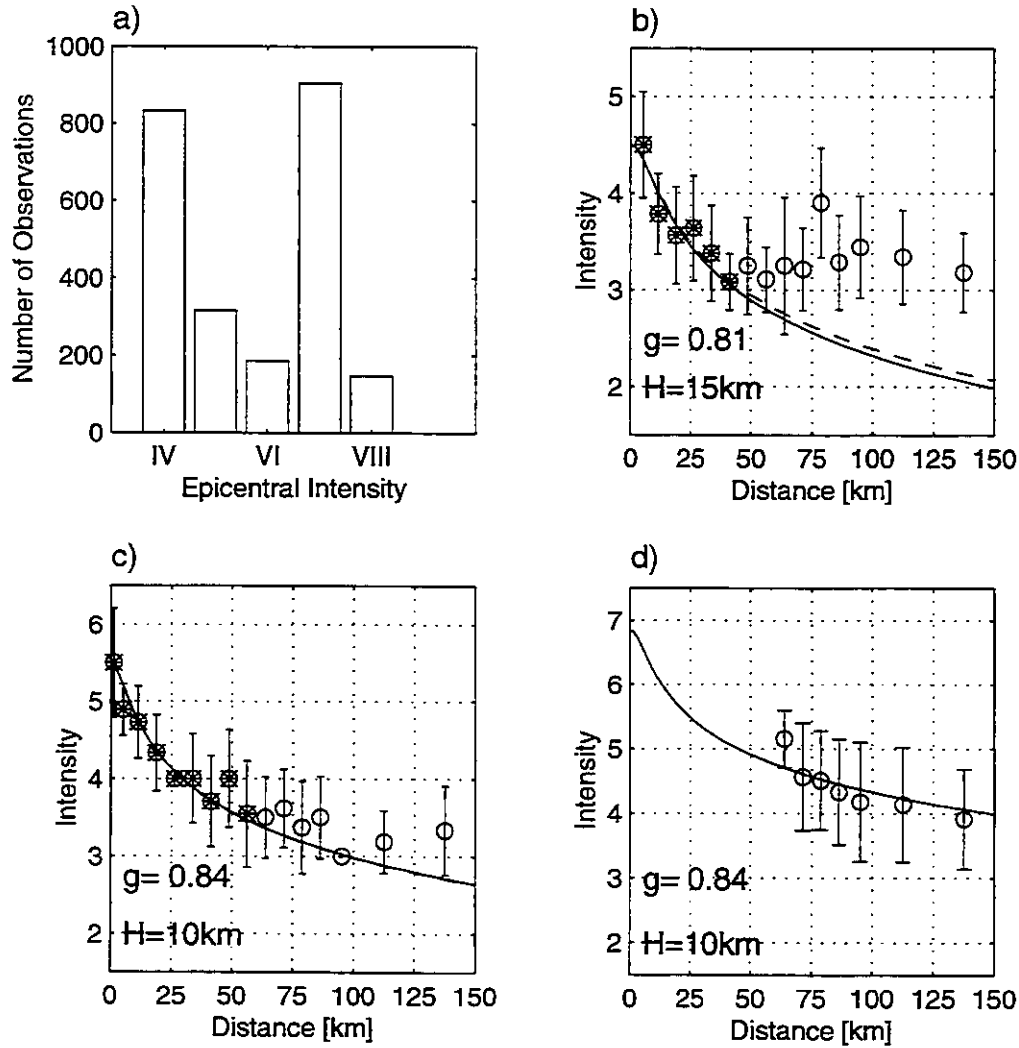

Figure 4.7: Alpine foreland: a) Number of observations for different epicentral intensities. b-d) Attenuation model: Only the data points labelled with stars were used to estimate the model parameter g. The dashed line indicates the best fit and the solid lines indicate the adopted model.

To illustrate the combination of epicentral intensity errors and attenuation model, figure 4.10 displays calculated probability distributions (bars) for an earthquake with intensity VII (with an error of ±0.5) in the Subalpine chains at a depth of 6 km. The determined probability distributions of the observed intensities for this region are shown by stars. For small distances (<2.5 km) the modelled variations in the intensities correspond to

the uncertainty in the epicentral intensity. Deviations between observed and modelled probabilities for greater distances occur, because no observations are available for intensity degrees I and II. However, the scattered attenuation law models the observed variation in the intensity data with good accuracy.
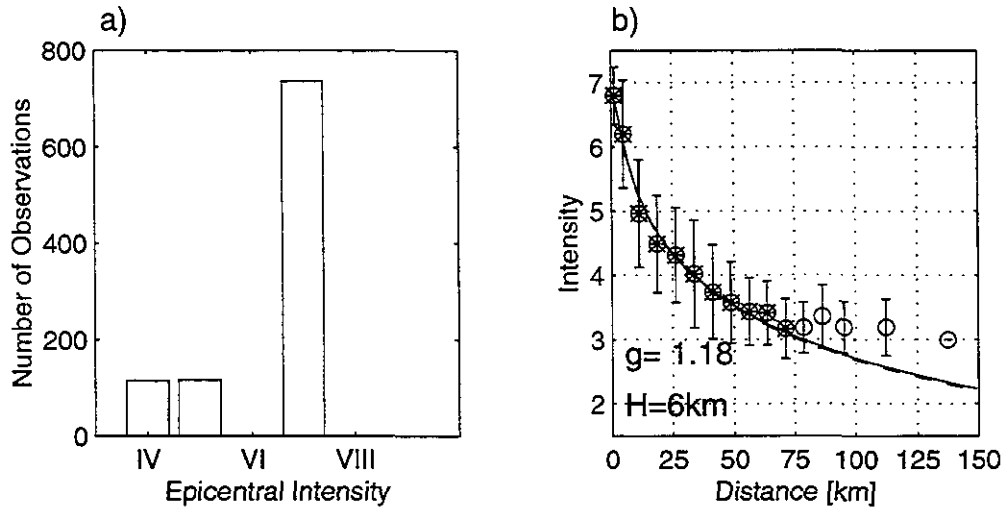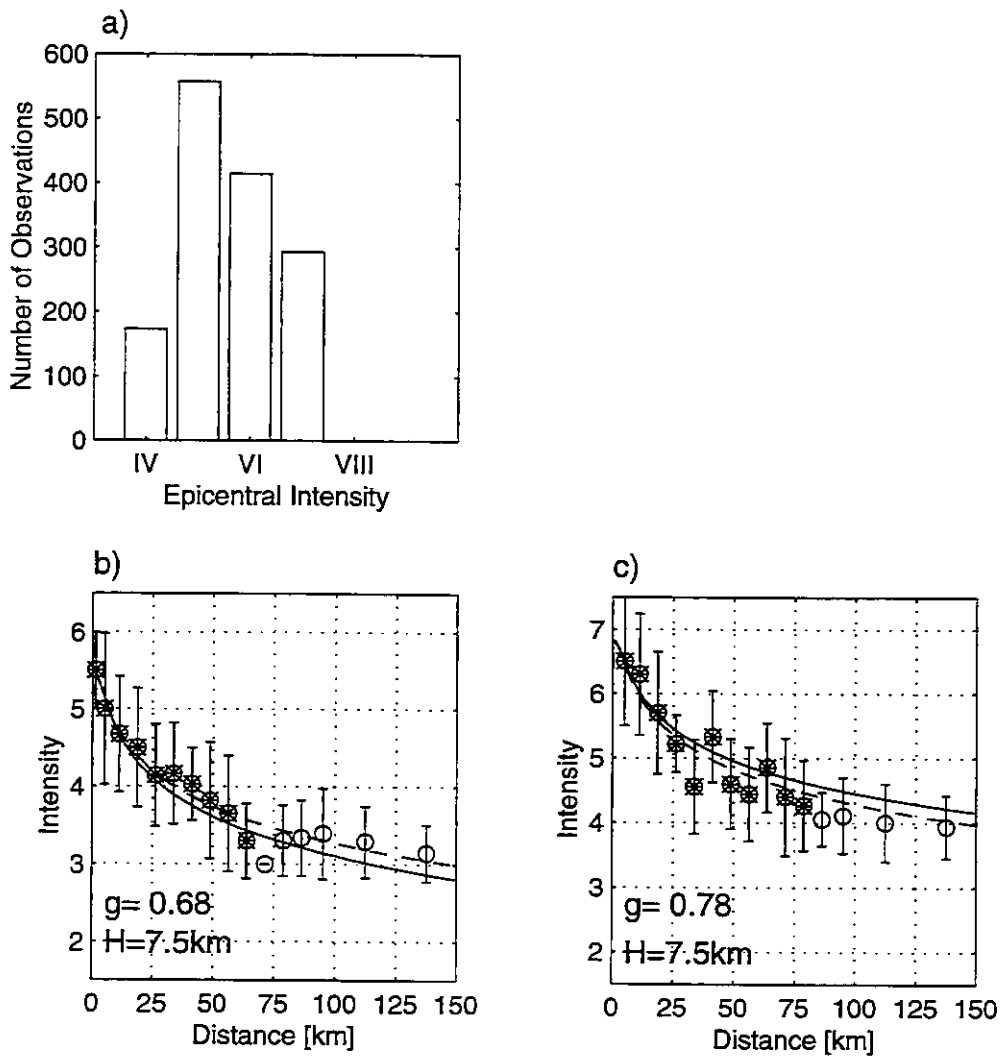

Figure 4.8: Subalpine chains: a) Number of observations for different epicentral intensities. b) Attenuation model: Only the data points labelled with stars were used to estimate the model parameter g. The dashed line indicates the best fit and the solid line indicates the adopted model.

Figure 4.9: Alpine chain: a) Number of observations for different epicentral intensities. b-c) Attenuation model: Only the data points labelled with stars were used to estimate the model parameter g. The dashed lines indicate the best fit and the solid lines indicate the adopted model.
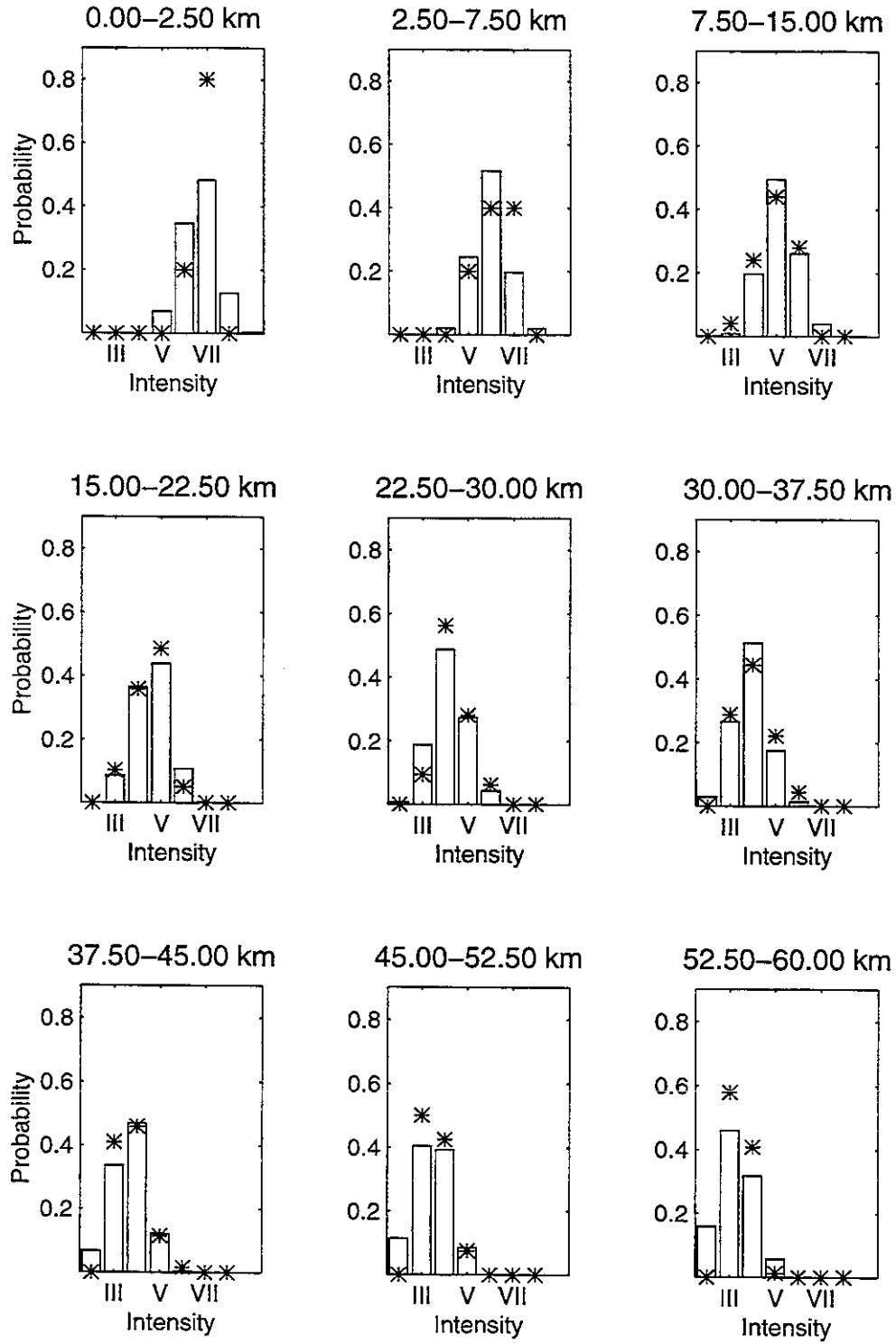
Figure 4.10:Modelled probability distributions (bars) for an event with epicentral intensity VII in the Subalpine chains for selected distance ranges. The determined probabilities of the observed intensities are labelled with stars.

4.2   Influence of Local Soil Conditions

The influence of local geologic settings on the intensity of shaking was clearly shown by recent earthquake catastrophes (Michoacan in Mexico City 1985 (Sánchez-Sesma et al., 1988), Armenia 1988 (Wyllie, 1989), Loma Prieta 1989 (Boatwright, 1991)). In the framework of a pilot study, carried out in the Canton Obwalden, a three-step approach was applied to study the influence of local geologic settings on macroseismic intensity: 1) intensities were calculated based on the Sponheuer attenuation laws, 2) calculated intensities were compared with observed intensities, and 3) relations of ground motion amplification versus soil type conditions were established (cf. Schindler et al., 1993).

Attenuation laws following Sponheuer's (1960) definition (cf. Chapter 4.1.1) have been used in the first step to calculate macroseismic intensities for all sites, where macroseismic observations were available. All sites have been classified according to their local geologic settings into geotechnical units, following the definitions of the simplified geotechnical map of Switzerland (scale 1:200'000, Rösli (1990)). Based on this classification, differences between observed and calculated intensities have been derived in the second step for all sites belonging to the same geotechnical unit. Figure 4.11 displays a typical result of such an analysis. The histogram shows the broad variation of the derived differences for observations on marly schists, with a mean difference of +0.42 intensity units and a standard deviation of 0.93. The large standard deviation may be caused by the rather rough classification of geologic settings based on geotectonic maps (Schindler et al., 1993). However, it was observed, that the differences derived are generally higher for unconsolidated soils and higher ground water levels.
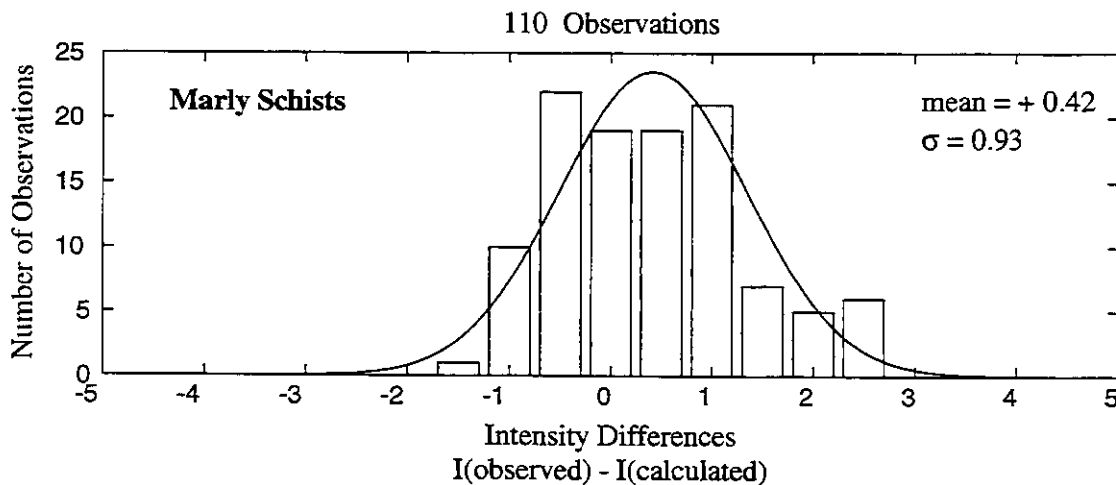

Figure 4.11:Variation in intensity differences between observed and calculated intensities for the geotechnical unit of marly schists (with a mean difference of 0.42 intensity units and a standard deviation of 0.93).

In the third step, preliminary intensity correction factors for different geotechnical units were defined. The correction values are summarized in table 4.6. In addition, the correction values applied in the U.S. for comparable geologic units are listed (Evernden and Thomson, 1985). Despite the rough classification in geotechnical units, and the

doubtful correlation of geotechnical units in Switzerland with geologic units in California, the derived correction scheme shows some similarity.

At this point it is necessary to define the local geologic settings for which the attenuation laws developed in chapter 4.1 are valid. The distribution of macroseismic observations versus geotechnical units (figure 4.12) shows that most of the observations have been made on unconsolidated soils (geotechnical unit 3 to 7 (Rösli, 1990)). It can be concluded, therefore, that the attenuation laws are more appropriate for unconsolidated soils. However, the modelled variation in intensity attenuation includes also the variation of local soil conditions.

More work has to be done before well-defined correction scheme can be derived, which account for local geologic settings. Studying significant local differences (Fäh (1985), Beer (1996)) seems to be more promising than a rather coarse classification. Also numerical waveform simulations, at present carried out for the city of Basel, will help to understand observed local anomalies (cf. Fäh, 1992).
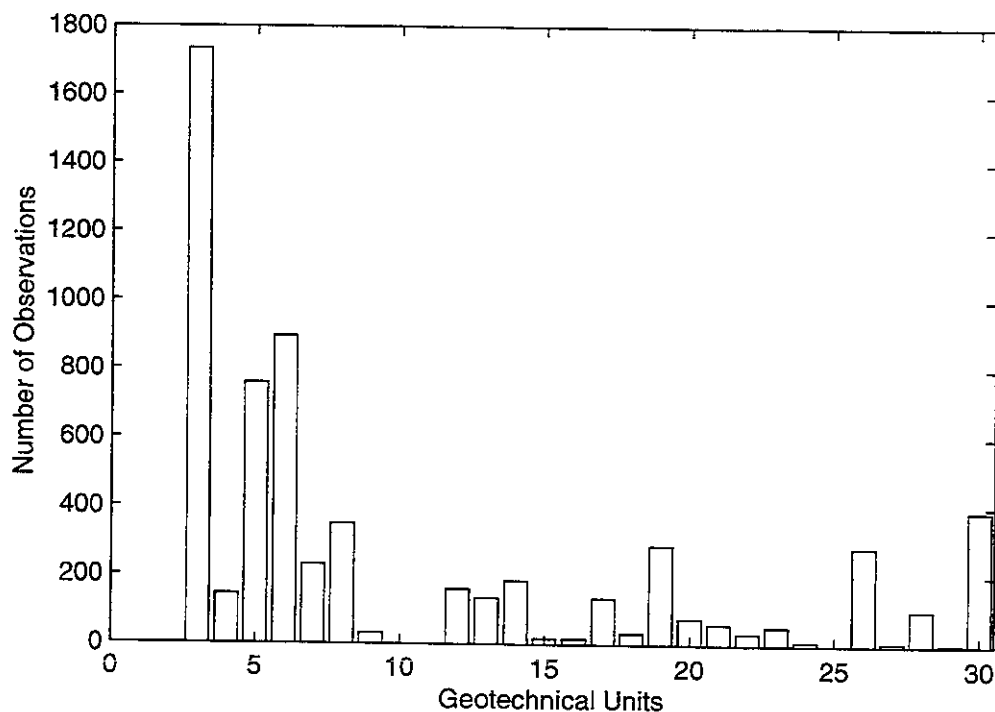

Figure 4.12:Number of macroseismic observations versus geotechnical units. Detailed descriptions of the geotechnical units are found in Rösli (1990). Units 3 to 7 correspond to unconsolidated soils, units 8 to 30 define rock outcrops.

Table 4.6: Values of intensity correction for different geologic settings. The first two rows are derived by Schindler et al. (1993) for geotechnical units in Switzerland (Rösli, 1990), the last two rows are derived by Evernden and Thomson (1985) for geologic units in California (defined by the California Division of Mines)

Geotechnical unit Switzerland	Intensity correction	Geologic unit California	Intensity correction
marly limestones massive limestones dolomite and gypsum	+0.4 +0.2 0	early Mesozoic sedimentary rocks	-0.5
marly schists with interca-lations of sandstone	+0.4	undivided Tertiary sedimentary rocks	0
various conglomerates	+0.2	Pliocene-Pleistocene sedimentary rocks	+0.7
unconsolidated sediments dependent on depth to ground water level 0 - 9 m 9 - 30 m > 30 m	 +1.5 +0.5 0	Quaternary sedimentary rocks dependent on depth to ground water level 0 - 9 m 9 - 30 m > 30 m	 +1.7 +0.7 +0.2

Chapter 5

APPLICATION TO SEISMIC HAZARD IN SWITZERLAND

5.1 Modelling of Macroseismic Intensity for Individual Earthquakes

The defined attenuation model (chapter 4) and error models of uncertainties in earthquake size and location (chapter 2) permit the calculation of ground motion probability distributions of individual earthquakes for specific sites. This is the first step in the method developed to calculate seismic hazard relations (cf. chapter 3.1). The ground motion probabilities for all earthquakes at a particular site define the "Earthquake Site Catalog" (ESC). For three individual earthquakes, expected ground motions are modelled in order to demonstrate the applicability of the developed model.

The earthquakes used are the event of 1991/11/20 in Vaz (Grisons), the event of 1964/03/14 in Sarnen and the Basel earthquake of 1356/10/18. The first two events are selected, because the amount and quality of macroseismic data are sufficient to check the calculated macroseismic intensities with observed intensities. The Basel event is used to show the applicability of the models for higher degrees of intensity. The intensities are calculated for a site near the epicenter and for a more distant site. The parameters of the earthquakes are summarized in table 5.1. Errors in epicentral intensity and location are modelled by probability distributions as discussed in chapter 2.

Table 5.1: Parameters of the 3 selected earthquakes

Date	I_0	ΔI_0	Lat.	Long.	Location error [km]	Depth [km]
1991 11 20	VI	0	46.721	9.528	2.5	7
1964 03 14	VII	0.5	46.950	8.280	5.0	7.5
1356 10 18	IX	1	47.467	7.6	10.0	10

The intensity distributions of the 1991/11/20 earthquake in Grisons are modelled for the city of Chur at an epicentral distance of 15 km, and for Zurich at an epicentral distance

of 130 km (figure 5.1). The attenuation model for the Alpine chain is used (cf. chapter 4.1.2). A probability of almost 90% is calculated for intensity IV and V together at Chur (figure 5.1a). This coincides with the observed intensity range of IV to V in Chur. Also for Zurich the calculated intensity III with a probability of 65% (figure 5.1b) is confirmed by the observations. In Zurich, 55% of the observations indicate an intensity III, 25% an intensity II and 20% an intensity IV.

The calculated intensity distributions for the 1964/03/14 earthquake in Sarnen show a broader range than the distribution of the previous example. This is mainly caused by the uncertainty of epicentral intensity. In Stans, which is at an epicentral distance of 10 km, there is a calculated probability of 75% for intensities V and VI together (figure 5.2a). The observed intensity in Stans was VI, which is well within the calculated range. The observed intensity of degree IV in Zurich (at a distance of 55 km) agrees very well with the calculated intensity distribution, which shows the highest probability for this intensity degree (figure 5.2b).

The 1356/10/18 earthquake near Basel has the highest uncertainties of all three examples in location as well as in epicentral intensity. Epicentral intensity estimates of different authors vary from intensity VIII to intensity X (Meyer et al. (1994) and references therein). To represent this uncertainty a probability distribution with 10% probability of intensity VIII, 60% of intensity IX and 30% of intensity X is chosen. The location error is assumed to be 10 km. A probability distribution defined by instrumental data is assumed to represent the uncertainty of hypocentral depth (cf. chapter 2.4). Intensities ranging from VI to X are calculated for Basel, which lies at a distance of 10 km. The broad scattering is caused by the various uncertainties which are considered in the calculation. Also for a rather distant site, e.g. Chur at a distance of 225 km, the wide range in intensity values is also apparent. However, the most probable intensity VI agrees with the observed isoseismal (Mayer-Rosa and Cadiot, 1979).The highest calculated intensities are based on the combination of the highest possible epicentral intensity (i.e. X) with the deepest assumed hypocenter (i.e. 25 - 30 km). This combination has more the character of a "worst case" scenario than of an exact modelling.

These three examples show that the developed attenuation models combined with the assessed error models predict properly intensity distributions for near as well as for distant sites. The models can therefore be used to calculate "Earthquake Site Catalogs", which represent the number of occurrences for different ground motion levels in history. Consequently, the ESC can be used to estimate recurrence parameters λ of a Poisson process.
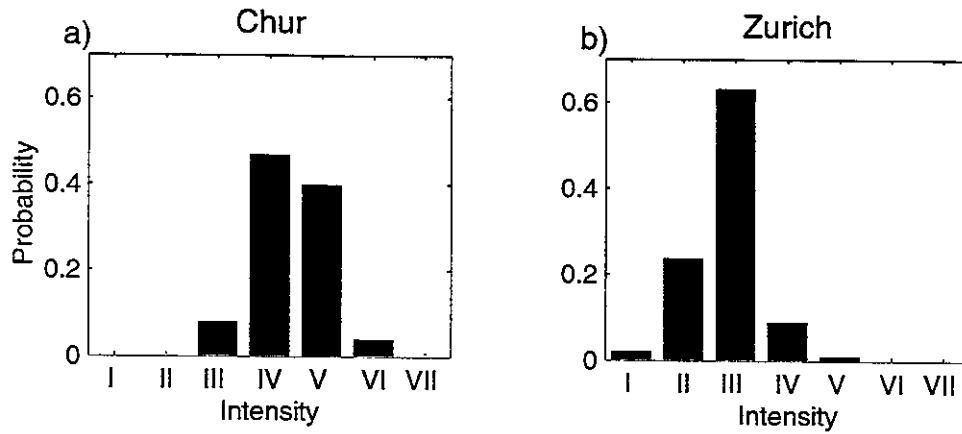
Figure 5.1: Calculated discrete intensity distributions for the 1991/11/20 earthquake with an epicentral intensity VI at two sites. a) for Chur at an epicentral distance of 15 km, and b) for Zurich at a distance of 130 km.
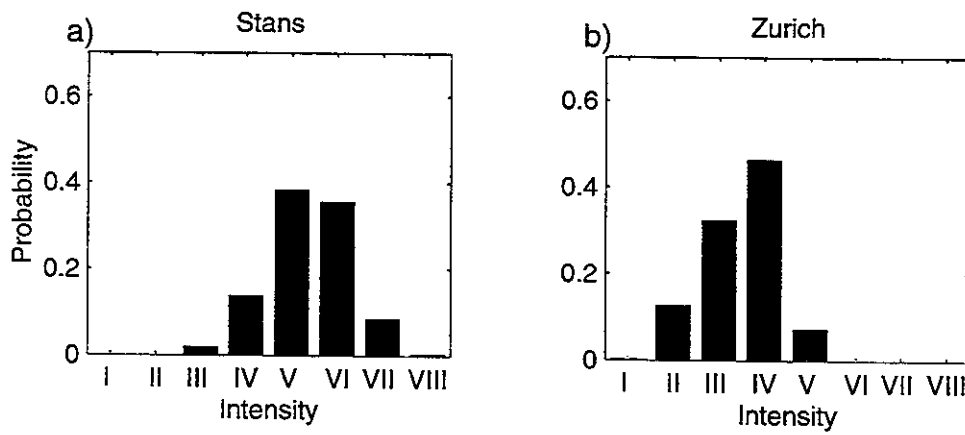

Figure 5.2: Calculated discrete intensity distributions for the 1964/03/14 earthquake with an epicentral intensity VII at two sites. a) for Stans at an epicentral distance of 10 km, and b) for Zurich at a distance of 55 km.
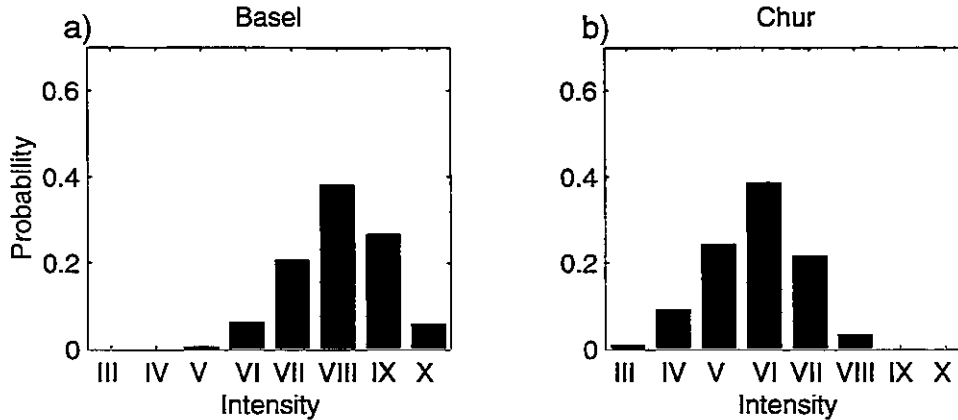
Figure 5.3: Calculated discrete intensity distributions for the 1356/10/18 earthquake with an epicentral intensity IX to X at two sites. a) for Basel at an epicentral distance of 10 km, and b) for Chur at a distance of 225 km.

5.2 Discussion of Seismic Hazard In Switzerland

As a result of this study hazard curves, i.e. return periods versus intensity, have been calculated for selected sites in Switzerland. The sites were chosen either because of their importance as an economic center or of their relative high seismic activity in the past. The economical centers are the cities of Zurich, Basel, Geneva, Bern, Chur and Lugano. Sites with a relative high seismic activity in the past are Brig, Sion, Samen, Yverdon, St. Moritz and Buchs. Return periods versus intensity are calculated for these 12 locations. Figure 5.4 shows the geographic locations of these twelve sites in Switzerland.

In a first step, the corresponding "Earthquake Site Catalogs" (ESC) are calculated (Appendix B), which contain the probability of occurrences for intensity V to XI since the 13th century. The ESCs show the contribution in intensity of all earthquakes in the extended Swiss Earthquake Catalog (see chapter 2.2) at a particular site. Distance distributions of the earthquakes which contributed to the site catalog (for intensity $\geq$V with a probability $\geq$0.1) are shown in Appendix B. These distributions show if the ESC is built up by earthquakes in the vicinity of the particular site or by earthquakes at greater distances.

In the second step, probability intervals of return periods are calculated by Bayesian estimation. In order to show the unbiased sample likelihood of intensity occurrences at a site, only a "minimal prior information" is used in the calculation (cf. chapter 3.5), which ensures that return periods increase with increasing intensity. However, the resulting return periods will still show broad distributions, if no occurrences are available (cf. chapter 3.5).
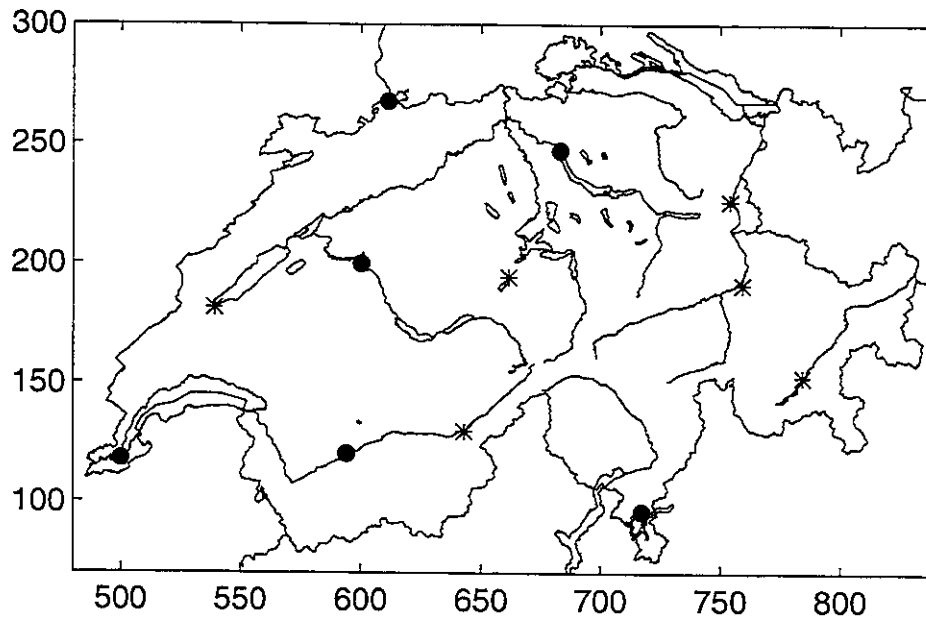
Figure 5.4: Geographic locations of the twelve sites, for which seismic hazard relations have been calculated. Points represent important economic centers, stars represent sites with a relative high seismic activity.

Figures 5.5 to 5.16 show return periods versus intensity for the selected twelve locations in alphabetical order. With the method developed in this study return periods are obtained as probability distributions. Two symmetric probability intervals around the median value are chosen in order to represent the probability distributions. The line indicated by crosses in figures 5.5 to 5.16 show the median of the probability distribution, the other four dotted lines border the 50% and the 90% symmetric probability interval, respectively. Return periods outside the 90% interval have, evidently, a probability of 10%. The lines connecting return periods of different intensities are only drawn in order to easily identify probability intervals. Only points indicated by crosses and circles have been calculated. For comparison, return periods calculated in the study by Sägesser and Mayer-Rosa (1978), which will be referred as SM78, are added by dashed lines.

In figure 5.5 the complete probability distributions for different intensity degrees are displayed. The figures 5.6 to 5.17 show only the points which border the 50% and 90% symmetric probability intervals. The probability distributions clearly demonstrate the great variance of estimated return periods, which is increasing with increasing intensities. This information is lost if only one representative value, e.g. the median or mean, is shown, which is usually the case in seismic hazard analysis.

Return periods estimated in SM78, i.e. calculated with standard hazard algorithms, lie within the 90% probability intervals for intensity degrees VI to VIII for ten out of the twelve locations. The return periods of SM78 for intensity V are slightly outside of the 90% intervals for Bern and Yverdon. Nevertheless, return periods estimated in SM78 are generally in the upper half of the 90% probability interval. Return periods of

intensity IX of SM78 are for all locations, except Brig and Sion, between 10'000 and 100'000 years. Values greater than 25'000 years are outside the symmetric 50% intervals. Two locations are selected to be discussed in detail, i.e. Brig, as an example of a location with a moderate to high seismic activity (figure 5.7), and Zurich as a site with low seismic activity (figure 5.16). The estimated return periods are summarized in tables 5.2 and 5.3, respectively.

Three prominent events occurred during the last 250 years in the Valais: the 1755/12/9 earthquake of Brig with an epicentral intensity of VIII (Volger, 1858), the 1855/07/25 earthquake of Visp with an intensity VIII to IX (Volger, 1858), and the 1946/07/25 earthquake in the Wildhorn area with an intensity VIII (Montandon, 1946). The effect of these three events can be recognized in the ESC for Brig (Appendix B4). The distance distribution (Appendix B14) of earthquakes which contributed to the site catalog shows the important influence of these near earthquakes. Return periods in SM78 for intensity VI to IX are within the 50% interval (figure 5.7). The uncertainty in return periods obtained by the developed method reflects the uncertainty of the input parameters. It has to be stressed, that in the method developed no assumptions have been made about the occurrences of earthquakes neither in size (for example Gutenberg-Richter relation (1944)) nor in space (by seismic source delineations (cf. Cornell, 1968).

The earthquake history for Zurich is quite different. The ESC (Appendix B13) shows a low seismic activity characterized by an almost negligible number of events with intensity $\geq$ VII. No earthquake is known in the past which produced severe damages in Zurich. The significant contributions in the upper intensity range stems from the 1356/10/18 earthquake near Basel. The distance distributions of earthquakes (Appendix B17) which contributed to the site catalog clearly shows that the main influence is produced by earthquakes at distances between 100 km and 150 km. Within this distance range are the active regions of central Switzerland, the Swabian Jura and Basel. Return periods in SM78 for intensity VI to IX are within the 90% interval. However, return period by SM78 are clearly outside the 50% (figure 5.15).

The earthquake history in Zurich exhibits the effect of the limited period of earthquake recording. In the developed method, estimated return periods of intensities which did not occur in the time period of observation, depend only on the length of this time period. The only information available is that no event of intensity IX occurred in Zurich during the time period of observations, i.e. in the past 700 years. This information is obviously not enough to estimate long return periods and consequently, large probability intervals for the return periods are obtained.

The long return periods which are obtained by the hazard analysis following Cornell's approach (1968) are an effect of the models used to describe the size distribution of earthquakes. The Gutenberg-Richter relation (equation (1-1)) (Gutenberg and Richter, 1944) assumes that the cumulative distributions of earthquakes versus intensity can be extrapolated to higher intensities. However, the short period of observations is insufficient either to prove or disprove this relation (cf. also Wesnousky, 1994).

Predictive probabilities (equation (3-13)) are calculated to estimate the chance of having zero events in a certain time period. The time period chosen depends on the specific purpose, but is usually related to the lifetime of an engineering structure. Such

probabilities are calculated for Brig (figure 5.17) and Zurich (figure 5.18) for a time period of 50 years. Calculated non-exceedance probabilities for Brig are 83.5% for intensity VIII, which is equal to the value obtained by SM78. For Zurich, predictive probabilities of non-exceedance are significantly lower than estimated by SM78. However, it is quite striking, that non-exceedance probabilities by SM78 for intensities VIII and IX are almost 1 (0.9995 for intensity IX).

Table 5.2: Return periods in years for Brig. The first two columns give the return period intervals calculated in this study, while the third column was calculated by Sägesser and Mayer-Rosa, 1978)

Intensity	Symmetric 50% return period interval (years)	Symmetric 90% return period interval (years)	Return period (SM78)
VI	[17, 27]	[13, 42]	18
VII	[44, 97]	[30, 220]	62
VIII	[185, 720]	[100, 3660]	340
IX	[1025, 6580]	[431, 55000]	2'000

Table 5.3: Return periods in years for Zurich. The first two columns give the return period intervals calculated in this study, while the third column was calculated by Sägesser and Mayer-Rosa, 1978)

Intensity	Symmetric 50% return period interval (years)	Symmetric 90% return period interval (years)	Return period (SM78)
VI	[34, 76]	[22, 180]	133
VII	[159, 735]	[79, 4180]	1000
VIII	[752, 5208]	[296, 45'000]	>10'000
IX	[2857, 25'000]	[980, >100'000]	>100'000

Figure 5.5-16:Return period versus intensity for twelve locations in Switzerland. Dotted lines give the values obtained in this study. Dotted lines with crosses gives median return periods, dotted lines with black points represent the 0.25 and 0.75 bounds of the probability intervals (50% probability intervals) and dotted lines with open circles represent the 0.05 and 0.95 bounds of the probability intervals (90% probability intervals), respectively. The dashed line represents return periods of the previous study (Sägesser and Mayer-Rosa, 1978)
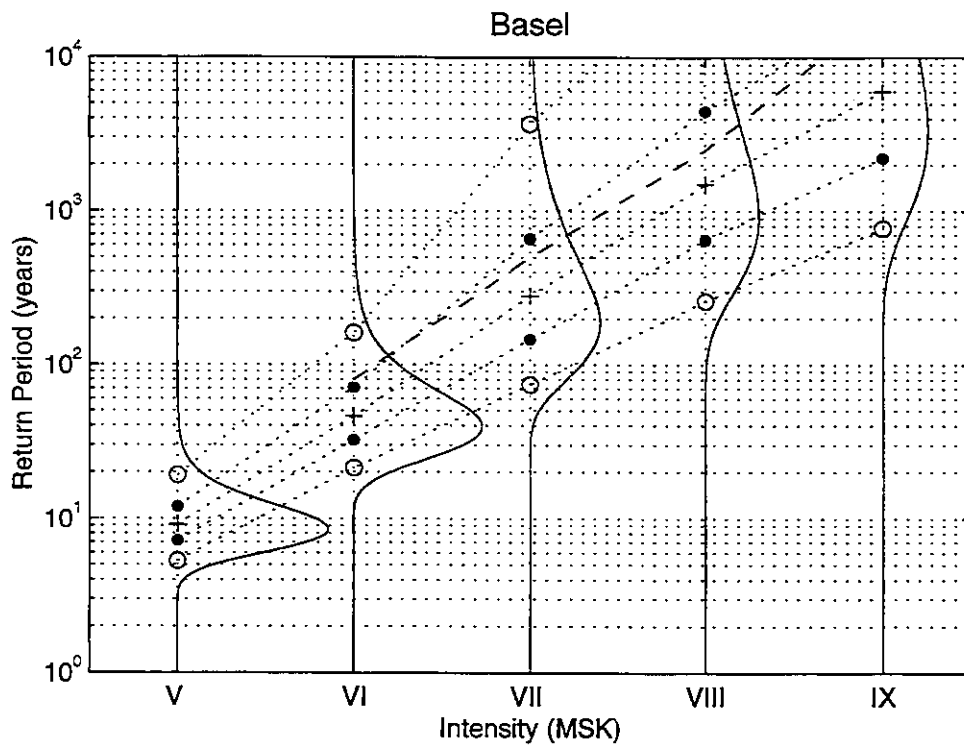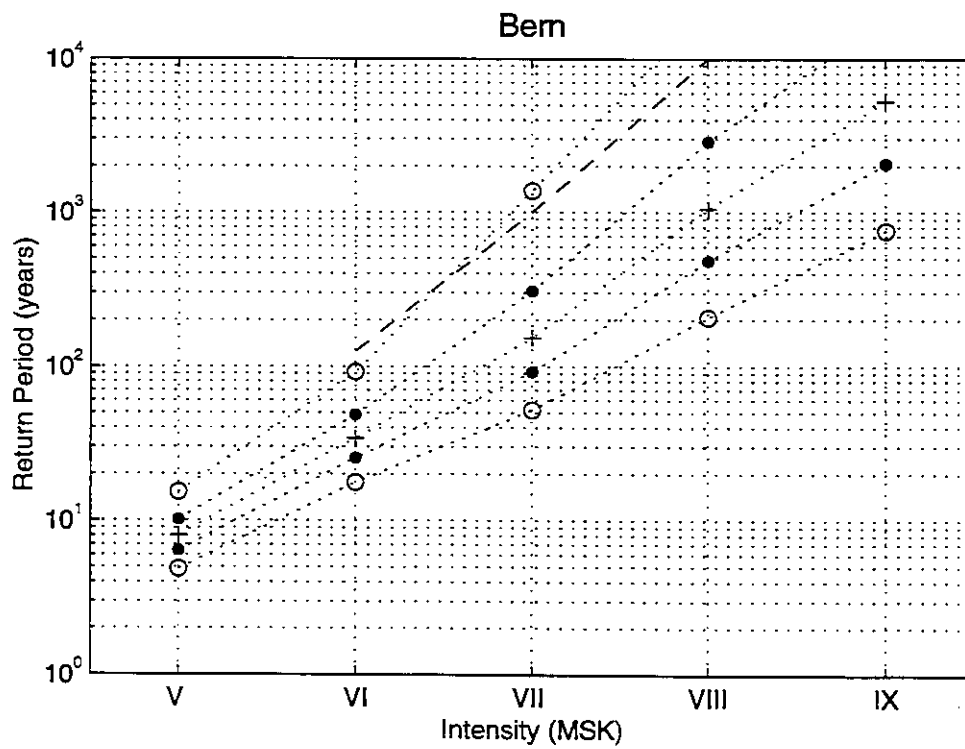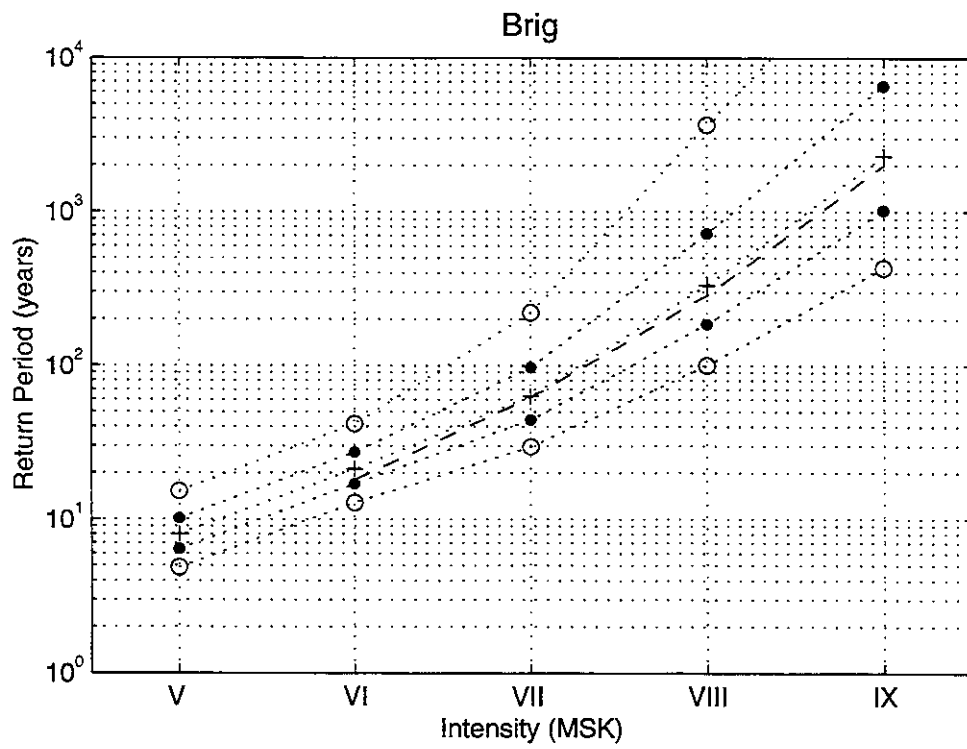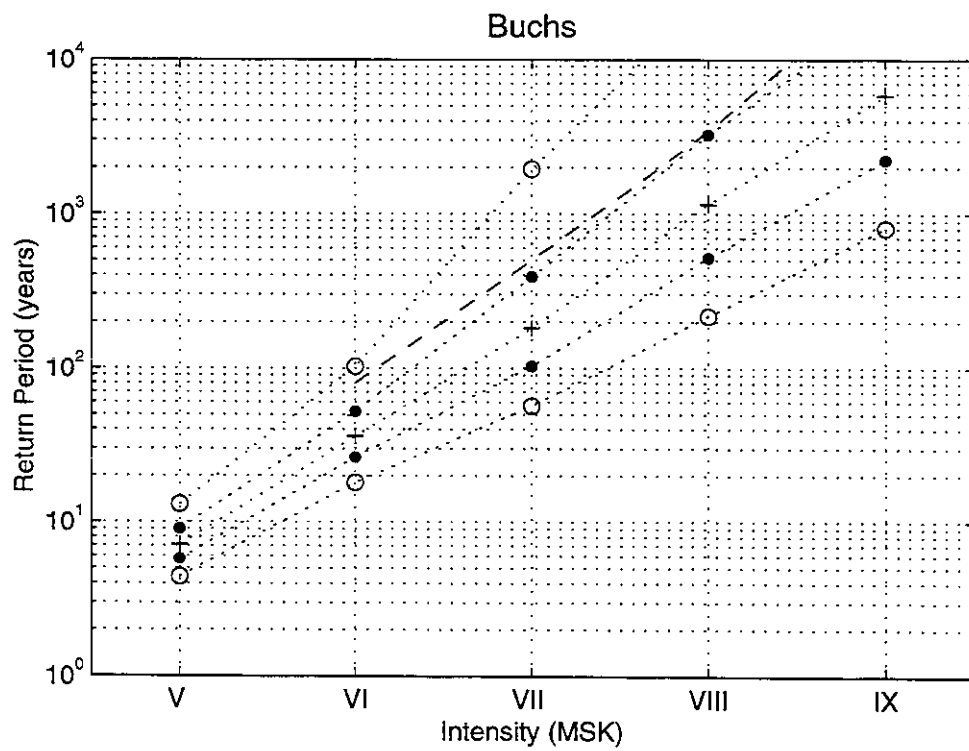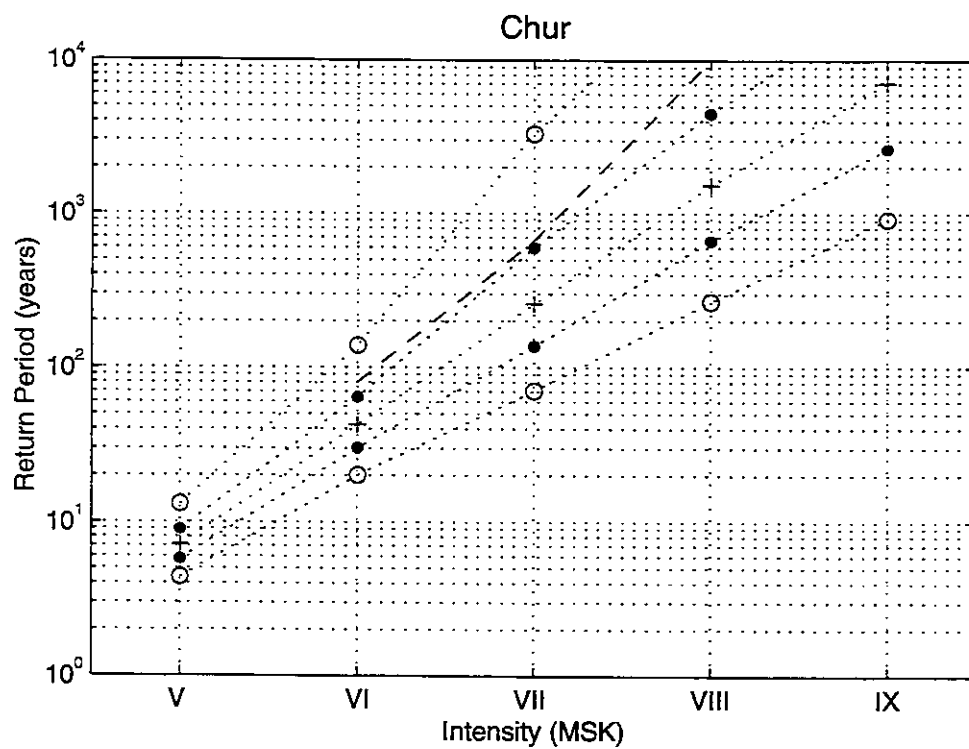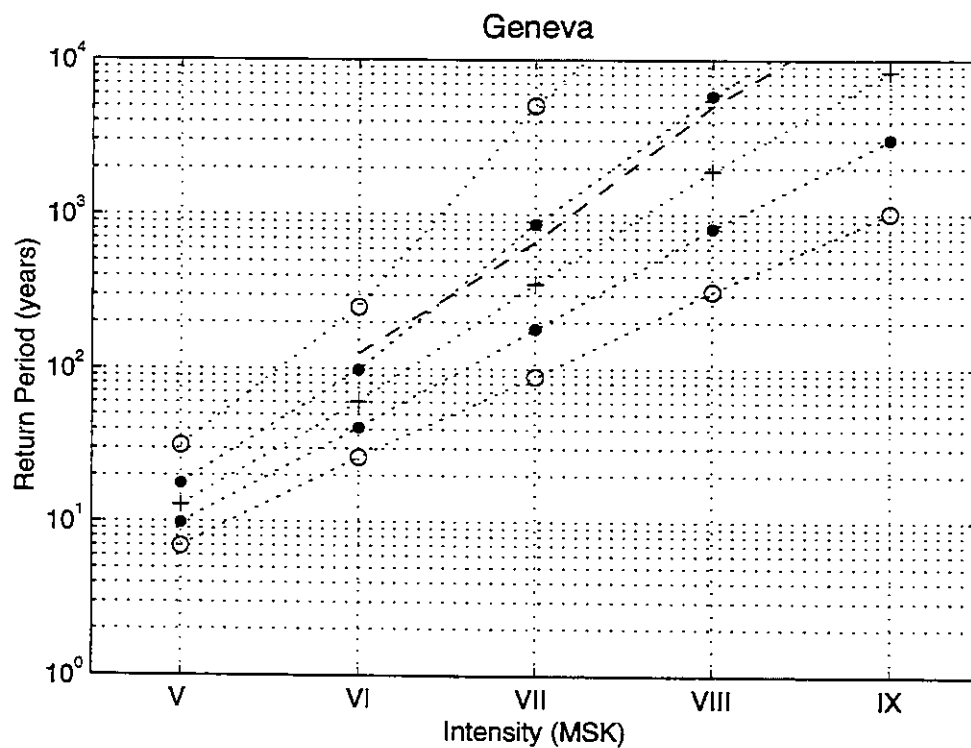
Figure 5.5

Figure 5.6
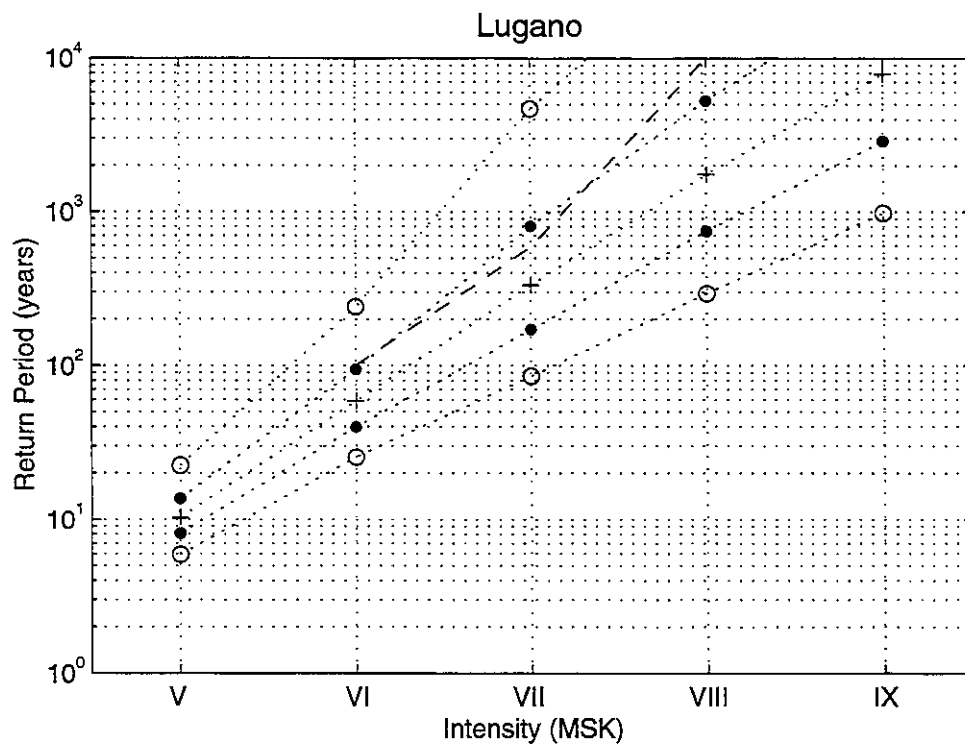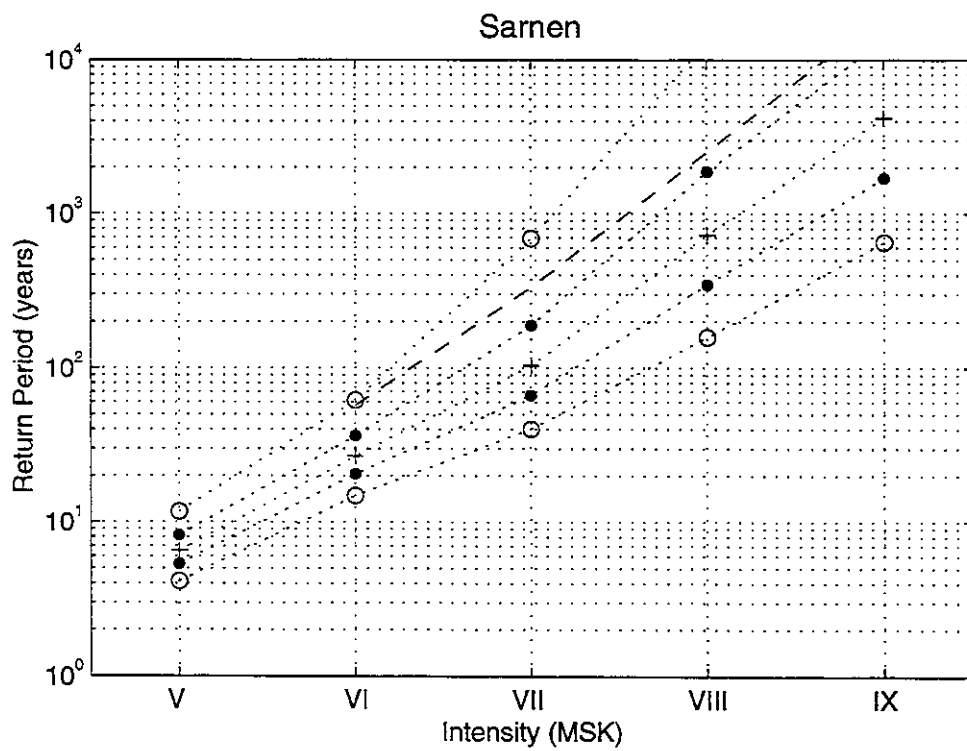
Figure 5.7

Figure 5.8
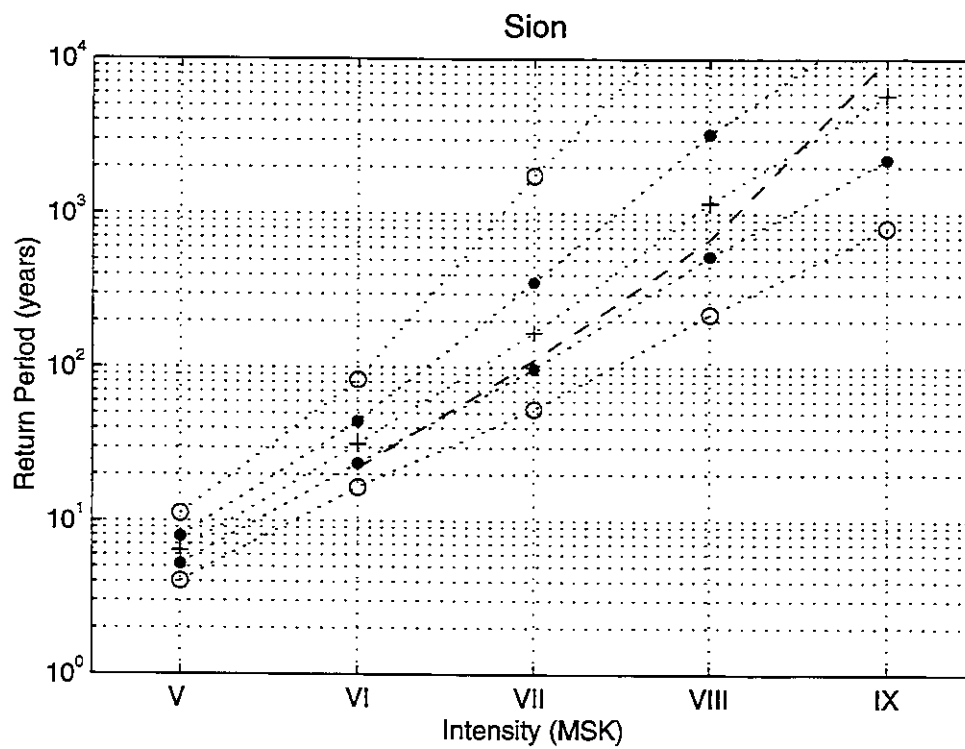
Figure 5.9

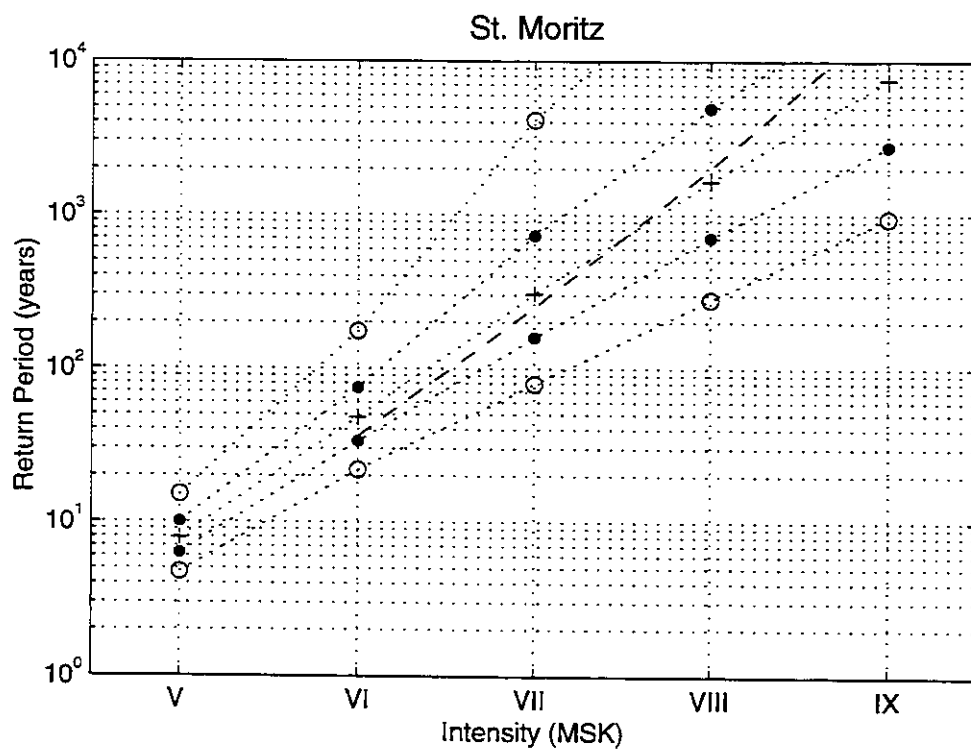Figure 5.10

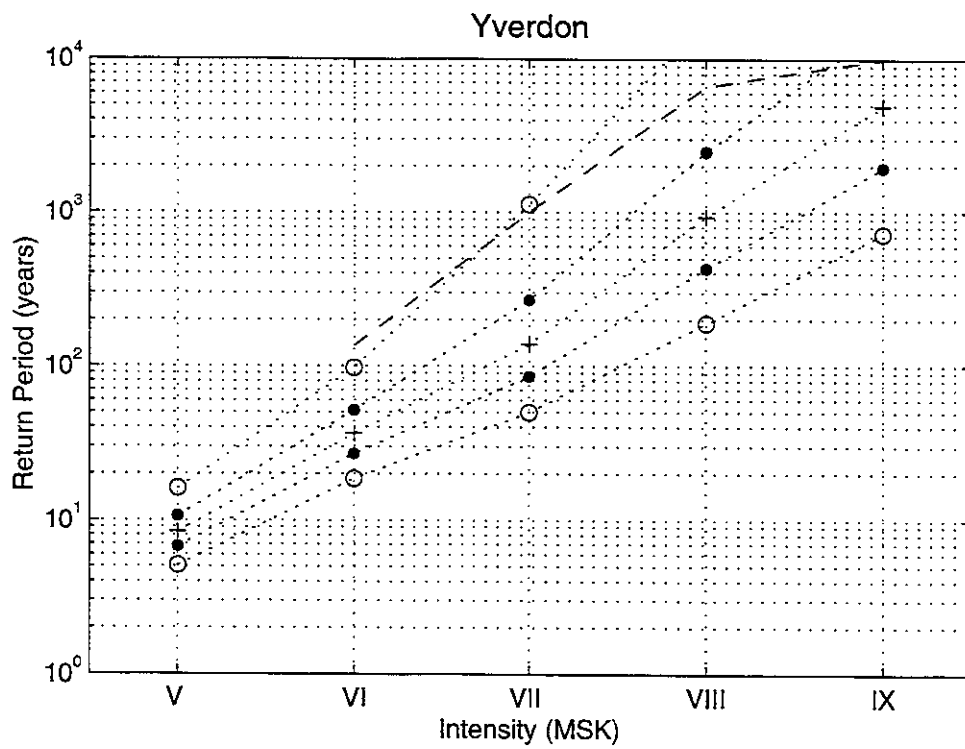Figure 5.11
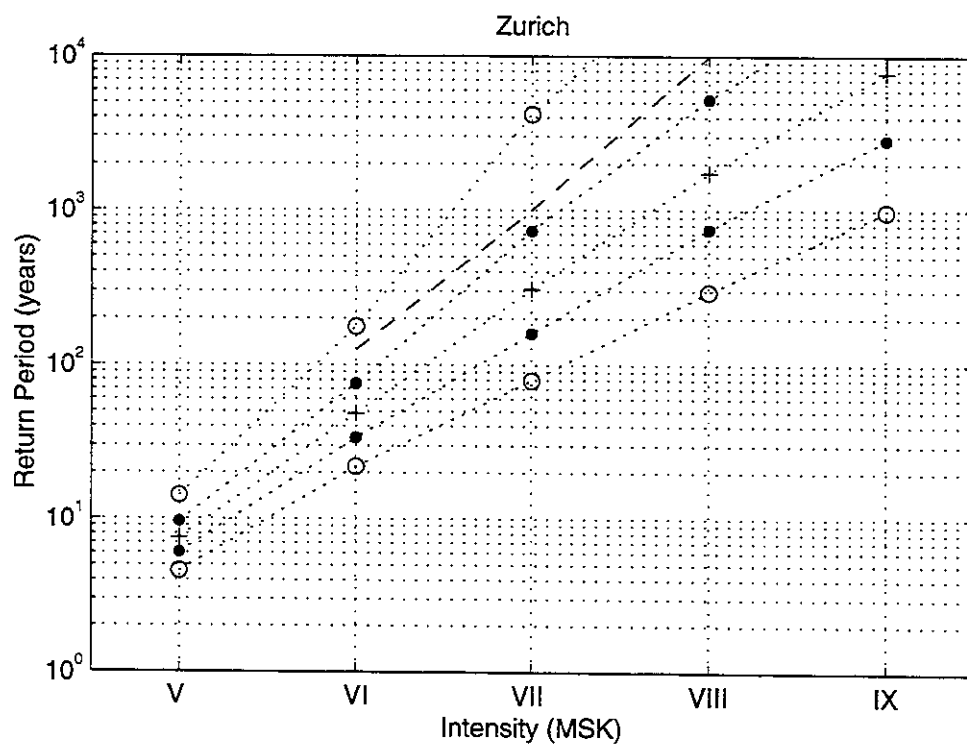

Figure 5.12

Figure 5.13

Figure 5.14

Figure 5.15

Figure 5.16

Figure 5.17:Probability of non-exceedance versus intensity for a time period of 50 years for Brig. The dotted line gives values obtained in this study, the dashed line is taken from the previous study by Sägesser and Mayer-Rosa (1978).
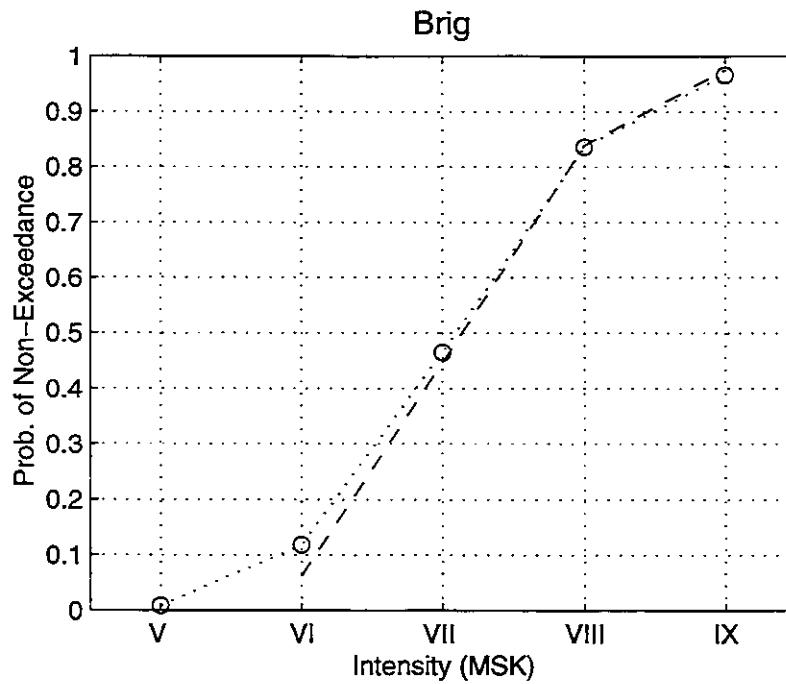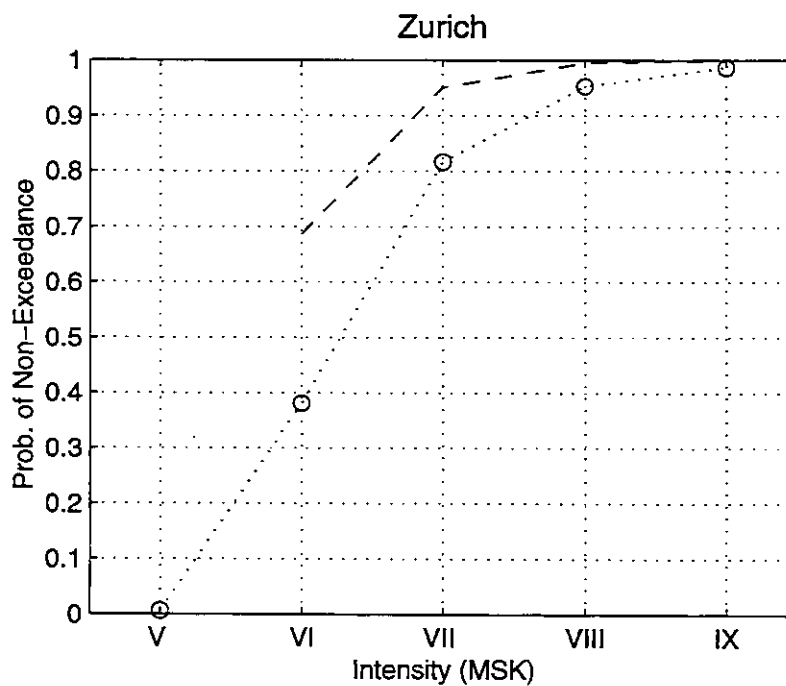

Figure 5.18:Probability of non-exceedance versus intensity for a time period of 50 years for Zurich. The dotted line gives values obtained in this study, the dashed line is taken from the previous study Sägesser and Mayer-Rosa (1978).

5.3   Conclusions and Recommendations

Earthquake data catalogs and ground motion attenuation laws are the main geophysical input in seismic hazard analysis. The earthquake data catalog provides the history of seismic activity. The longer the time of observation, the better the seismic activity can be described. However, the further we go back in history, the more uncertain the acquired seismological data become. It is therefore essential to represent the uncertainty of these data appropriately before they are used for seismic hazard analysis. In this study probability distributions have been defined in order to represent the uncertainty in earthquake size (i.e. macroseismic intensity or magnitude) and in earthquake location. Probability distributions proved to be well-suited to describe the uncertainties. They can be assessed for historical data as well as for instrumental data. Furthermore, they completely fit into the probabilistic concept of seismic hazard assessment.

Ground motion attenuation relations for intensity have been defined. Three regions could be delineated which are characterized by different attenuation parameters. The formulation of attenuation relations by discretized normal distributions takes into account the definition of intensity as an integer value. The intensity distribution of earthquakes in Switzerland can be modelled with the proposed attenuation relations. Calculation of possible "scenarios" describing future earthquakes can also be modelled.

The uncertainties of the data as well as of the suggested models have to be used to determine the uncertainty in the final hazard estimates. The developed method based on Bayesian statistics permits to take into account these uncertainties. This method for quantifying uncertainties represents a major improvement over the widely used hazard algorithms. This new procedure also avoids the delineation of earthquake sources, which are difficult to define in regions where the spatial seismicity distribution is obviously not related with significant tectonic features.

The results of seismic hazard assessment obtained by the method developed have been compared with results from a previous study. The latter results were almost always within the confidence limits calculated by the new method. However, longer return periods (i.e. return periods for higher intensities in regions with low seismic activity) obtained by the previous study could not be confirmed. Extrapolating intensity-frequency laws to unobserved higher intensities as done in standard hazard studies yields return periods larger than 10'000 years. The limited period of earthquake observations and reporting is insufficient to prove or disprove these high return periods.

Three main recommendations can be made for future work:

- The estimation of long return periods in regions with low seismic activity cannot be achieved only by historic earthquake data, since the time period of observations is too short. Return periods for these earthquakes are probably better determined by palaeo-seismological investigations. The method developed is open to take such results into account as prior estimates. An assessment of such prior estimates of return periods is highly recommended.

- Earthquake hazard defined in intensity degrees is of limited use for engineering purposes. With the method developed seismic hazard can also be calculated for other ground motion parameters. But first, attenuation laws have to be developed for these parameters. Future work should, therefore, address the attenuation of the various types of ground motion parameters (e.g. spectral amplitudes) as well as the conversion of epicentral intensities into magnitude estimates.

- The effect of local geologic settings is important for site-specific seismic hazard. It cannot sufficiently be treated by a rather rough classifications into soil classes based on intensity anomalies. Specific studies, especially in areas of high seismic risk, are necessary.

REFERENCES

Algermissen, S.T. and D.M. Perkins (1976): A Probabilistic Estimate of Maximum Acceleration in Rock in the United States. U.S. Geol. Surv. Open-File Rep., 76-416, 45 pp.

Algermissen, S.T., D.M. Perkins, P.C. Thenhaus, S.L. Hanson and B.L. Bender (1982): Probabilistic Estimates of Maximum Acceleration and Velocity in Rock in the Contiguous United States. U.S. Geol. Surv. Open-File Rep., 82-1033, 99 pp.

Anagnos T. and A.S. Kiremidjian (1984): Stochastic Time-predictable Model for Earthquake Occurrences. Bull. Seism. Soc. Am., 74, 2593-2611.

Araya, R. and A. der Kiureghian (1988): Seismic Hazard Analysis: Improved Models, Uncertainties and Sensitivities. Earthquake Engineering Research Center, University of California at Berkeley, Report No. UCB/EERC-90/11, 155 pp.

Beer, C. (1996): Ph.D Thesis, ETH Zurich, in preparation.

Benjamin, J.R. and C.A. Cornell (1970): Probability, Statistics and Decision for Civil Engineers. McGraw-Hill, New York, 684 pp.

Bender, B. and D.M. Perkins (1987): Seisrisk III: A Computer Program for Seismic Hazard Estimation. U.S. Geological Survey Bulletin 1772, Denver, Colorado.

Blake, A. (1941): On the Estimation of Focal Depth from Macroseimsic Data. Bull. Seism. Soc. Am., 31, 225-231.

Boatwright, J., L.C. Seekins, T.E. Fumal, H. Liu and C.S. Mueller (1991): Ground Motion Amplification in the Marina District. Bull. Seism. Soc. Am., 81, 1980-1997.

Campell, W.K. (1985): Strong Motion Attenuation Relations: A Ten Year Perspective. Earthquake Spectra, 1(4), 739-804.

Coppersmith, K.J. and R.R. Youngs (1986): Capturing Uncertainty in Probabilistic Seismic Hazard Assessment Within Intraplate Tectonic Environments. Proc. 3rd U.S. National Conf. on Earthquake Engineering, Charleston, South Carolina, vol. I, 301-312.

Cornell, C.A. (1968): Engineering Seismic Risk Analysis. Bull. Seism. Soc. Am., 58, 1583-1606.

Deichmann, N. and L. Rybach (1989): Earthquakes and Temperature in the Lower Crust below the Northern Alpine Foreland of Switzerland. In: Mereu, R.F., St. Mueller and D.M Fountain (Ed.): Properties and Processes of Earth's Lower Crust. Geophysical Monograph 51, IUGG Volume 6, 197-213.

Deichmann, N. and M. Baer (1990): Earthquake Focal Depths Below the Alps and Northern Alpine Foreland of Switzerland. In: Freeman, R., P. Giese and St. Mueller (Eds.): The European Geotraverse: Integrative Studies. European Science Foundation, Strasbourg, France, 277-288.

Deichmann, N. (1992): Structural and Rheological Implications of Lower-Crustal Earthquakes below Northern Switzerland. Phys. Earth and Planet Interiors, 69, 270-280.

Egozcue, J.J., A. Barbat, J.A. Canas and J. Miquel (1991): A Method to Estimate Intensity Occurrence Probabilities in Low Seismic Activity Regions. Earthquake Engineering and Structural Dynamics, 20, 43-60.

Egozcue, J.J. (1994): Períodos de Retorno y su Estima. In: Barbat, A. and J.M. Canet: Estructuras Sometidas A Acciones Sismicas. Centro Internacional de Métodos Numéricos en Ingeniería, Universitat Polytecnica de Cataluña, 719-740.

Evernden, J.F. (1970): Study of Regional Seismicity and Associated Problems. Bull. Seism. Soc. Am., 60, 393-446.

Evernden, J.F., W.M. Kohler and G.D. Clow (1981): Seismic Intensities of Earthquakes of Conterminous United States - Their Prediction and Interpretation. U.S. Geological Survey Prof. Paper 1223, Washington, D.C., 56 pp.

Evernden, J.F. and J.M. Thomson (1985): Predicting Seismic Intensities. In: J.I. Ziony (Ed.): Evaluating Earthquake Hazards in the Los Angeles Region - An Earth-Science Perspective. U.S. Geological Survey Prof. Paper 1360, Washington, D.C., 151-202.

Fäh, D. (1985): Seismische Mikrozonierung in der Schweiz. Diploma Thesis, ETH Zürich, 126 pp.

Fäh, D. (1992): A Hybrid Technique for the Estimation of Strong Ground Motion in Sedimentary Basins. Ph.D. Thesis, ETH Zurich, 226 pp.

Forell, F.A. (1880). Les Tremblements de Terre Étudiés par la Commission Sismologique Suisse. Archive des Sciences Physiques et Naturelles. 3e pér. t.4, Genève, 369-372.

Gardner, J.K. and L. Knopoff (1974): Is the Sequence of Earthquakes in Southern California, with Aftershocks Removed, Poissonian? Bull. Seism. Soc. Am., 64, 1363-1367.

Grünthal, G. (1991): Die seismische Gefährdung im östlichen Teil Deutschlands und deren Berücksichtigung in erdbebengerechten Baunormen. Kolloquium Erdbebeningenieurwesen, Potsdam, DGEB-Publikation Nr. 5, 37 pp.

Grünthal, G. (Ed.) (1993): European Macroseismic Scale 1992 (up-dated MSK-scale).

Conseil de l'Europe, Cahiers du Centre Européen de Géodynamique et de Séismologie, volume 7, Luxembourg, 79 pp.

Grünthal, G., C. Bosse, D. Mayer-Rosa, E. Rüttener, W. Lenhardt and P. Melichar (1994): Joint Seismic Hazard Assessment for Austria, Germany and Switzerland. Proc. of the 10th European Conference on Earthquake Engineering, Vienna, in press.

Guidoboni, E. and M. Stucchi (1993): The Contribution of Historical Records of Earthquakes to the Evaluation of Seismic Hazard. Annali di Geofisica, 36, 201-215.

Gutenberg, B. and C.F. Richter (1944): Frequency of Earthquakes in California. Bull. Seism. Soc. Am., 34, 185-188.

Gutenberg, B. and C.F. Richter (1949): Seismicity of the Earth. Princeton University Press, 273 pp.

Gutenberg, B. and C.F. Richter (1956): Earthquakes, Magnitude, Energy and Acceleration. Bull. Seism. Soc. Am., 46, 105-145.

Hall, J.F. (Ed.) (1994): Northridge Earthquake January 17, 1994; Preliminary Reconnaissance Report. Earthquake Engineering Research Institute, Report 94-01, 104 pp.

Howell, B.F. and T.R. Schultz (1975): Attenuation of Modified Mercalli Intensity with Distance from the Epicenter. Bull. Seism. Soc. Am., 65, 651-665.

Joyner, W.B. and D.M. Boore (1988): Measurements, Characterization, and Prediction of Strong Ground Motion. Proc. Earthquake Engineering and Soil Dynamics II, GT Div/ASCE, Park City, Utah, 43-102.

Karnik, V. (1969): Seismicity of the European Area, Part I. D. Reidel Publishing Co., Dordrecht, Holland, 364 pp.

Karnik, V. (1971): Seismicity of the European Area, Part II. D. Reidel Publishing Co., Dordrecht, Holland, 218 pp.

Kiremidjian, A.S. and T. Anagnos (1984): Stochastic Slip-predictable Model for Earthquake Occurrences. Bull. Seism. Soc. Am., 74, 739-755.

Kövesligethy, R. von (1906): Seismischer Stärkegrad und Intensität der Beben. Gerlands Beitr. Geophysik, 8, 25 pp.

Kradolfer, U. (1989): Seismische Tomographie in der Schweiz mittels lokaler Erdbeben. Ph.D Thesis, ETH Zürich, 109 pp.

Lee, W.K.H. and J.C. Lahr (1975): HYPO71 (revised): A Computer Program for Determining Hypocenter, Magnitude, and First Motion Pattern of Local Earthquakes. U. S. Geol. Surv. Open-File Rep., 75-311, 100 pp.

Lenhardt, W. (1993): Austrian Earthquake Catalogue (1201 - 1993). Computer File, Ze-

ntralanstalt für Meteorologie und Geodynamik, Wien.

Lomnitz, C. (1973): Poisson Processes in Earthquake Studies. Bull. Seism. Soc. Am., 64, 735-758.

Maurer, H. (1993). Seismotectonics and Upper Crustal Structure in the Western Swiss Alps. Ph.D Thesis, ETH, Zurich, 159 pp.

Mayer-Rosa, D. and H. Merz (1976): Seismic Risk Maps of Switzerland. Description of the Probabilistic Method and Discussion of the Input Parameters. In: A.R. Ritsema (Ed.): Seismic Risk Assessment for Nuclear Power Plants, Proc. of ESC Symposium, Luxembourg. KNMI De Bilt, The Netherlands, 45-52.

Mayer-Rosa, D. and B. Cadiot (1979): A Review of the 1356 Basel Earthquake.Tectonophysics, 126, 329-374.

Mayer-Rosa, D. (1986): Attenuation of Seismic Ground Motion in Switzerland. Terra Cognita, 6, 590-592.

Mayer-Rosa, D. and M. Baer (1993): Earthquake Catalog of Switzerland. Swiss Seismological Service, Computer-File.

McGuire, R. K. (1976): FORTRAN Computer Program for Seismic Risk Analysis. U.S. Geological Survey, Open-File Report 76-67, 90 pp.

McGuire, R.K. (1993): Computation of Seismic Hazard. Annali di Geofisica, 36, 181-200.

Medvedev, S.V., W. Sponheuer and V. Karnik (1965): Seismic Intensity Scale MSK 1964. Academy of Sciences of the USSR, Soviet Geophysical Committee, Moscow, 10 pp.

Merz, H.A. and C.A. Cornell (1973): Seismic Risk Analysis Based on a Quadratic Magnitude Frequency Law. Bull. Seism. Soc. Am., 63, 1999-2006.

Meyer, B., R. Lacassin, J. Brulhet and B. Mouroux (1994): The Basel 1356 Earthquake: Which Fault Produced it? Terra Nova, 6, 54-63.

Meyer, S.L. (1975): Data Analysis for Scientists and Engineers. John Wiley & Sons, New York, 513 pp.

Montandon, F. (1942): Les Séismes de Forte Intensité en Suisse. Revue pour l'Étude des Calamités, Extrait de fascicules 18-19 et 20-21, Genève.

Montandon, F. (1946): Les Trois Recents Séismes du Valais Central. Extrait de la Revue pour l'étude des calamites, Tome IX, fasc. 25, Gevève.

Montandon, F. (1953): Les tremblements de terre destructive en Europe. Catalogue par territoires séismiques de l'an 1000 à 1940, Genève.

Mortgat, C.P. and H.C. Shah (1979): A Bayesian Model for Seismic Hazard Mapping. Bull. Seism. Soc. Am., 69, 1237-1251.

Mueller, St. and D. Mayer-Rosa (1980): The New Seismic Hazard Maps for Switzerland. Rev. Geofisica, 13, 7-19.

Press, S.J. (1989): Bayesian Statistics: Principles, Models, and Applications. John Wiley & Sons, New York, 237 pp.

Rösli, U. (1990): Vereinfachte Geotechnische Karte der Schweiz, Erfassung auf ARC/ INFO. Bundesamt für Wasserwirtschaft, Bern.

Roth, Ph., N. Pavoni and N. Deichmann (1992): Seismotectonics of the eastern Swiss Alps and Evidence for Precipitation-induced Variations of Seismic Activity. Tectonophysics, 207, 183-197.

Sägesser, R. and D. Mayer-Rosa (1978): Erdbebengefährdung in der Schweiz. Schweizerische Bauzeitung, Zürich, 78/7, 3-18.

Sánchez-Sesma, F.J., S. Chávez-Pérez, M. Suárez, M.A. Bravo and L.E. Pérez-Rocha (1988). The Mexico Earthquake of September 19, 1985 - On the Seismic Response of the Valley of Mexico. Earthquake Spectra 4, 569-589.

Schindler, C., C. Beer, D. Mayer-Rosa, E. Rüttener, J.J. Wagner, J.M. Jaquet and C. Frischknecht (1993): Earthquake Hazard Assessment in the Canton Obwalden using a Geographic Information System (GIS). In: Floods and Geological Hazards, Swiss National Committee of the UN-IDNDR, Report 1991-1993.

Shah, H.C., C.P. Mortgat, A. Kiremidjian and T.C. Zsutty (1975): A Study of Seismic Risk for Nicaragua, Technical Rep. 11, John A. Blume Earthquake Engineering Center, Stanford University, 187 pp.

Sieberg, A. (1940): Beiträge zum Erdbebenkatalog Deutschlands und angrenzender Gebiete für die Jahre 58 bis 1799. Mitteilungen des Deutschen Reichs-Erdbebendienstes Heft 2, Berlin, 112 pp.

Smit P. and D. Mayer-Rosa (1993): Swiss National Strong Motion Network - Strong Motion Network Bulletin 1992. Swiss Seismological Service, Zurich, 92 pp.

Smit P. (1994): Swiss National Strong Motion Network - Strong Motion Network Bulletin 1993. Swiss Seismological Service, Zurich, 43 pp.

Sponheuer, W. (1952): Erdbebenkatalog Deutschlands und der angrenzenden Gebiete für die Jahre 1800 bis 1899. Akademie-Verlag, Berlin.

Sponheuer, W. (1960): Methoden zur Herdtiefenbestimmung in der Makroseismik. Freiberger Forschungshefte, C88, Akademie Verlag, Berlin, 116 pp.

Stepp, J.C. (1971): An Investigation of Earthquake Risk in the Pudget Sound Area by

Use of Type I Distribution of Largest Extremes. Ph.D. Thesis, Pennsylvania State University, University Park, 131 pp.

Swiss Seismological Service (1911-1963): Jahresberichte des Schweizerischen Erdbebendienstes, Zurich.

UNO (1989): International Decade for Natural Disaster Reduction. Resolution 44/236, adopted at the 44th Session of the United Nations General Assembly, 22 December 1989.

Veneziano, D., C.A. Cornell and T. O'Hara (1984): Historical Method of Seismic Hazard Analysis. Technical Report NP-3438, Electric Power Research Institute, Palo Alto, California, 178 pp.

Volger, G.H.O. (1857): Untersuchungen über das Phänomen der Erdbeben in der Schweiz; 1. Teil: Chronik der Erdbeben in der Schweiz. Gotha.

Volger, G.H.O. (1858): Untersuchungen über das Phänomen der Erdbeben in der Schweiz; 3. Teil: Die Erdbeben im Wallis. Gotha.

Wanner, E. (1932): Erdbebenkatalog der Schweiz für die Jahre 1856 - 1879. Jahresbericht des Schweizerischen Erdbebendienstes 1932, Kap. 3, 16-21.

Wechsler, E. (1987): Das Erdbeben von Basel 1356, Teil 1: Historische und kunsthistorische Aspekte. Publication Series of the Swiss Seismological Service, No. 102, ETH Zürich, 128 pp.

Wesnousky, S.G. (1994): The Gutenberg-Richter or Characteristic Earthquake Distribution, Which Is It? Bull. Seism. Soc. Am., 84, 1940-1959.

Wyllie, L.A. and J.R. Filson (Eds.) (1989): Armenia Earthquake Reconnaissance Report. Earthquake Spectra, Special Supplement, 89-01, 175 pp.

Youngs, R.R. and K.J. Coppersmith (1985): Implications of Fault Slip Rates and Earthquake Recurrence Models to Probabilistic Seismic Hazard Estimates. Bull. Seism. Soc. Am., 75, 939-964.

APPENDIX A

Earthquake Catalog

Region   5.5 - 11.0 longitude East

              45.5 - 48.5 latitude North

Time window 1300 - 1993

Intensity   ≥ VI or

Magnitude   ≥ 5.0

Format:

1. column: year

2. column: month

3. column: day

4. column: hour, minutes and seconds

5. column: latitude (in deg E)

6. column: longitude (in deg N)

7. column: intensity (MSK)

8. column: magnitude

9. column: main source of information (for a full description of the references see
              Mayer-Rosa and Baer (1993))

Year	Mo	Da	Ho	Mi	Sec	Lat	Long	Int	Mag	Ref
1334	12	4	23:	0:	.0	45.72	10.85	VIII-IX		SCM
1346	11	24	23:	0:	.0	47.47	7.62	VIII		SED
1356	10	18	21:	0:	.0	47.47	7.60	IX		SED
1357	5	0	0:	0:	.0	48.17	7.50	VII		KSB
1358	0	0	0:	0:	.0	46.87	9.53	VI		SED
1363	7	3	0:	0:	.0	47.80	7.10	VI		SED
1369	2	1	0:	0:	.0	45.58	8.22	VII-VIII		SCM
1369	11	26	0:	0:	.0	45.50	9.25	VII		SCM
1372	6	1	0:	0:	.0	47.47	7.60	VII		SED
1375	0	0	0:	0:	.0	46.90	8.40	VIII		SED
1378	6	1	0:	0:	.0	47.00	9.00	VI		SED
1382	4	20	0:	0:	.0	46.00	7.00	VI		SED
1384	12	24	0:	0:	.0	47.75	7.08	VI		SED
1391	3	23	0:	0:	.0	47.67	7.30	VII		SED
1394	3	22	0:	0:	.0	46.30	7.97	VIII		SED
1396	12	26	0:	0:	.0	45.67	9.67	VII		SCM
1397	12	26	2:	0:	.0	45.67	9.67	VIII		SCM
1403	1	17	0:	0:	.0	45.50	11.00	VII-VIII		SCM
1415	6	21	0:	0:	.0	47.45	7.58	VI		SED
1416	7	22	0:	0:	.0	47.52	7.57	VI		SED
1428	12	13	0:	0:	.0	47.53	7.60	VII		SED
1444	1	30	4:	0:	.0	47.80	7.10	VI		SED
1492	11	7	0:	0:	.0	47.50	7.65	VI		SED
1498	9	3	14:	0:	.0	46.50	7.43	VI-VII		SED
1504	2	29	0:	0:	.0	46.78	10.20	VIII		SED
1508	0	0	0:	0:	.0	46.65	9.80	VI		SED
1512	0	0	0:	0:	.0	46.38	8.97	VII		SED
1513	9	28	0:	0:	.0	46.35	9.13	VI		SED
1521	1	26	10:30:		.0	45.55	10.22	VI		SCM
1523	5	19	2:	0:	.0	46.78	6.63	VI		SED
1531	10	10	20:	0:	.0	47.03	9.07	VI		SED
1533	11	17	0:	0:	.0	47.48	9.33	VI		SED
1533	11	26	0:	0:	.0	47.38	9.63	VI		SED
1534	10	2	0:	0:	.0	47.52	8.30	VI		SED
1537	3	1	0:	0:	.0	47.52	7.43	VI		SED
1540	9	1	0:	0:	.0	45.53	10.22	VI		SCM
1541	1	6	0:	0:	.0	46.62	8.57	VII		SED
1542	11	8	0:	0:	.0	47.82	10.05	VI		SED
1552	2	9	2:	0:	.0	47.82	7.10	VI		SED
1555	11	2	0:	0:	.0	46.00	10.00	VI		SCM
1569	8	6	0:	0:	.0	47.43	7.60	VII		SED
1572	2	9	7:	0:	.0	47.52	7.53	VI		SED
1573	6	30	0:	0:	.0	46.87	9.53	VI		SED
1573	12	20	0:	0:	.0	47.03	9.02	VI		SED
1574	0	0	0:	0:	.0	48.50	7.90	VII		Ley
1574	5	3	0:	0:	.0	46.20	6.20	VII		SED
1576	9	26	6:	0:	.0	45.67	9.67	VI		SCM
1577	2	2	2:	0:	.0	46.77	7.57	VI		SED
1577	9	22	0:	0:	.0	47.53	7.62	VI		SED

A2

Year	Mo	Da	Ho Mi Sec	Lat	Long	Int	Mag	Ref
1578	9	28	0: 0: .0	47.40	8.50	VI		SED
1584	3	1	11: 0: .0	46.33	6.97	VII		SED
1584	3	10	0: 0: .0	46.33	6.93	VII		SED
1584	5	4	0: 0: .0	46.35	6.97	VI		SED
1588	6	11	0: 0: .0	47.75	8.83	VII		SED
1593	3	8	0: 0: .0	45.68	9.67	VI-VII		SCM
1593	10	10	0: 0: .0	47.03	9.05	VI		SED
1594	3	20	0: 0: .0	47.03	9.05	VI		SED
1594	11	11	0: 0: .0	47.03	9.05	VI		SED
1597	0	0	0: 0: .0	46.20	8.07	VI		SED
1600	9	0	0: 0: .0	45.67	7.83	IX		SCM
1601	9	8	1: 0: .0	46.83	8.50	VIII-IX		SED
1606	8	22	0: 0: .0	45.68	9.67	VI-VII		SCM
1607	4	2	0: 0: .0	46.78	6.63	VI		SED
1610	11	29	0: 0: .0	47.47	7.55	VII-VIII		SED
1614	2	28	0: 0: .0	47.52	7.62	VI		SED
1614	10	4	0: 0: .0	47.45	7.57	VI		SED
1616	2	29	0: 0: .0	46.83	8.40	VIII		SED
1617	7	5	0: 0: .0	48.00	7.87	VI		Ley
1618	8	25	0: 0: .0	46.32	9.45	VII		SED
1620	1	29	0: 0: .0	46.60	7.65	VI		SED
1621	5	21	16: 0: .0	47.22	7.30	VII		SED
1622	7	25	0: 0: .0	46.78	10.25	VI		SED
1622	8	3	0: 0: .0	46.80	10.25	VII		SED
1623	2	20	0: 0: .0	46.30	9.78	VI		SED
1650	1	8	0: 0: .0	47.20	9.47	VI		SED
1650	5	6	0: 0: .0	47.50	7.55	VI		SED
1650	9	7	0: 0: .0	47.55	7.53	VII		SED
1650	9	10	3: 0: .0	47.52	7.65	VI-VII		SED
1650	9	11	3: 0: .0	47.48	7.63	VI-VII		SED
1655	3	29	0: 0: .0	48.50	9.07	VII-VIII		Ley
1655	4	11	0: 0: .0	48.50	9.07	VII		Ley
1661	1	9	21: 0: .0	47.03	9.07	VI		SED
1661	3	11	0: 0: .0	45.70	9.85	VII-VIII		SCM
1661	3	12	0: 0: .0	45.75	9.75	IX		SCM
1663	9	10	21: 0: .0	46.92	9.17	VI		SED
1666	9	1	0: 0: .0	47.58	9.33	VI		SED
1669	9	30	12:45: .0	48.50	7.75	VII		Ley
1674	12	6	8: 0: .0	47.08	9.07	VI		SED
1676	6	17	20: 0: .0	45.50	8.00	VIII		SCM
1681	1	27	21: 0: .0	47.12	9.15	VI		SED
1682	5	12	2: 0: .0	47.91	6.48	VIII		KSB
1683	5	25	0: 0: .0	46.08	10.67	VI-VII		SCM
1684	2	26	19: 0: .0	46.37	8.08	VII		SED
1693	1	9	0: 0: .0	46.75	6.58	VI		SED
1695	9	1	0: 0: .0	46.88	9.67	VI		SED
1701	9	7	0: 0: .0	46.92	8.98	VI		SED
1702	12	9	4: 0: .0	46.93	9.02	VI		SED
1703	1	20	19: 0: .0	45.75	10.82	VII		SCM

Year	Mo	Da	Ho Mi Sec	Lat	Long	Int	Mag	Ref
1711	2	9	3:30: .0	47.45	7.62	VI-VII		SED
1712	8	11	23: 0: .0	46.30	7.02	VI		SED
1720	12	20	4:30: .0	47.50	9.58	VIII		SED
1721	7	3	6:45: .0	47.45	7.70	VII		SED
1724	3	20	0: 0: .0	45.82	10.07	VI		SCM
1729	1	13	21:30: .0	46.63	7.63	VII		SED
1730	1	10	0: 0: .0	47.38	9.43	VI		SED
1733	7	8	0:30: .0	47.13	7.37	VI		SED
1736	6	12	19: 0: .0	47.48	7.62	VI		SED
1751	12	26	0: 0: .0	47.58	8.52	VI		SED
1754	9	19	11: 0: .0	46.28	7.12	VII		SED
1755	10	1	0: 0: .0	47.12	9.02	VI		SED
1755	12	9	13:30: .0	46.32	7.98	VIII		SED
1755	12	21	3: 0: .0	46.32	8.00	VI		SED
1755	12	30	0: 0: .0	46.30	7.98	VI		SED
1756	6	7	7:50: .0	47.13	6.85	VI		SED
1765	4	7	13: 0: .0	46.87	8.23	VI		SED
1770	3	20	15:55: .0	46.48	7.18	VI-VII		SED
1770	10	9	6:30: .0	47.03	8.37	VI		SED
1771	8	11	7:30: .0	47.30	9.03	VI		SED
1771	8	15	0: 0: .0	45.67	10.00	VI		SCM
1771	12	27	0: 0: .0	47.33	10.17	VI		SED
1772	7	3	0: 0: .0	47.67	9.13	VII		SED
1773	11	25	17: 0: .0	47.03	9.02	VI		SED
1774	2	28	0: 0: .0	46.87	9.53	VI		SED
1774	4	17	23:30: .0	46.95	7.43	VII		SED
1774	9	10	15:25: .0	46.85	8.67	VIII		SED
1775	1	23	3:25: .0	46.85	8.55	VI-VII		SED
1776	11	28	2:15: .0	47.77	7.30	VII		SED
1777	2	7	1: 0: .0	46.88	8.25	VII		SED
1777	3	25	0: 0: .0	46.88	8.25	VII		SED
1777	3	28	0: 0: .0	46.88	8.25	VII		SED
1777	12	20	4: 0: .0	47.90	7.60	VI		Ley
1778	1	27	0: 0: .0	47.25	9.55	VII		SED
1778	1	28	2:30: .0	47.90	7.60	VI-VII		Ley
1780	2	22	18: 0: .0	47.03	8.32	VI		SED
1781	9	10	0: 0: .0	45.50	9.65	VI-VII		SCM
1781	9	10	11:30: .0	45.50	9.67	VII		SCM
1783	7	28	17:30: .0	45.85	10.80	VI		SCM
1784	10	15	12: 3: .0	45.63	5.91	VI-VII		LvG
1784	11	29	21:10: .0	47.85	7.43	VI		SED
1785	11	18	0: 0: .0	46.60	10.10	VII		SED
1787	8	27	0:45: .0	47.30	11.00	VII		Ley
1795	12	6	0: 0: .0	47.20	9.42	VII		SED
1796	4	20	6:12: .0	47.20	9.42	VIII-IX		SED
1799	5	29	0: 0: .0	45.50	10.25	VI-VII		SCM
1803	12	12	15:30: .0	45.92	6.83	VI		SED
1805	11	30	5: 0: .0	46.57	9.78	VI		SED
1810	5	1	0: 0: .0	45.75	10.83	VII		SCM

A4

Year	Mo	Da	Ho Mi Sec	Lat	Long	Int	Mag	Ref
1811	6	6	22:15: .0	46.87	9.53	VI		SED
1812	7	17	3: 0: .0	47.73	7.67	VI-VII	4.0	SED
1813	9	22	1:30: .0	46.83	9.80	VI		SED
1817	3	11	20:10: .0	45.88	6.75	VI		SED
1822	2	19	8:45: .0	45.81	5.81	VII-VIII		LvG
1822	11	28	10:45: .0	48.50	8.40	VI-VII		Ley
1823	11	21	21:30: .0	48.12	7.68	VI-VII		Ley
1823	12	3	21: 0: .0	48.12	7.68	VI		Ley
1826	12	15	19: 0: .0	47.20	9.68	VI		SED
1827	1	24	0: 0: .0	46.77	7.57	VI		SED
1827	2	26	20: 0: .0	46.28	8.00	VI		SED
1827	4	2	0:20: .0	46.73	10.18	VII		SED
1828	2	8	14:20: .0	48.40	9.32	VI-VII		Ley
1828	12	13	20:40: .0	46.77	7.35	VI		SED
1828	12	15	19:50: .0	47.57	9.58	VI	4.5	SED
1830	9	12	10:45: .0	48.25	9.47	VI		Ley
1830	9	23	4:15: .0	48.32	9.47	VI		Ley
1831	1	29	22: 0: .0	48.00	6.60	VI		Ley
1835	4	18	17:25: .0	46.68	7.83	VI		SED
1835	10	29	2:47: .0	47.42	9.42	VI-VII		SED
1835	10	31	2:30: .0	47.38	9.37	VI		SED
1836	11	5	6: 0: .0	47.47	7.55	VI-VII	3.9	SED
1837	1	24	0:58: .0	46.32	7.97	VII		SED
1837	1	24	1:30: .0	46.58	8.10	VI		SED
1837	1	24	1:58: .0	45.67	8.33	VII		SCM
1839	8	9	8:45: .0	45.50	10.17	VI		SCM
1839	8	11	19: 0: .0	45.90	6.12	VII		SED
1839	8	16	17:30: .0	45.90	6.12	VII		SED
1841	12	2	19:53: .0	45.75	5.91	VI-VII		LvG
1842	3	30	0:30: .0	46.23	7.12	VI		SED
1843	9	6	8:20: .0	47.33	6.87	VI		SED
1846	8	17	5:45: .0	46.78	6.58	VI		SED
1846	8	17	6:15: .0	46.77	6.58	VII		SED
1851	1	1	0: 0: .0	46.28	7.98	VI		SED
1851	3	10	15:13: .0	47.63	9.50	VI	4.3	SED
1851	8	24	1:30: .0	46.50	8.08	VI		SED
1852	7	29	12:40: .0	46.43	9.85	VI		SED
1852	7	29	13: 0: .0	46.43	9.85	VI		SED
1853	8	11	10:10: .0	47.22	7.57	VII		SED
1855	7	25	11:50: .0	46.23	7.85	VIII-IX		SED
1855	7	26	9:15: .0	46.23	7.88	VIII		SED
1855	7	26	13:20: .0	46.23	7.82	VII-VIII		SED
1855	7	2	10: 0: .0	46.25	7.82	VII		SED
1855	8	24	0: 0: .0	46.25	7.88	VI		SED
1855	8	26	9: 0: .0	46.25	7.92	VI		SED
1855	10	28	1:45: .0	46.25	7.92	VII		SED
1855	11	6	3:30: .0	46.23	7.92	VI		SED
1856	2	1	8:20: .0	47.22	7.57	VI		SED
1856	8	6	13:45: .0	46.25	7.87	VI-VII		SEH

Year	Mo	Da	Ho:Mi:Sec	Lat	Long	Int	Mag	Ref
1857	2	1	23:12: .0	45.75	10.47	VII		SCM
1857	8	28	0: 0: .0	46.78	10.27	VII		SED
1857	12	0	0: 0: .0	45.67	9.67	VI-VII		SCM
1861	11	14	21: 0: .0	47.35	8.87	VI		SED
1866	4	14	0: 0: .0	47.15	10.02	VI		SED
1866	8	11	0: 0: .0	45.72	10.78	VII		SCM
1867	5	14	3: 0: .0	46.80	6.75	VI		SED
1867	12	17	11: 0: .0	47.07	7.23	VI		SED
1868	2	20	0: 0: .0	45.62	10.72	VI		SCM
1869	12	14	7: 0: .0	47.70	7.60	VI	3.4	SED
1871	2	21	15:55: .0	48.50	8.40	VI		Ley
1873	4	10	19:30: .0	46.87	7.32	VI		SED
1874	2	20	18: 5: .0	47.33	8.45	VI		SED
1874	12	1	19:30: .0	46.15	7.80	VII		SED
1876	4	2	4:55: .0	47.00	6.95	VI		SED
1876	4	29	0: 0: .0	45.73	10.78	VII-VIII		SCM
1876	4	29	10:50: .0	45.73	10.83	VIII		SCM
1876	4	29	13:15: .0	45.67	10.83	VI		SCM
1876	4	29	20: 0: .0	45.73	10.83	VII		SCM
1876	4	29	23: 0: .0	45.73	10.83	VI		SCM
1876	4	29	23:15: .0	45.67	10.83	VII		SCM
1876	5	1	10:50: .0	45.73	10.83	VI-VII		SCM
1876	5	7	4:48: .0	46.70	6.50	VI		SED
1876	5	29	10:30: .0	45.73	10.83	VI		SCM
1877	5	2	19:40: .0	47.23	8.70	VI		SED
1877	10	1	0: 0: .0	45.75	10.80	VI-VII		SCM
1877	10	8	4: 0: .0	45.83	6.50	VII		SED
1877	10	8	4:20: .0	45.70	6.97	VI-VII		SCM
1877	10	8	5:12: .0	46.03	6.23	VII		LvG
1877	10	22	20:30: .0	46.03	7.75	VI		SED
1879	1	14	6:45: .0	45.70	10.67	VII		SCM
1879	1	14	6:55: .0	45.70	10.67	VII		SCM
1879	12	30	11:27: .0	46.12	6.75	VI		SED
1880	1	27	20:10: .0	45.70	6.97	VI		SCM
1880	7	4	8:20: .0	46.25	8.05	VII		SED
1880	7	4	19:30: .0	46.28	7.88	VI		SED
1880	9	19	10: 1: .0	46.82	7.18	VI		SED
1880	9	21	18:50:27.0	46.82	7.18	VI		SED
1881	1	27	13:19:53.0	46.90	7.50	VII		SED
1881	3	2	0: 0: .0	45.53	8.00	VI		SCM
1881	11	18	3:50: .0	47.20	9.42	VI-VII		SED
1881	11	25	17:25: .0	46.30	6.97	VII		SED
1882	1	23	0: 0: .0	47.50	10.55	VI		LvG
1882	2	27	6:30: .0	45.88	9.98	VI-VII		SCM
1882	9	13	0:40: .0	48.00	6.60	VI		Ley
1882	9	18	0: 0: .0	45.73	10.83	VII-VIII		SCM
1884	9	12	0: 0: .0	45.57	9.85	VI		SCM
1885	4	13	10:25: .0	46.57	7.38	VII		SED
1885	6	28	1:26: .0	46.55	7.37	VI		SED

Year	Mo	Da	Ho Mi Sec	Lat	Long	Int	Mag	Ref
1886	9	29	17:28: .0	46.75	10.05	VI		SED
1886	10	9	18:20: .0	48.45	7.92	VII		Ley
1886	11	28	22:30: .0	47.30	10.80	VII-VIII	5.2	AEC
1887	6	11	21:30: .0	48.38	7.88	VI		Ley
1887	10	1	0: 0: .0	45.75	10.75	VII		SCM
1891	1	9	20:34: .0	47.37	9.62	VI-VII		SED
1891	1	23	20: 5: .0	47.38	9.43	VI		SED
1892	1	5	0: 0: .0	45.53	10.48	VI-VII		SCM
1892	3	5	0: 0: .0	45.62	7.80	VII		SCM
1894	11	27	0: 0: .0	45.58	10.12	VI-VII		SCM
1895	10	12	1:45: .0	45.77	10.83	VI		SCM
1896	1	6	17:40:42.0	45.77	10.83	VI		SCM
1896	1	22	0:47: .0	47.90	8.18	VI		Ley
1898	2	22	10:44: .0	46.80	6.60	VII		SED
1898	5	6	13:10: .0	46.60	7.68	VII		SED
1898	6	14	3:55: .0	47.12	9.50	VII		SED
1899	2	14	16:58: .0	48.12	7.65	VII		Ley
1899	5	30	8: 0: .0	47.30	10.50	VI		Ley
1900	6	3	3:40: .0	48.15	7.55	VI-VII		Ley
1901	5	22	7:58: .0	47.63	7.40	VI		LvG
1901	10	30	14:49: .0	45.53	10.42	VIII-IX		SCM
1901	10	30	14:51:41.0	45.60	10.50	VII-VIII		LvG
1904	3	28	13:20: .0	46.77	7.32	VI		SED
1905	4	29	1:46: .0	45.92	6.93	VII-VIII		SED
1905	8	13	10:21: .0	45.90	7.00	VI-VII	5.6	SED
1905	12	5	0: 0: .0	46.85	9.52	VI		SED
1905	12	10	0: 0: .0	45.92	10.30	VII	4.7	LvG
1905	12	25	17: 5:48.0	46.80	9.40	VII	4.9	SED
1905	12	26	0:20:30.0	46.80	9.40	VI	4.2	SED
1910	5	26	6:12: 5.0	47.40	7.30	VII		SED
1910	7	13	8:32: .0	47.30	10.90	7.1	4.8	AEC
1910	12	7	18:51: .0	47.73	7.57	VI		SED
1911	4	24	17:19: .0	47.17	10.33	VI	3.7	SED
1911	11	16	21:25:48.0	48.22	9.00	VIII		Ley
1911	11	23	1:59: .0	48.20	9.03	VI		Ley
1912	1	19	5:45: .0	48.20	9.03	VI		Ley
1913	4	21	20:25: .0	47.25	8.60	VI		SED
1913	7	20	12: 6:22.0	48.23	9.01	VII		Ley
1914	8	30	11:22:38.0	47.32	9.65	VI	3.5	SED
1914	10	27	9:23:18.0	46.00	9.00	VI-VII		SED
1915	8	25	2:11:36.0	46.03	7.03	VII	4.4	SED
1917	6	20	23: 9: .0	47.72	9.02	VI	5.0	SED
1917	12	30	7:50: .0	47.48	10.95		4.5	Ley
1918	4	24	14:21: .0	45.80	9.55	VI		SCM
1924	4	15	12:48:54.0	46.25	7.92	VII	5.1	SED
1924	12	11	16:33: 3.0	48.26	9.09	VI		Ley
1925	1	8	2:45: .0	46.87	6.50	VII		SED
1925	7	21	12: 1:58.0	46.08	6.20	VI	3.4	SED
1926	6	28	22: 0:40.0	48.13	7.68	VII		Ley

Year	Mo	Da	Ho Mi Sec	Lat	Long	Int	Mag	Ref
1926	12	15	13:58:52.0	46.75	7.18	VI 4.3		SED
1927	12	16	10:44:30.0	48.27	9.02	VI		Ley
1929	3	1	10:32:10.0	46.77	6.75	VII-VIII	4.4	SED
1930	10	7	23:27: .0	47.35	10.70	7.8	5.3	AEC
1931	4	14	22:12:52.0	45.80	10.40	VI-VII	4.4	SCM
1932	2	19	12:57: .0	45.65	10.80	VII-VIII		SCM
1933	8	12	9:56:57.0	46.68	6.78	VII	4.4	SED
1933	11	8	0:51: .0	47.35	10.70	6.8	4.6	AEC
1935	1	31	12:39:33.0	47.68	9.08	VI	4.5	SED
1935	2	5	1:30: .0	48.30	8.20	VI		Ley
1935	6	27	17:19:30.0	48.04	9.47	VII-VIII	5.6	Ley
1936	3	15	1:26: .0	47.65	9.48	VI	4.3	SED
1936	6	22	3:44:55.0	45.50	10.77	VI	4.3	SCM
1937	7	7	22: 2:49.0	46.37	10.65	VI	4.1	LvG
1938	4	11	6:42: .0	48.04	9.47	VI		Ley
1942	2	17	11:14:42.9	46.66	7.64		3.2	SED
1942	6	20	14:42: .0	45.90	10.90	VI	3.6	SCM
1942	7	17	10:26:41.4	48.26	8.98	VI	4.8	SED
1943	4	25	11:35: 6.9	48.28	9.00	VI	4.8	SED
1943	5	2	1: 8: .6	48.27	9.04	VII	4.9	SED
1943	5	28	0:24: 8.5	48.15	8.79		5.1	SED
1943	6	1	13:53: 5.0	48.26	8.98	VI-VII		Ley
1943	7	4	4:37: 9.0	48.27	8.98	VI		Ley
1943	7	14	4:16:36.1	48.22	8.81	VI	4.3	SED
1943	10	13	23:24: 7.7	48.29	9.00	VI	5.0	SED
1943	10	17	2:30:12.0	48.30	9.00	VI		Ley
1943	12	27	18:50:31.3	48.36	9.17	VI-VII	4.8	SED
1946	1	25	17:31:47.0	46.38	7.52	VIII	5.7	SED
1946	1	26	3:15:16.0	46.32	7.52	VI-VII		SED
1946	2	4	4:11:28.0	46.30	7.52	VI-VII	4.2	SED
1946	5	30	4:41: .0	46.30	7.42	VII	4.4	SED
1947	4	14	21:30:41.0	48.25	9.05	VI		Ley
1947	6	28	13:13: .0	48.26	9.05	VI-VII		Ley
1947	12	25	20:42:34.0	45.70	10.20	VI	4.2	SCM
1948	7	19	18:11:31.3	46.27	10.91		5.0	SED
1951	10	18	19:57:44.0	48.28	9.02	VI		Ley
1954	5	19	9:34:58.5	46.36	7.07	VI-VII	5.3	SED
1955	11	23	6:39:12.0	47.41	5.98	VI		LvG
1956	8	1	9:40:33.0	48.30	9.02	VI		Ley
1957	8	29	3:45:53.0	48.19	9.18	VI	4.3	SED
1958	3	30	16:10:12.0	45.76	5.80	VI		LvG
1958	9	15	16:21:51.0	45.70	5.71	VI		LvG
1958	9	30	8:45: .0	47.20	10.60	6.6	4.5	AEC
1959	9	4	8:36:53.0	48.35	7.63	VI		LvG
1959	9	4	8:56:54.0	48.38	7.72	VII		Ley
1960	2	19	2:30:14.0	45.73	10.45	VI	4.5	SCM
1960	3	23	23: 8:50.0	46.37	8.15	VII	4.7	SED
1960	5	13	3:55:34.0	48.42	7.33	VI		Ley
1961	8	9	13: 4:29.1	46.80	10.36	VI	4.0	SED

Year	Mo	Da	Ho Mi Sec	Lat	Long	Int	Mag	Ref
1961	8	25	12:22: .0	47.40	10.60	VI	4.1	AEC
1964	2	17	12:19: 1.0	46.90	8.25	VII	4.8	SED
1964	3	14	2:37:22.0	46.95	8.28	VII	4.8	BOL
1968	6	18	5:27:33.2	45.73	7.96	VI	5.2	SED
1968	6	27	15:43:40.0	46.30	6.80	VI-VII	4.6	SED
1968	8	19	0:36:41.0	46.31	6.73	VI		SED
1969	2	26	1:28: 2.6	48.38	9.06	VII	4.4	BOL
1970	1	22	15:25:17.3	48.43	8.98	VII	4.5	BOL
1971	6	8	2:22: 2.0	48.35	8.93	VI	4.2	Ley
1971	9	29	7:18:51.7	47.11	9.03	VII		SED
1972	5	18	8:11: 1.0	48.28	9.03	VII	4.8	Ley
1976	9	15	23:39:10.0	48.32	9.07	VI	4.0	Ley
1977	9	2	22:47:14.0	48.03	9.32	VI-VII	3.9	Ley
1978	1	16	14:31:17.0	48.30	9.03	VI-VII	4.6	Ley
1978	9	3	5: 8:32.0	48.28	9.03	VII-VIII	5.7	Ley
1980	7	15	12:17:22.0	47.63	7.52	VI	4.4	SED
1984	12	29	11: 2:37.0	48.11	6.50	VI	4.8	Ley
1991	11	20	1:54:17.4	46.72	9.53	VI	5.0	SED

APPENDIX B

Earthquake Site Catalogs

Figures B2 to B13 display "Earthquake Site Catalogs" for intensity degrees V to IX since the 13th century for the twelve selected sites (in alphabetical order). They show the calculated probabilities of occurrences for the different intensity degrees following the procedure described in figure 3.1.

The twelve selected sites are:

B2:	Basel
B3:	Bern
B4:	Brig
B5:	Buchs
B6:	Chur
B7:	Geneva
B8:	Lugano
B9:	Sarnen
B10:	Sion
B11:	St. Moritz
B12:	Yverdon
B13:	Zurich

Figures B14 to B17 show the distance distributions of the "Earthquake Site Catalogs" for intensity $\geq$V and for a probability of ≥ 0.1. On these figures it can be recognized in which distance to the site the earthquakes occurred that contributed to the "Earthquake Site Catalog".

B14:	Basel / Bern / Brig
B15:	Buchs / Chur / Geneva
B16:	Lugano / Sarnen / Sion
B17:	St. Moritz / Yverdon / Zurich

Basel
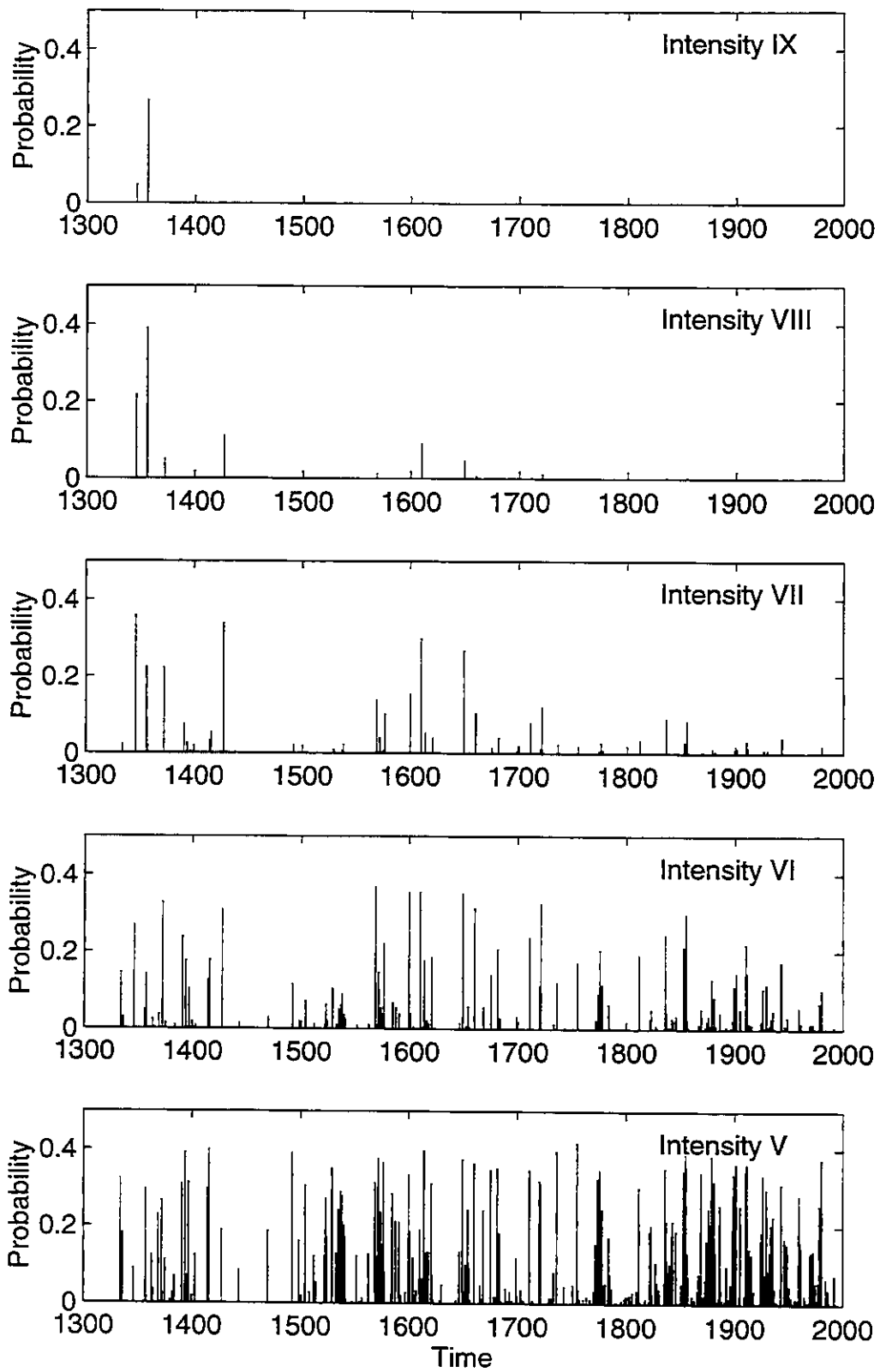
Bern
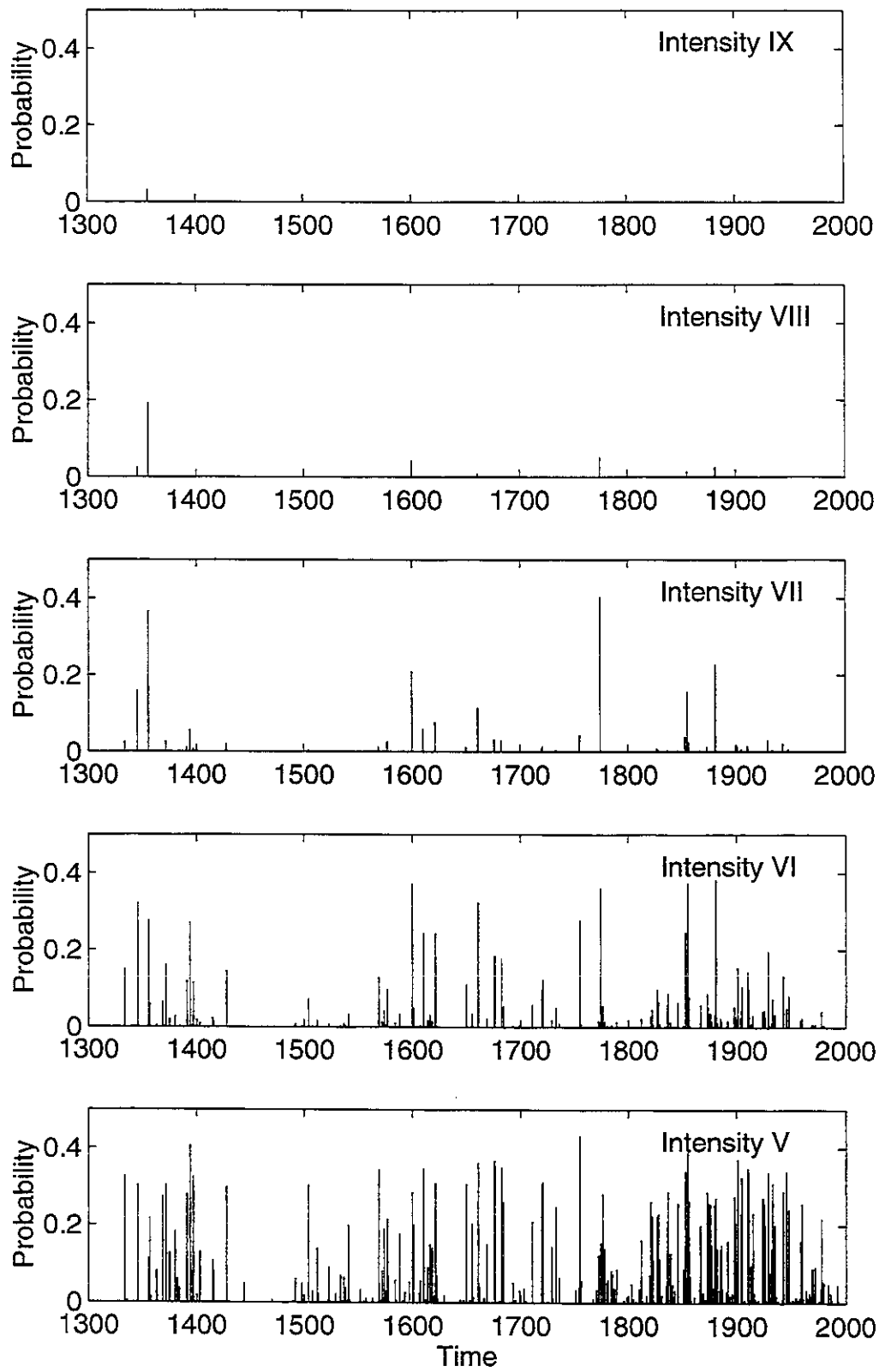
Brig
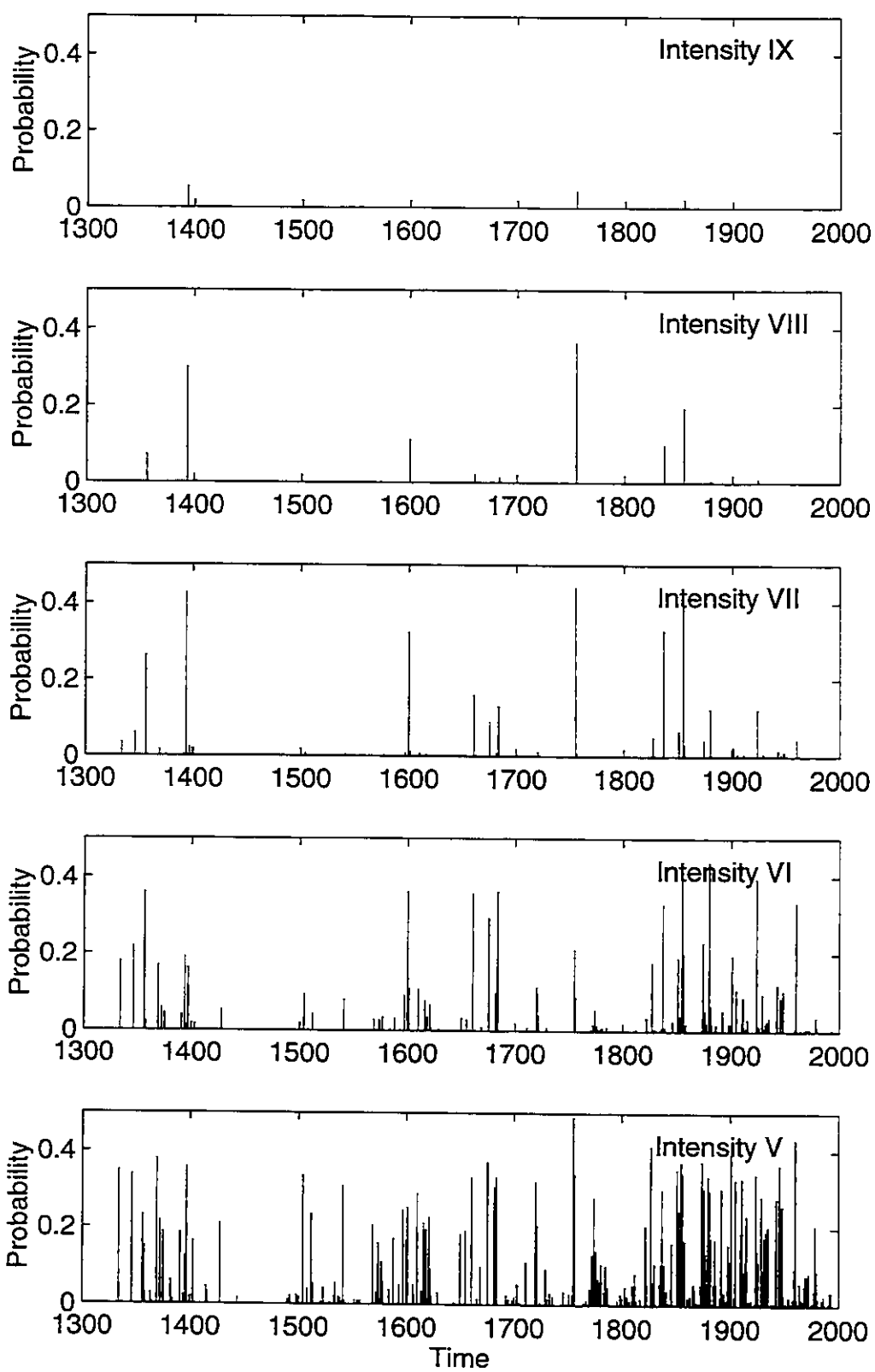
Buchs
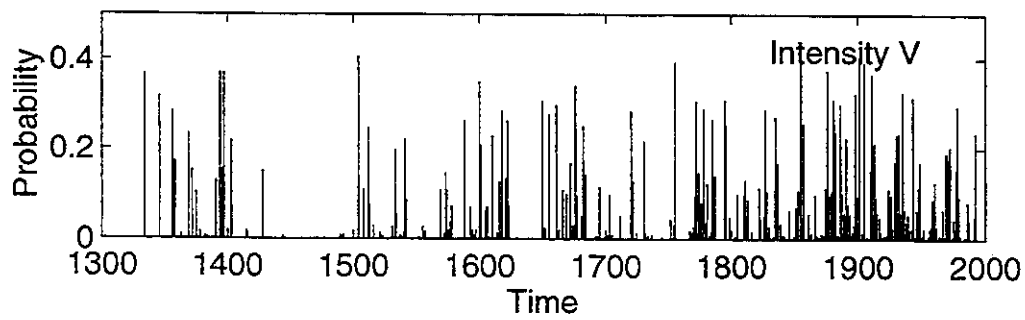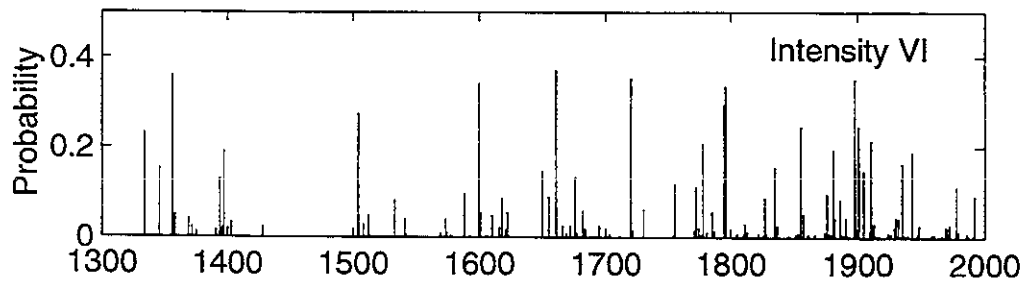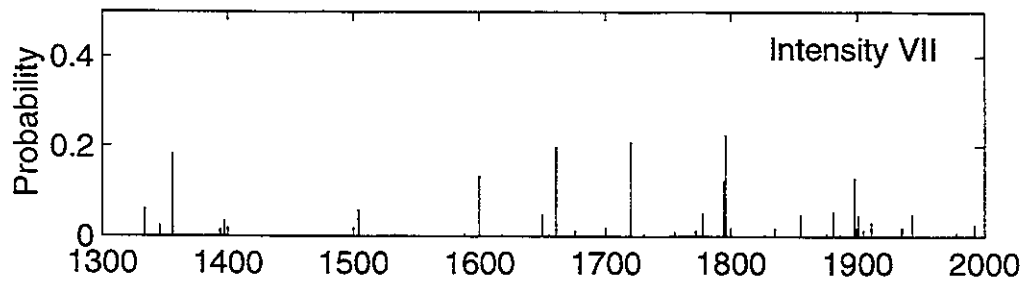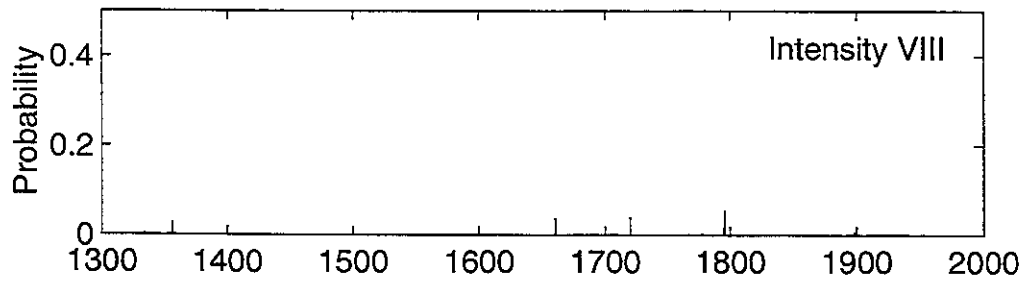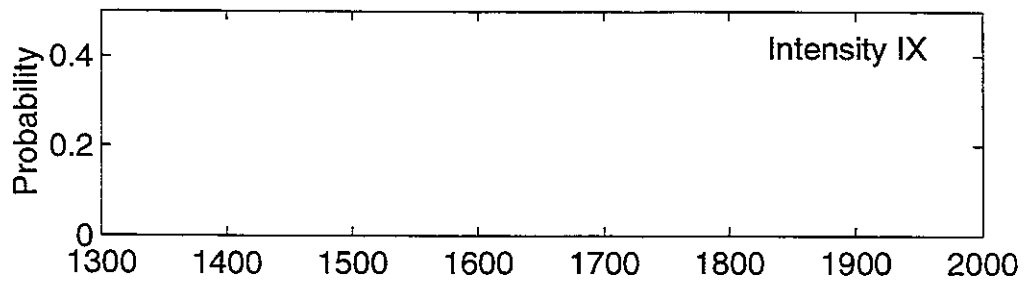
Chur
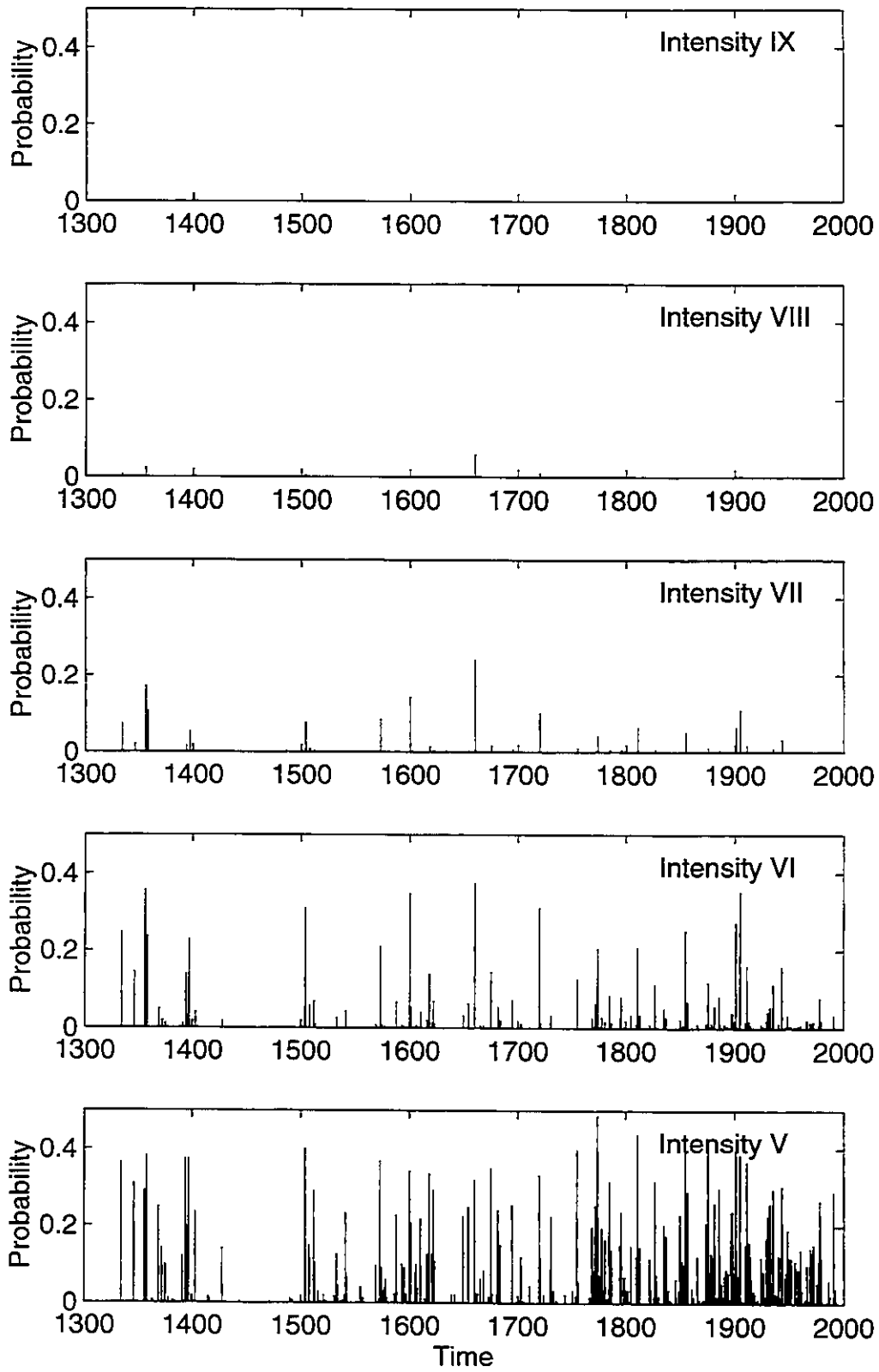
Geneva
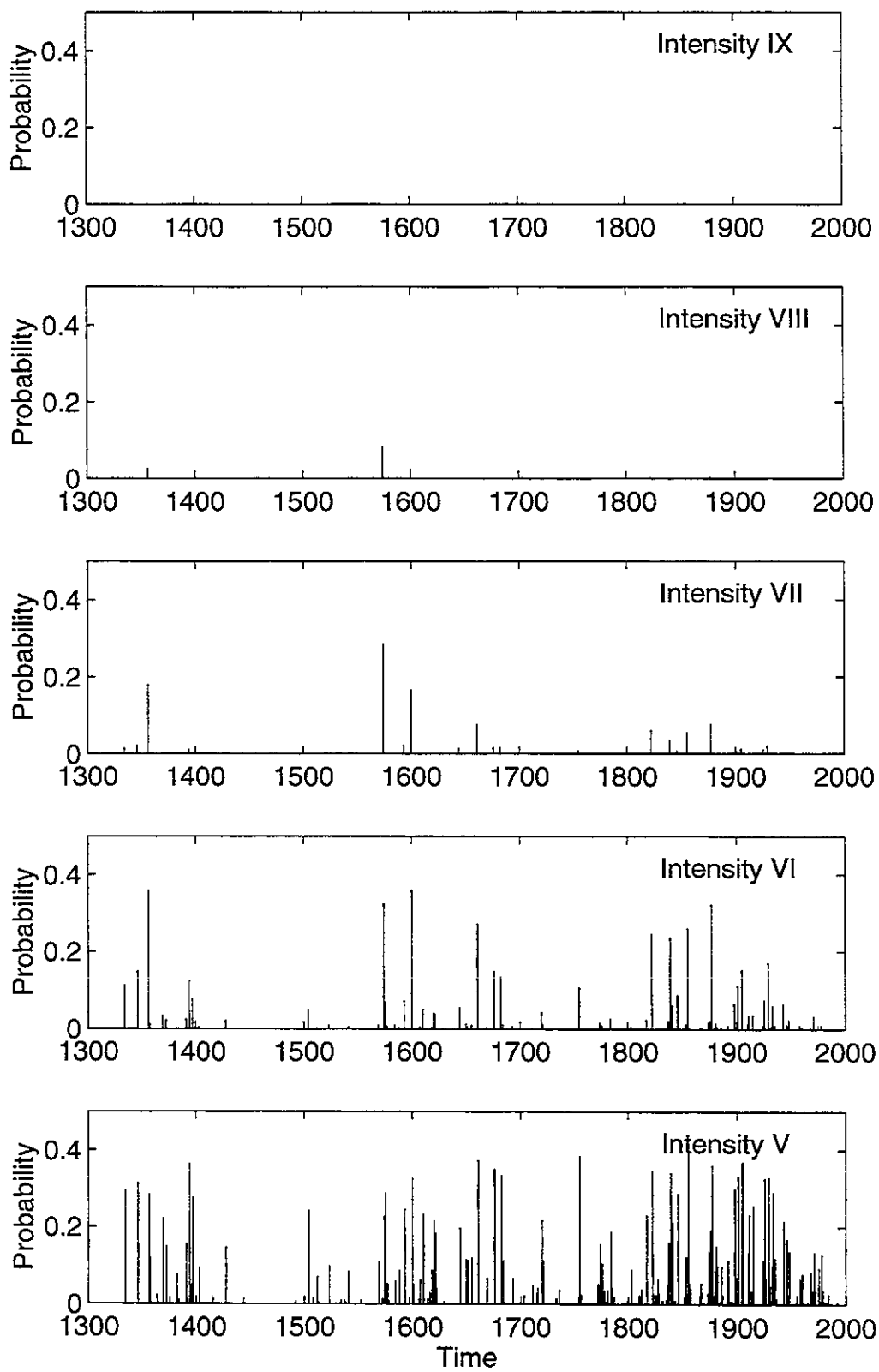
Lugano
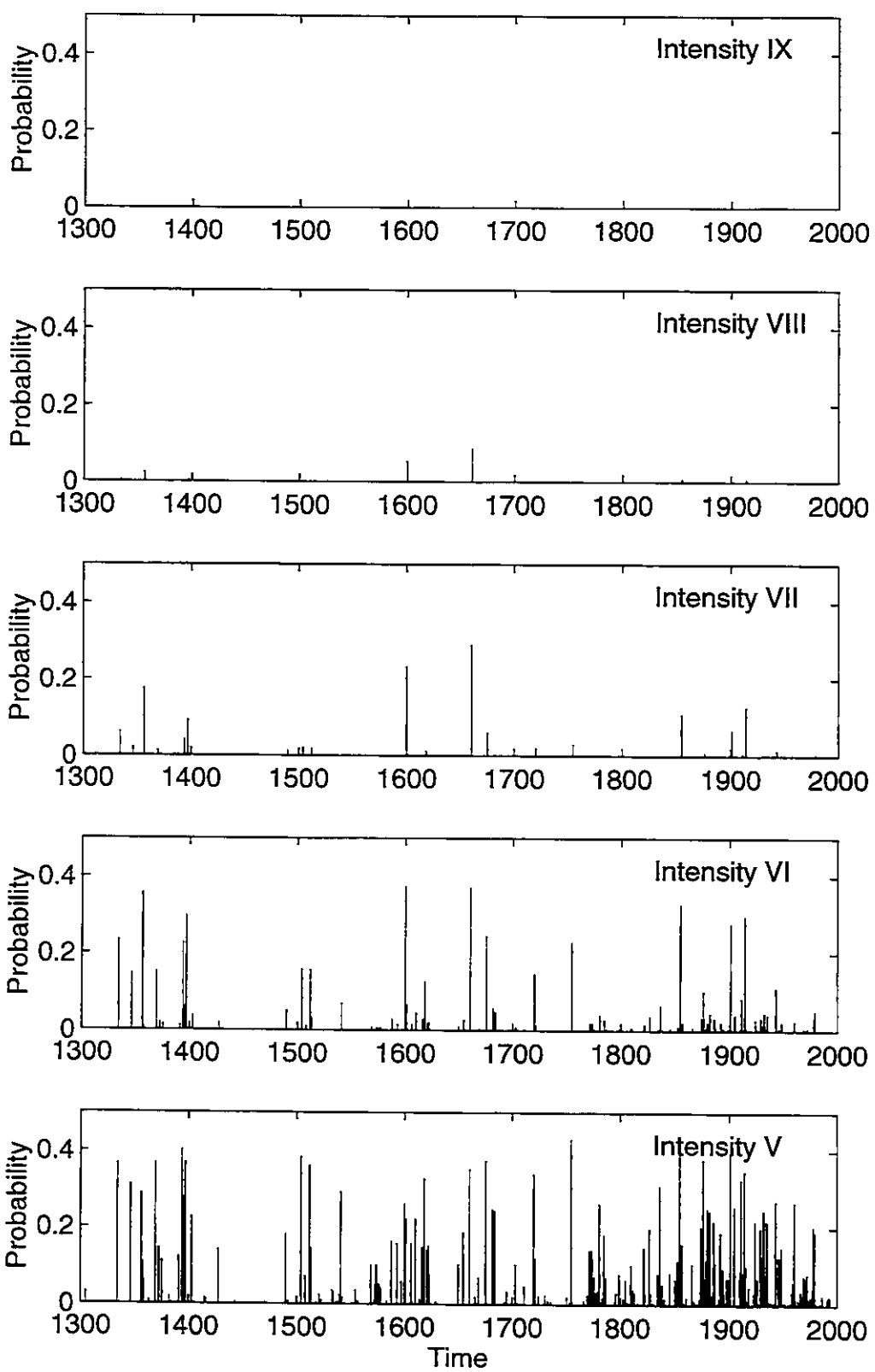
Sarnen

Sion

St. Moritz

Yverdon

Zurich

Basel

Bern

Brig

Buchs

Chur

Geneva
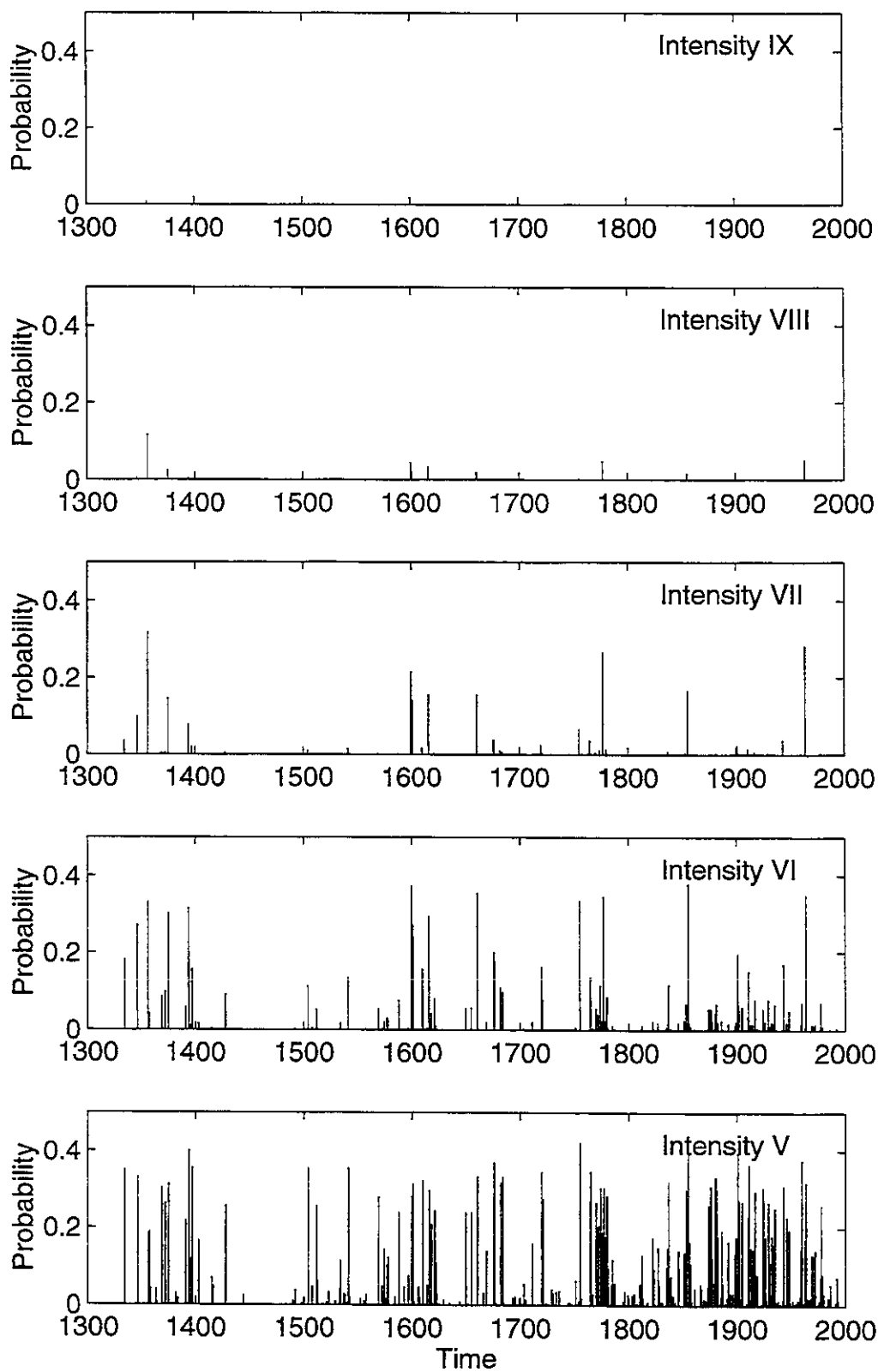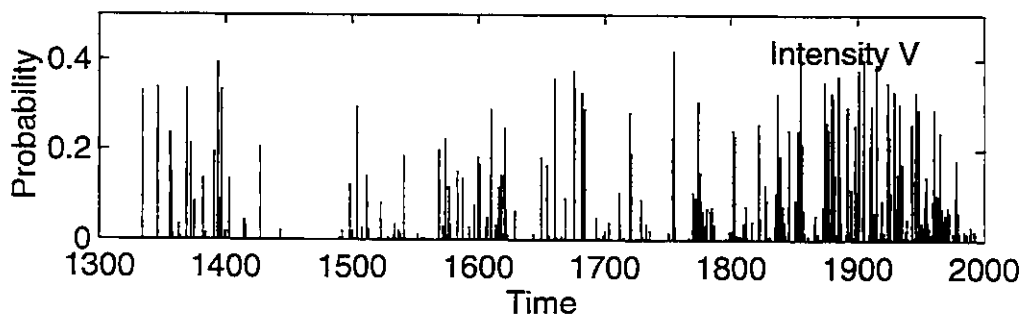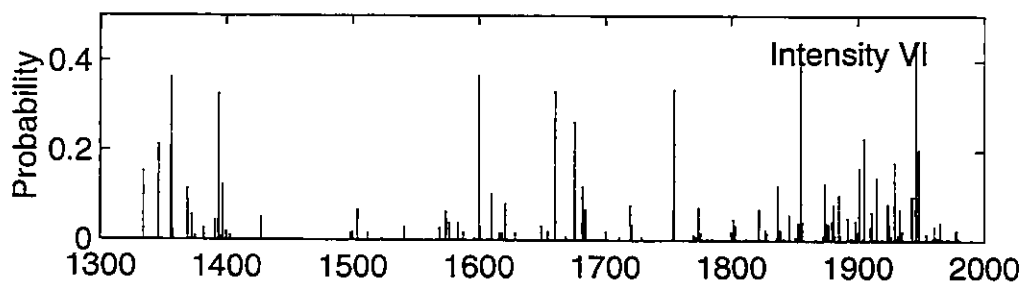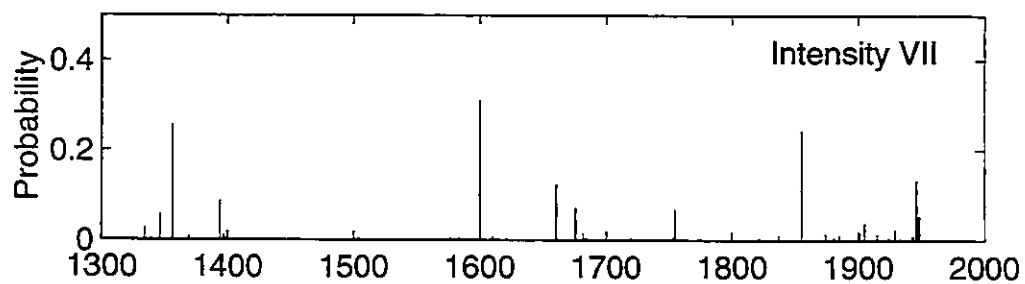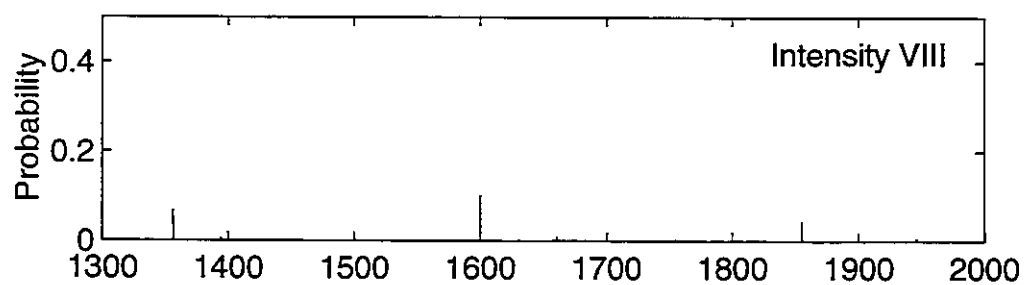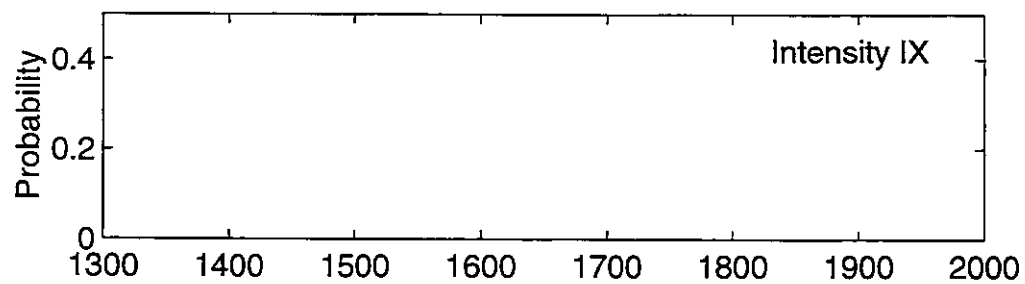
St. Moritz
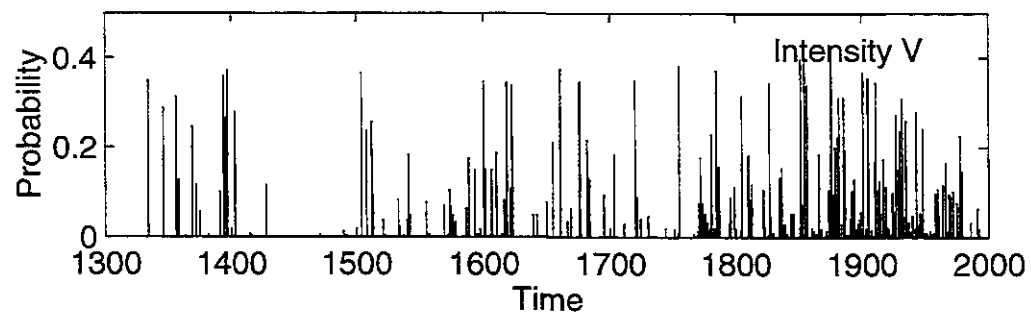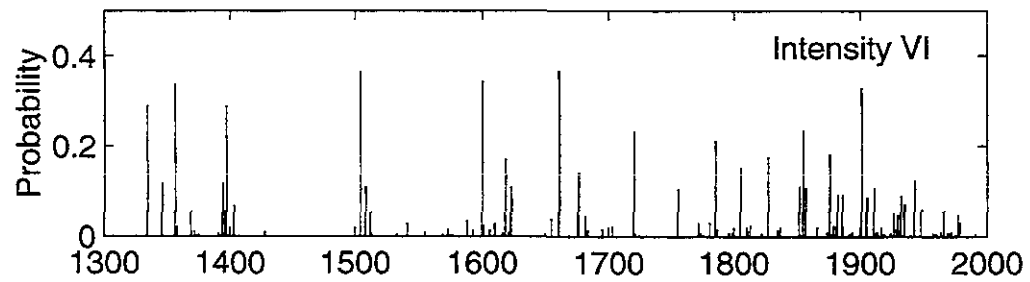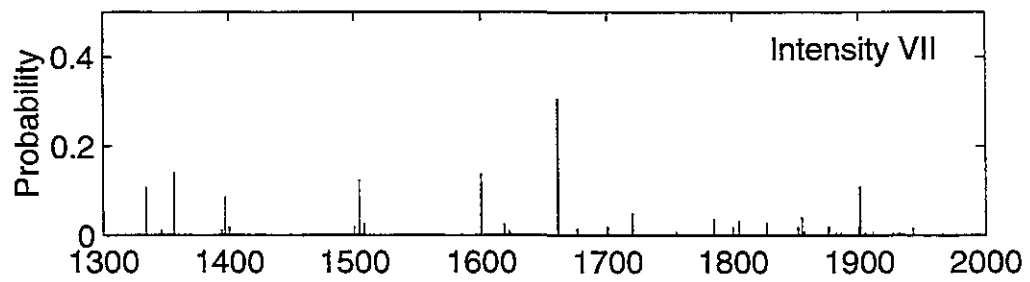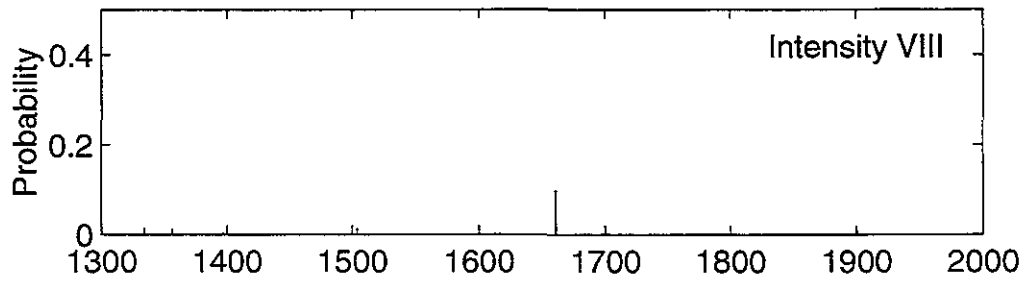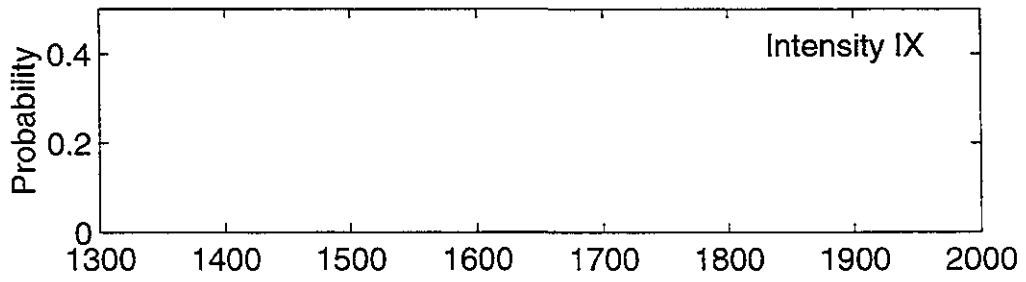
Yverdon
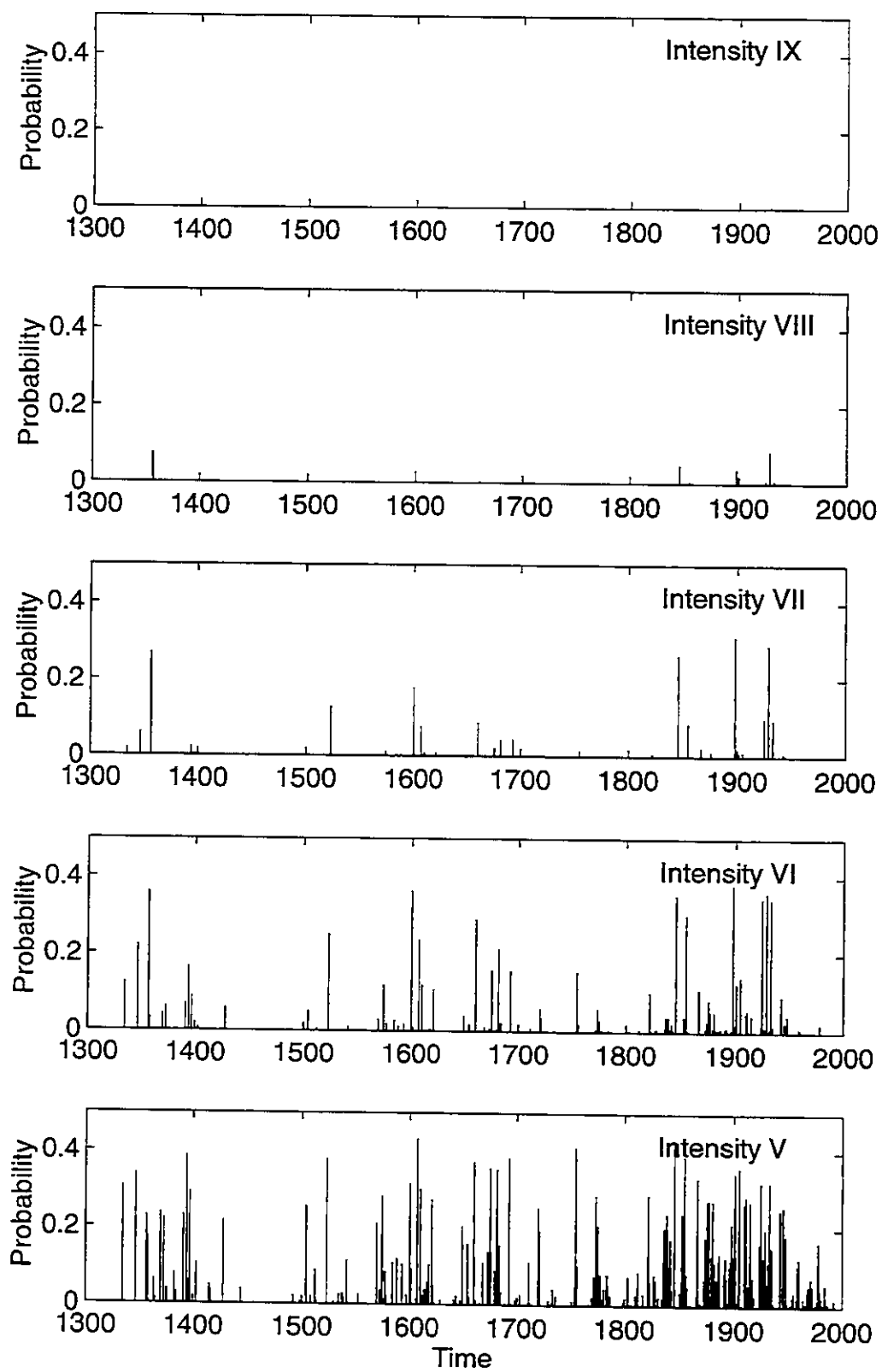
Zurich
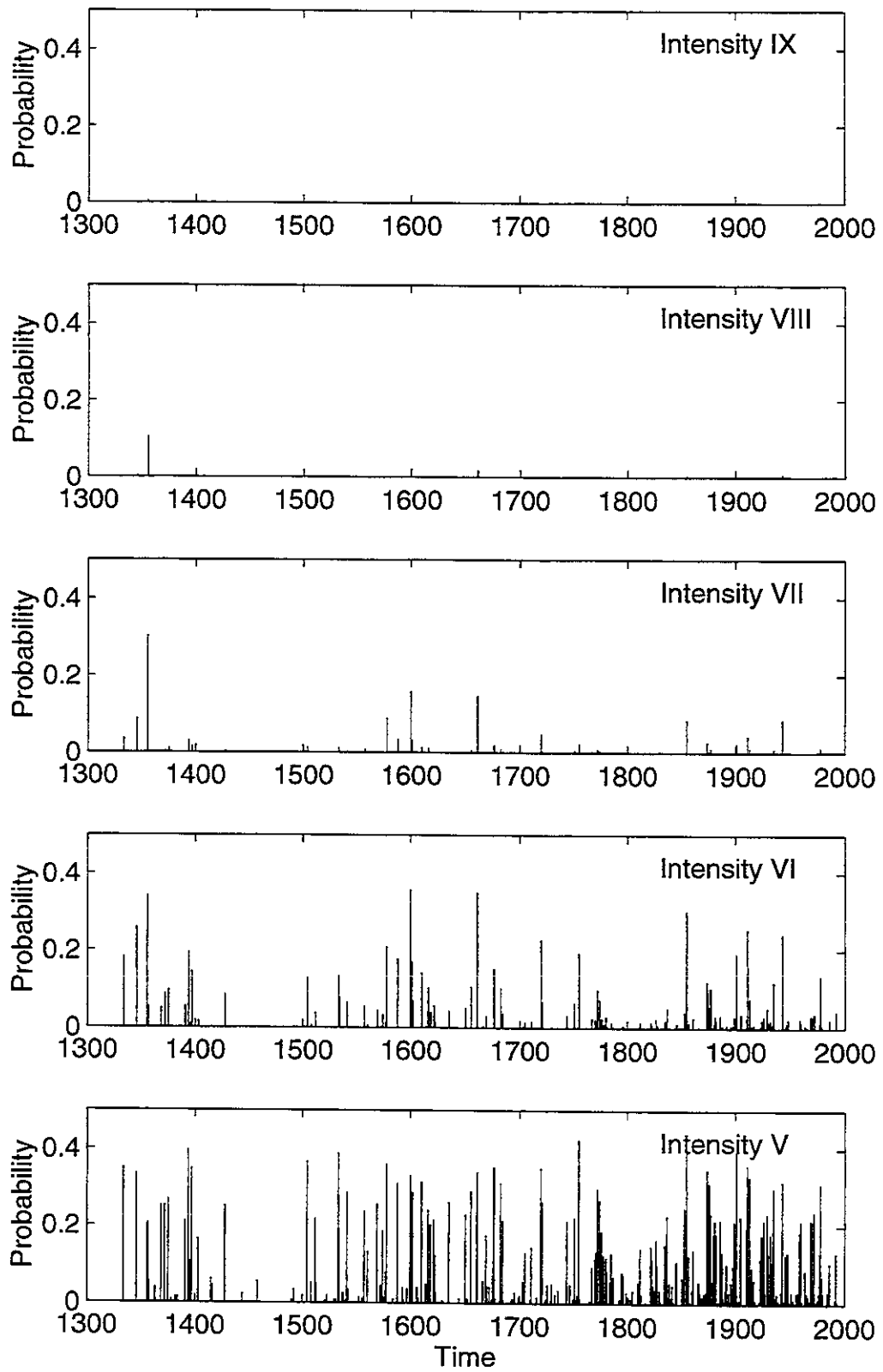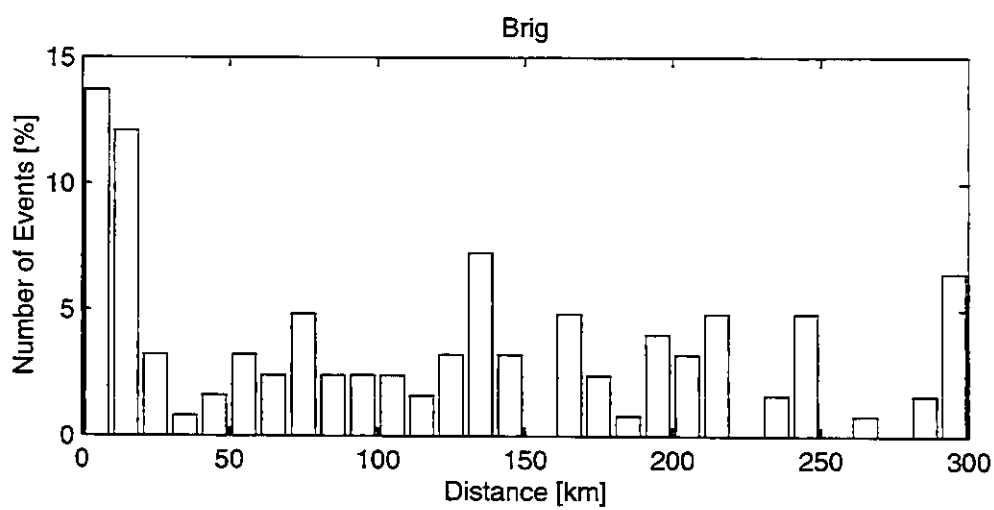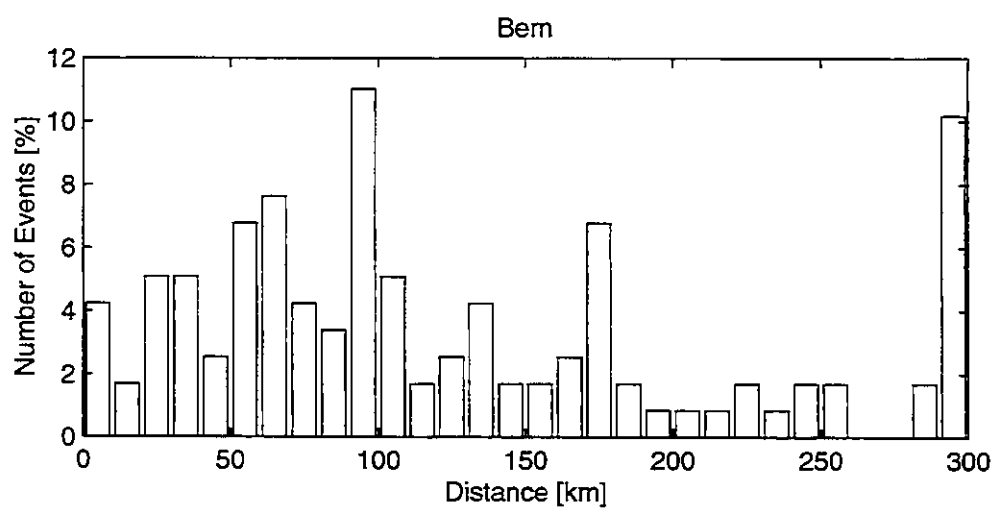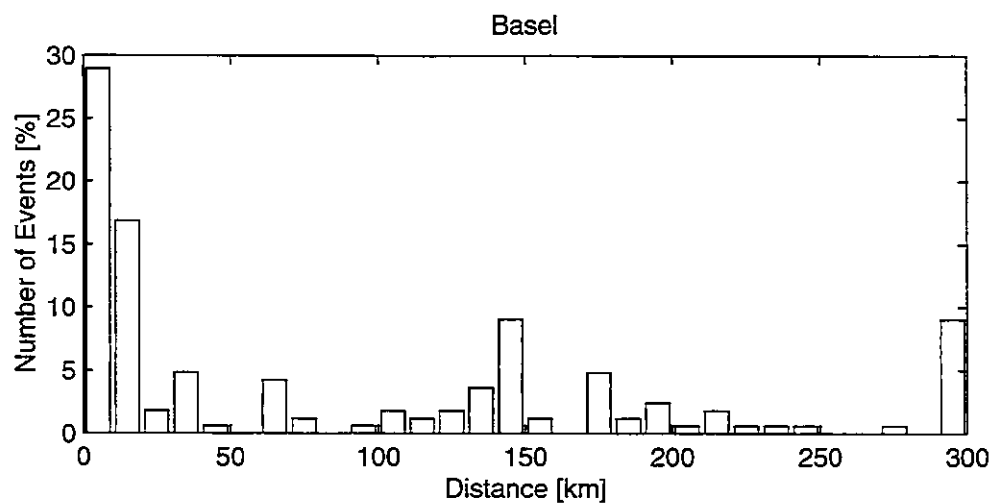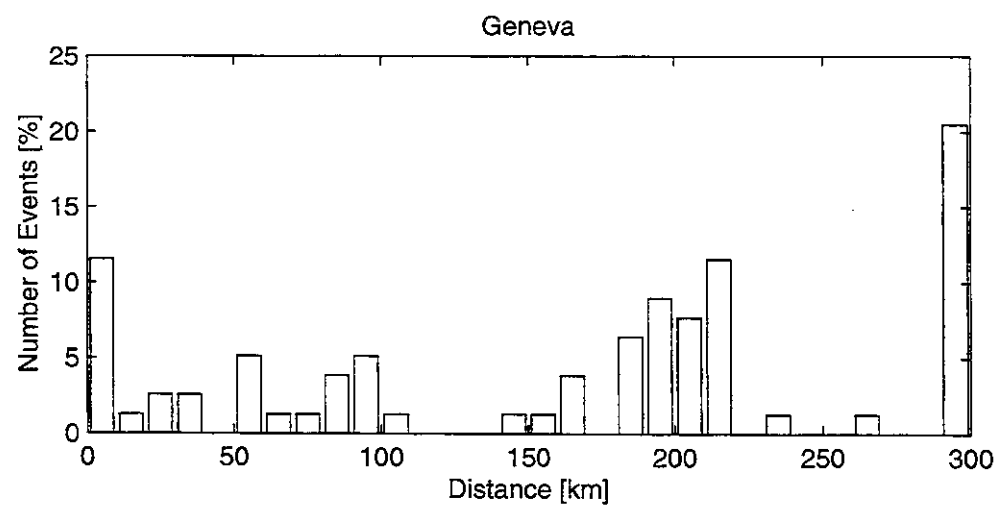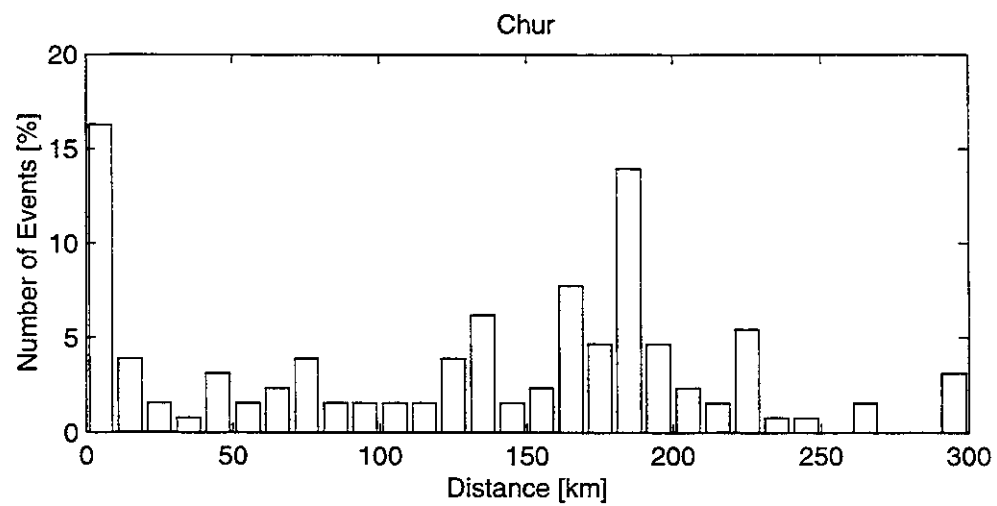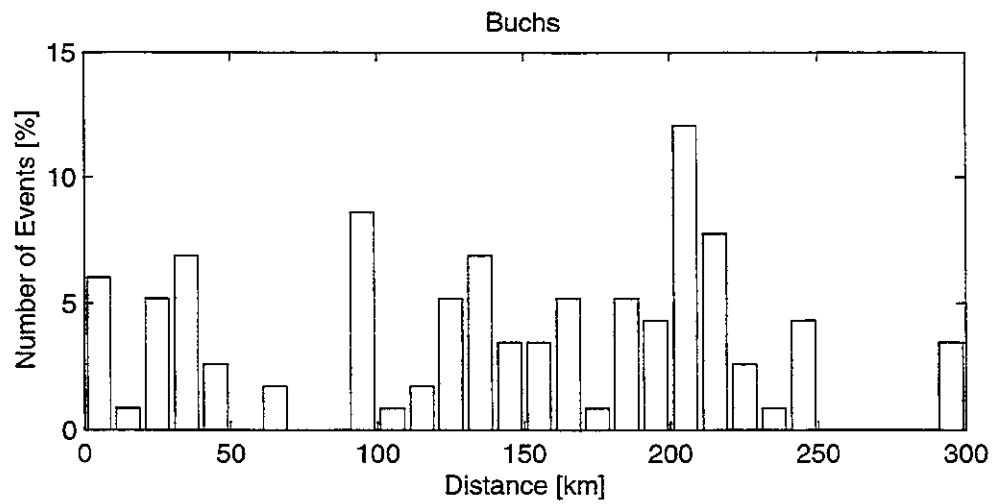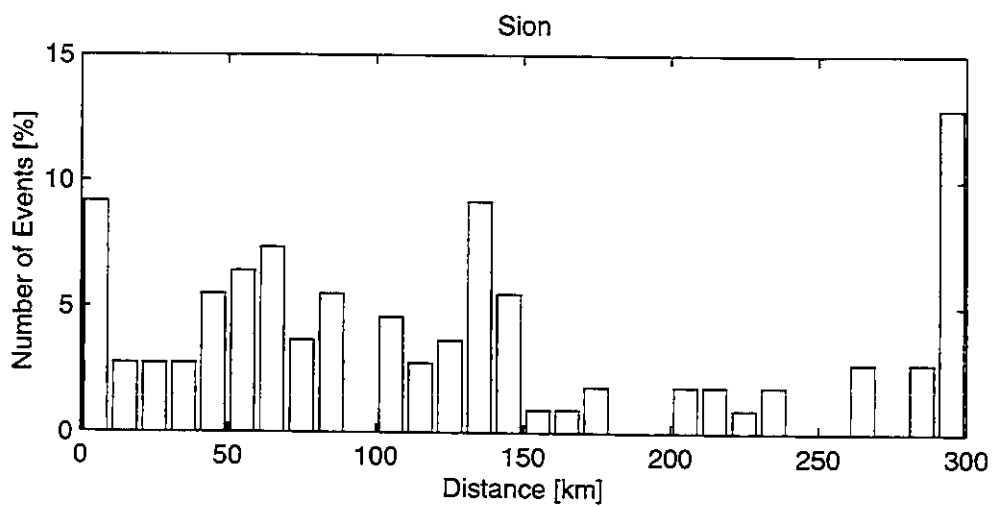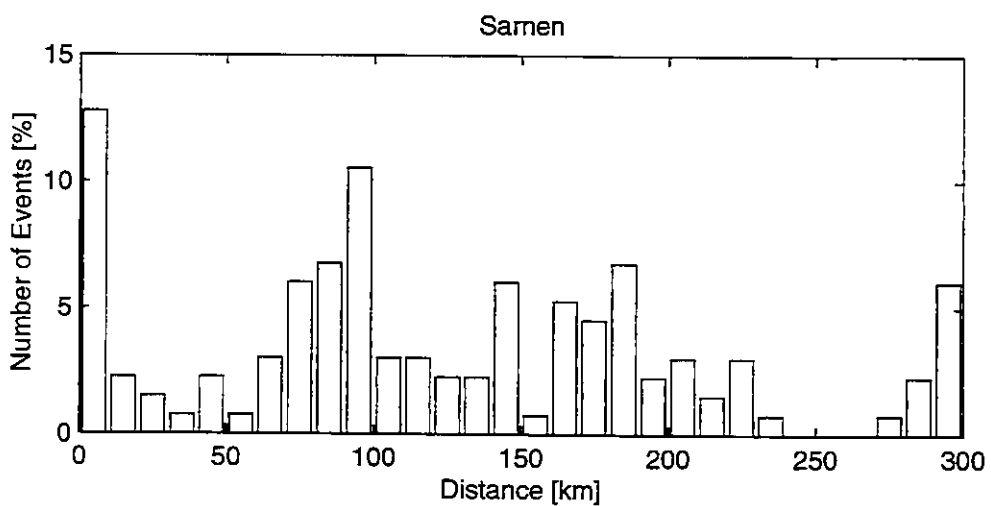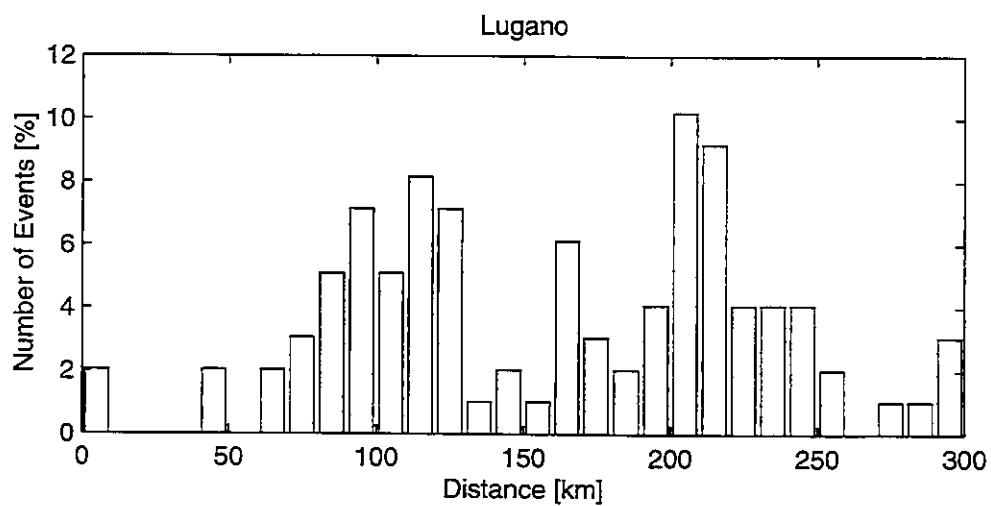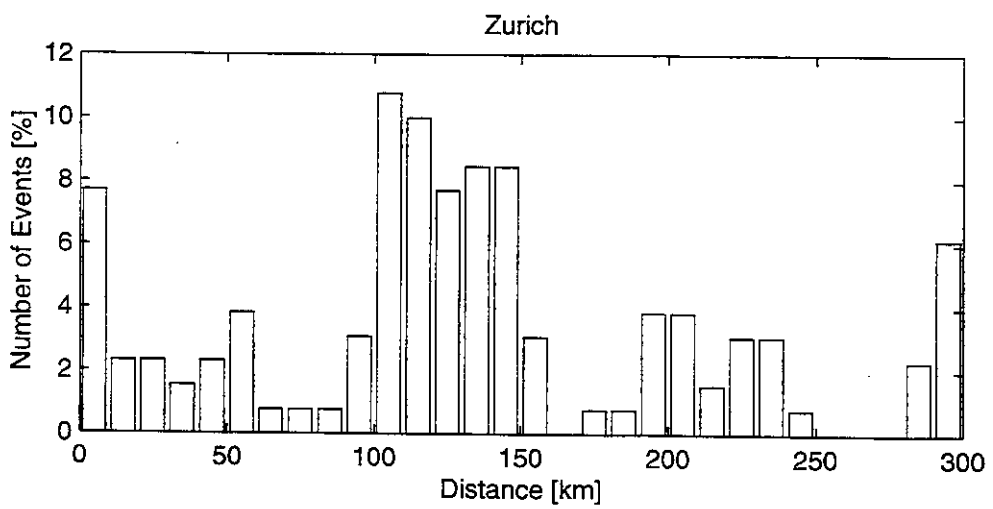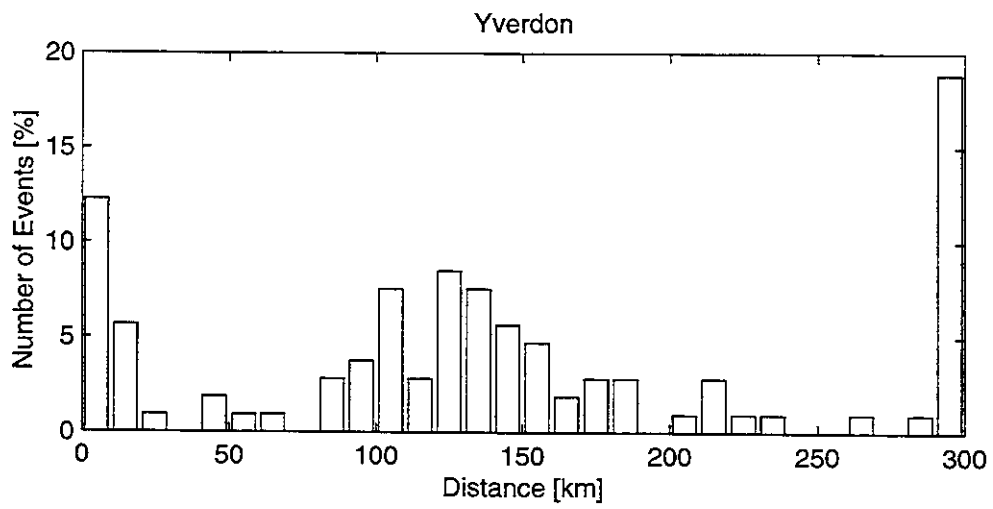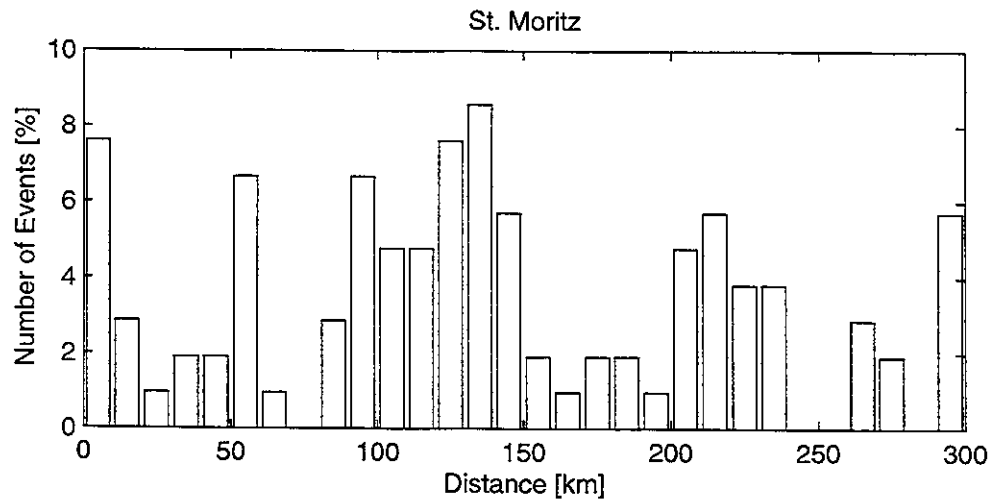
APPENDIX C

Program BayHaz

Author: **Erik Rüttener**

Release: **1.0 (January, 1995)**

Syntax: **bayhaz**

Description

Program BAYHAZ creates an "Earthquake Site Catalog" taking into account error models for earthquake size, standard deviations for earthquake location errors, depth distribution models and scattered attenuation models. Besides the "Earthquake Site Catalog", probabilities of number of occurrences based on a mixed Bernoulli trial are calculated (cf. chapter 3.4). Needed input files are (cf. source code (header information) for the exact format description):

- file containing earthquake data catalog. Each earthquake needs flags that indicate which error model, which standard deviation, which depth model and which attenuation model has to be used;
- file describing earthquake size error models;
- file describing depth distribution models;
- file describing attenuation models.

Structure of the Source Code

The source code is found in the file bayhaz.f. There is a Makefile available that allows a quick compiling of the code. Needed files containing subroutines are:

- calc_prob.f
- epidiffusion.f
- mixber_tine.f
- grkr.f

Program OUTNEW

Author: **Erik Rüttener**

Release: **1.2 (January, 1995)**

Syntax: **outnew(data,gm,is1,is2,ip1,ip2,ip3,ip4)**

Description

MATLAB interface module which calculates prior and posterior distributions following Bayesian inference. Needed input is the file that contains the probabilities of number of occurences (this is the output of program BAYHAZ).

Structure of Source Code

Outnew calls different routines that calculate standard Bayesian distributions and weighted Bayesian distributions, each of them either with informative, minimal informative or non-informative prior distributions (controlled by the parameters is1 and is2). Figure C.1 displays the flowchart of Outnew. Help outnew displays the description of all needed parameters.

The output are median values, 50% and 90% probability intervals of the posterior distribution.
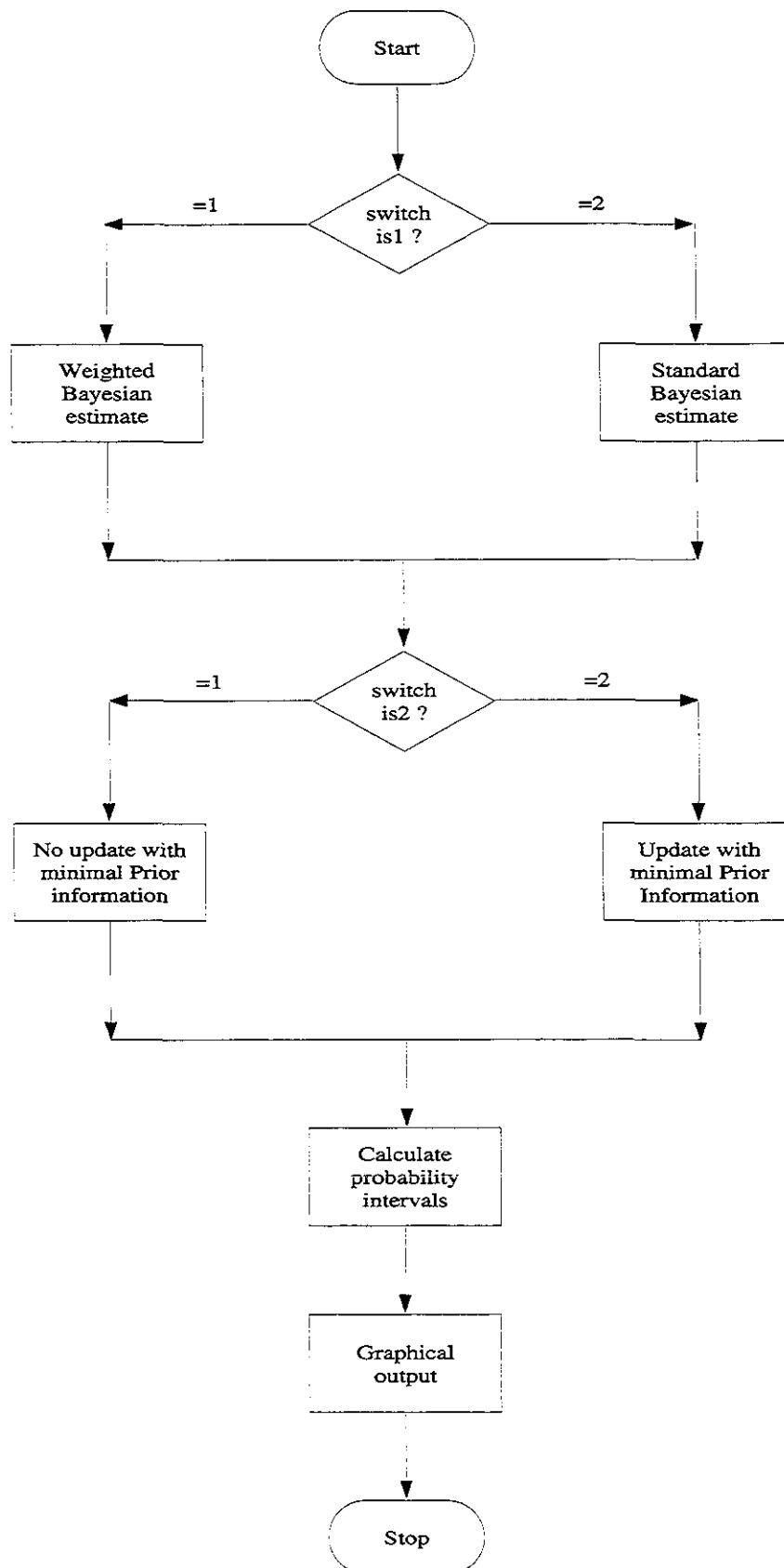
Figure C.1:Flowchart of OUTNEW

Beiträge zur Geologie der Schweiz
Matériaux pour la Géologie de la Suisse
Contributions to Geology of Switzerland

Geophysik-Géophysique-Geophysics